SSD 52.4

Final Report

for the

POSITIVE DEPLOYABLE SOLAR ARRAY DEVELOPMENT PROGRAM

(1 July 1964 - 30 September 1964)

Contract No. NAS 5-3988

Submitted To

GODDARD SPACE FLIGHT CENTER

Greenbelt, Maryland

Prepared By

FAIRCHILD HILLER
SPACE SYSTEMS DIVISION

1455 Research Boulevard
Rockville, Maryland

TABLE OF CONTENTS

TABLE OF CONTENTS (Continued)

LIST OF ILLUSTRATIONS

LIST OF ILLUSTRATIONS (Continued)

ABSTRACT

This final report presents the results of a study to select an optimum design for a compact storable solar array system for use with spin stabilized satellites. In this study several concepts of both flexible and rigid solar panels were considered. The elimination of less favorable concepts were made on the basis of minimum weight, high power to weight ratios, environmental compatibility, reliability, minimum packaged volumes, state-of-the-art materials and moderate cost. The study has culminated in a final design using a flexible substrate with a scissors type extension mechanism. The scissors are driven by spring loaded screw jacks and controlled during deployment by a centrifugal brake mechanism. A dynamic, thermal and a structural analysis of the final configuration is included.

During this study it was found that for smaller payloads the flexible panel is generally more favorable if package volume and weight are primary considerations. It is possible, however, that a rigid panel may be better, if package depth is extremely limited. For depths of package less than 1.50 inches the flexible array is not practical.

The most critical requirements imposed on the design was found to be 1 g condition and the limited depth of the package. The effect of these are to increase the weight of the extension mechanism and drive system. The most important item for further development is the flexible substrate, especially in the area of manufacturing processes and testing. A more efficient packaging arrangement could be made if the geometry of the spacecraft and launch vehicle were specified.

1.0 INTRODUCTION

Fairchild Hiller's Space Systems Division has conducted a study for the Goddard Space Flight Center directed toward increasing packaging density for satellite borne solar cell arrays. High density packaging is desired to provide greater array area, and hence; an increment in available power within the limitations of space and weight constraints placed on a given spacecraft application. This increased available power allows a greater flexibility in design of subsystems.

The method of approach applied to the design problem by Fairchild Hiller Corporation is described graphically in Figure 1.1. This procedure was designed to enable an optimum selection among the various possible alternates in minimum time.

1.1 SUMMARY

The design offered for evaluation in this report utilizes a flexible substrate driven by a scissor linkage extension system. The design study has shown that this approach offers the best packaging efficiency and lowest weight of the several configurations studied. The design chosen used the ground rules listed below.

- The solar array package dimensions shall be no greater than thirteen inches wide by twenty-five inches long by four inches deep. It shall deploy to the dimensions of one foot wide by eight feet long with solar cells mounted on the two sides of this area. The deployment mechanism shall be capable of maintaining a rigid configuration in the earth's gravitational field. The relationships between the array and the spacecraft are given in Figure 1.1. The further stipulation has been made that for ground deployment the x axis will be vertical.

- The array shall be capable of positive deployment and of maintaining dimensional integrity while spinning on the body of a spacecraft at an initial rate (before deployment) of 80 - 160 revolutions per minute and a final rate (after deployment) of 20 - 40 revolutions per minute.
- The total weight including mechanisms, wiring, interconnectors, and solar cells with attached six mil glass slips shall not exceed twelve pounds.
- The deployment mechanism shall be capable of reliable operation in the hard vacuum of space.
- Substrate surfaces shall be compatible with RTV-40 or similar cell bonding materials.
- The packaged array shall be capable of withstanding shock, vibration and accelerations such as might be experienced by arrays during launch.
- All materials shall be nonmagnetic, capable of withstanding radiations (including both ultra-violet and hard particles) experienced in space, and capable of withstanding humidity (up to 95% RH at $30^{\circ}C$ for twenty-four hours).
- The packaged arrays shall be capable of long-term (100 days) storage at temperatures which may vary from $-20^{\circ}C$ to $+60^{\circ}C$. They also shall be capable of withstanding hard vacuum conditions for extended periods (one to five years) without excessive deterioration.
- The extended array shall be capable of withstanding a thermal cycling test at 10^{-7} torr pressure from $-70^{\circ}C$ to $+70^{\circ}C$ for 1000 cycles at a nominal rate of two hours per cycle.

- Structure shall be capable of meeting the above condition without degrading the performance of the attached cells.

For the purposes of analysis the following guidelines have also been assumed.

- The satellite to which the panels attach will weight 110 pounds and be a homogenious three-foot diameter cylinder.
- There will be a total of four panels which will deploy radially from the center of gravity of the system.
- There will be no ground deployment fixtures for the panels nor any modification of the undeployed package dimensions unless it can be shown that a considerable improvement in the design is obtained.
- The array is not to be designed for any particular voltage or current but rather a general system of series-parallel connection is to be considered.

To arrive at a configuration FHC considered several designs of both flexible and rigid types. An elimination of all but two of each type was then performed based on a preliminary analysis and examination considering:

- Simplicity of design
- Structural integrity
- Ease of manufacture
- State-of-the-art materials
- Package Size
- Vibration characteristics

A more detailed design was then developed and analysed for each of the remaining concepts. A final selection was then made based on weight, volume, reliability and the criteria mentioned above.

It was found that the rolled flexible concept offers the greatest possibilities for future applications of small arrays, because it does offer more dense packaging than the rigid systems.

The application of the flexible concept to arrays larger than 8 square feet was not considered during the study, since this is beyond the scope of the program.

For the smaller payloads the flexible panel is generally best if packaged volume and weight are primary considerations. A rigid panel is best, however, for small payloads if the depth (four inches depth used in this study) is very small. The study has shown that for depths less than 1.50 inch diameter the flexible type is impractical because the small radius; (1) creates considerable bending loads on the rolled-up cells, and (2) increases the bend angle of the cell-to-cell connections.

The study has also shown that the most critical design requirement is the deployment under one "g" conditions. The gravity effect increases the weight of the extension mechanism and drive system. Some reduction in weight could be achieved by deploying the panel downward. This would tend to simulate the forces caused by spinning of the vehicle.

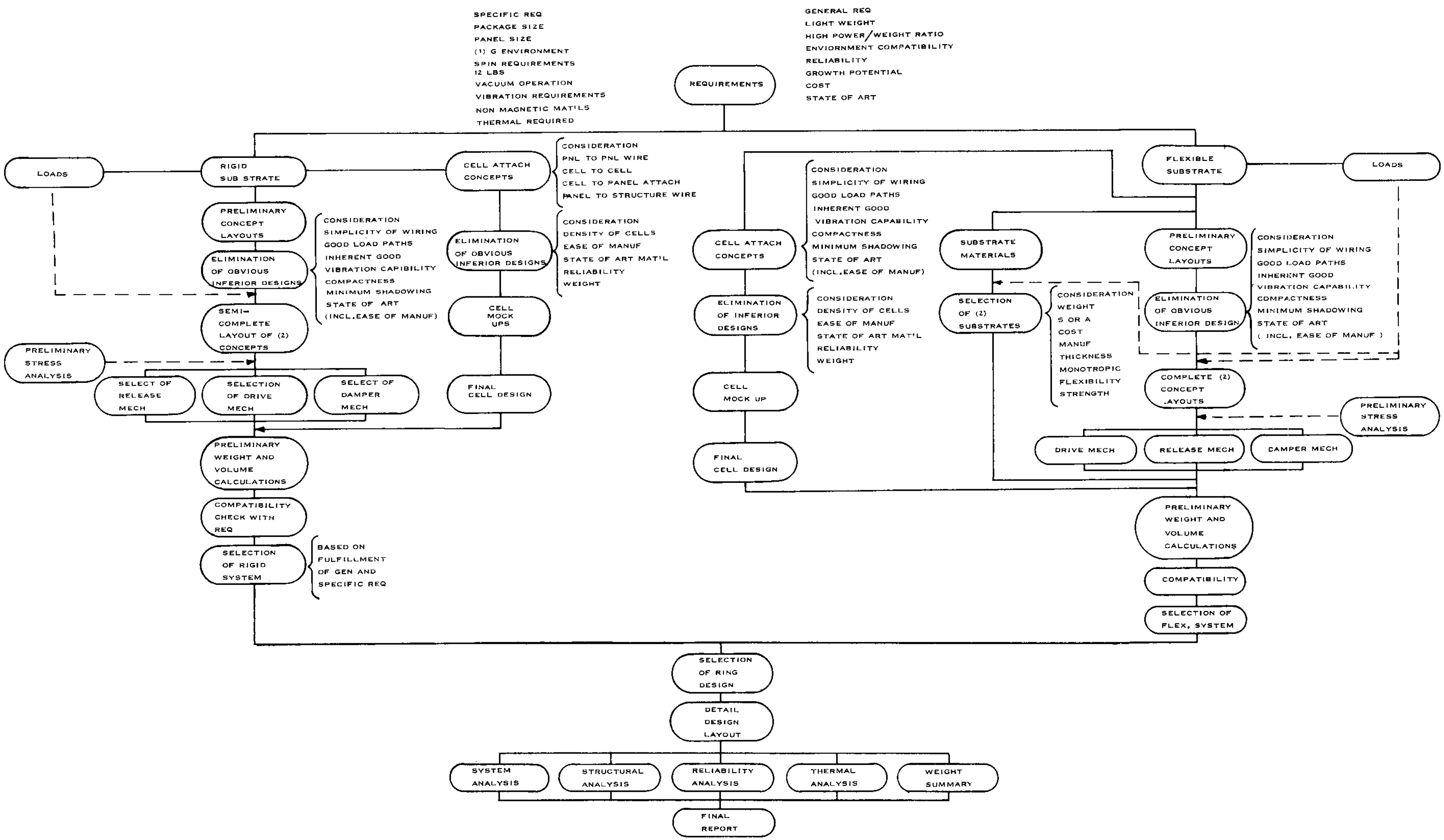

FIGURE 1.1 PROGRAM OUTLINE

2.0 DESIGN

2.1 INTRODUCTION

The deployable solar array design study has concentrated on developing an optimum system for deploying a one-foot by eight-foot array of solar cells from a minimum stored volumn. The design criteria used in the study is based on the guidelines covered in Section 1.0.

2.2 EXTENSION CONCEPTS ANALYSIS

There are $(2)^6 - 1 = 63$ different combinations of translation and rotation possible for each member of a mechanism deploying along any arbitrary path of the coordinate system shown in Figure 2.1.

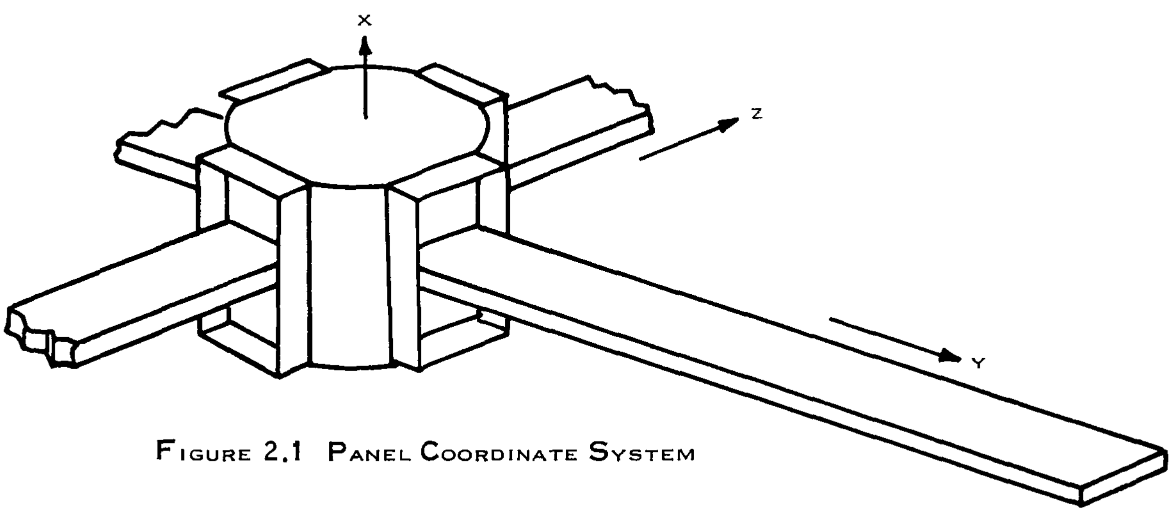

FIGURE 2.1 PANEL COORDINATE SYSTEM

For the design of the deployable array, however, certain restrictions are imposed that reduce this number considerably. They are:

- The center of gravity of the extension mechanism must remain in the z plane
- The panel must lie in a plane parallel to the x plane when fully deployed
- Panel size to be one-foot by eight-feet when deployed

- The dimensions of the extension mechanism package will be 13 by 25 by four inches or less
- The mechanism is to be as simple as possible.

The first restriction reduces the possibilities to $(2^5 - 1) = 31$ since any component of translation in the z direction will fall outside of the z plane. All seven combinations of pure rotation (ω) may be eliminated since the longest package dimension is much smaller than the largest deployed panel dimension, making a one piece panel obviously impossible.

It will also be noted that translation along the x axis alone is not a possibility. In addition, translation along the x axis and any combination of rotation is also impossible. Further, it is not possible to satisfy the restriction with only pure translation except along the y axis. Therefore, fifteen possibilities remain which will satisfy the conditions imposed upon the mechanism, but since simplicity is desired, those systems with three or less components of motion were found to be attractive. They are:

- r_y (Translation along y axis)
- r_y, ω_z (Translation along y axis, rotation about an axis parallel to z)
- r_y, ω_x (Translation along y axis, rotation about an axis parallel to x)
- r_y, r_x, ω_z (Translation in the z plane, rotation about an axis parallel to z axis)
- r_y, ω_x, ω_z (Translation along y axis, rotation about an axis lying in a plane parallel to the y plane).

Only these five concepts were studied.

For pure translation along the y axis only a self rigidizing device or a rigid sliding mechanism can be used. The self rigidizing type includes inflatable bags, inflatable bags with stressed stiffened skins, inflatable bags with hardening skins, inflatable bags with hardening cores, foam filled bags, extruded foams and plastics and bags with inflated cellular cores.

All of these rigidized systems were eliminated after a survey of the existing state-of-the-art. The more obvious objections to these systems are: difficulty in horizontal deployment under one "g" conditions, difficulty in demonstration of concepts that require special environments for deployment, high weight (especially the foam in place type), and high development cost. Possibly the greatest objection, however, is the inability to test flight hardware prior to launch.

Other r_y systems that were considered in this study are; 1) preformed metal tapes which assume some predetermined shape when deployed from a roll, 2) metallic or other thin sheets that can be taken from a roller or other storage device and fabricated into a stable section as it is being deployed, 3) thin sheets mechanically formed during deployment into a stable section, and, 4) rigid sliding devices including sliding pages, telescoping boxes, tubes or other shapes.

Mechanisms that translate along the y axis with a z component of rotation are scissors or linkages whose plane is normal to the z axis. Likewise, translation along the y axis with a component of x rotation are linkages lying in a plane normal to the x axis.

A parallel or other four-bar linkage lying in a plane normal to z can provide motion to guide an object along a path with both x and y translation and z rotation. (Steam shovels or back hoes are examples).

The last motion considered can be obtained from any plane linkage deployed in the y direction and lying in a plane canted at some angle to the x and y planes. None of the concepts chosen for further study used the latter motion, but it has possibilities if the solar panel is to be tilted with respect to the spin plane.

As a result of the foregoing analysis, several extension systems were conceived and are described in the following paragraphs.

2.3 CONCEPT DESCRIPTION

Following the development plan of Figure 1.1, the concepts are grouped in rigid substrate and flexible substrate categories.

2.3.1 Rigid Substrates

2.3.1.1 Configuration A (Half Scissors, Figure 2.2)

This configuration consists of four rigid panels hinged at their ends and deployed along the y axis (r_y motion). The deployment motion is controlled by links driven by screwjacks or other linear drive mechanisms mounted in the housing. Solar cells are mounted to both sides of the panels.

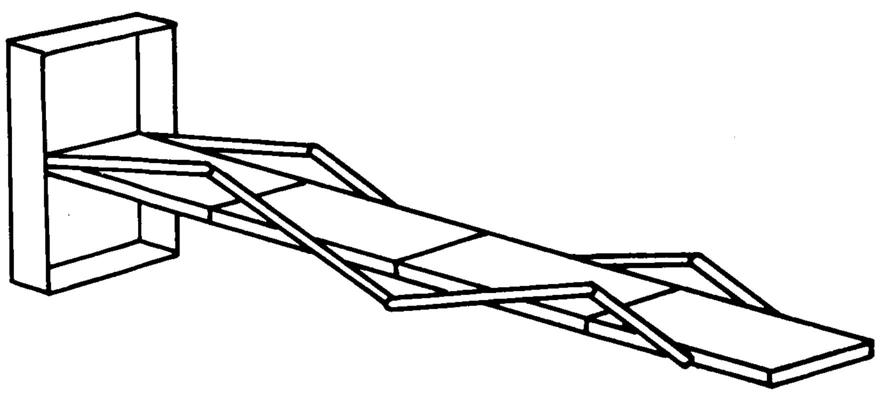

FIGURE 2.2 CONFIGURATION A (HALF SCISSORS)

2.3.1.2 Configuration B (Full Scissors, Figure 2.3)

The full scissors design is composed of two sets of hinged panels forming two solar array surfaces when deployed. The extension, drive damping and release systems are similar to the half scissor design mentioned previously. Cells are mounted only on the outer surfaces.

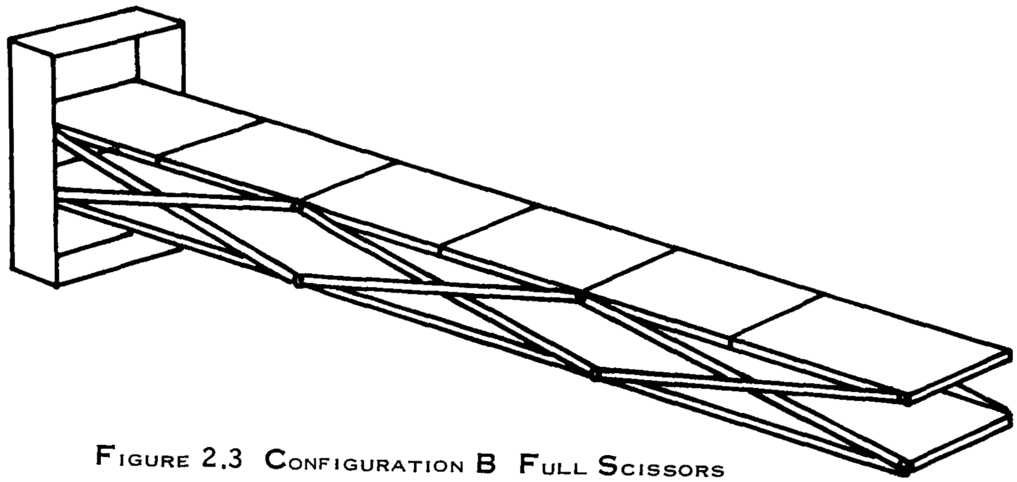

FIGURE 2.3 CONFIGURATION B FULL SCISSORS

2.3.1.3 Configuration C (Sliding Plate, Figure 2.4)

This configuration consists of three flat, solar cell covered plates sliding from a cell covered box. The box must initially be rotated upward 90° before deployment. The design of the slide connecting the plates is similar to that found in a filing cabinet.

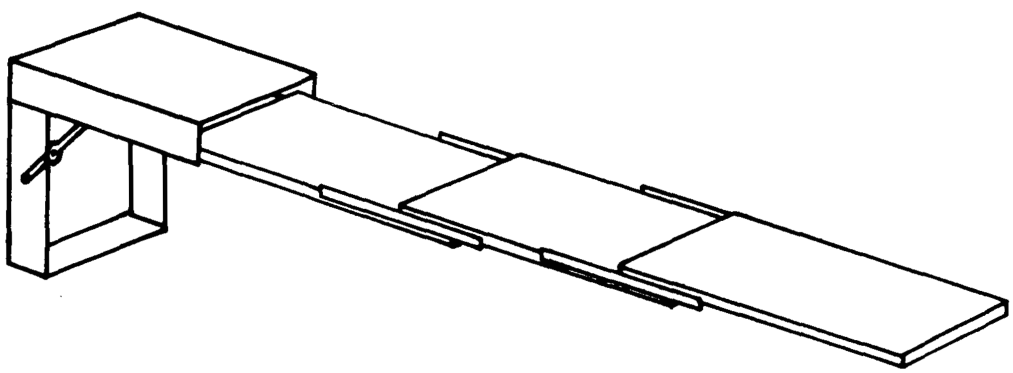

FIGURE 2.4 CONFIGURATION C (SLIDING PLATE)

2.3.1.4 Configuration D (Parallel Link, Figure 2.5)

This design consists of four cell covered plates connected by a set of parallel links. During deployment the plates rotate and translate outward from the housing to their final position. The drive system requirements would be similar to those of Configurations A and B.

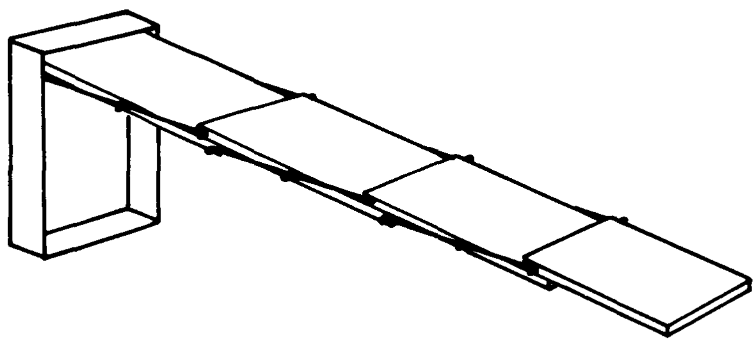

FIGURE 2.5 CONFIGURATION D (PARALLEL LINK)

2.3.1.5 Configuration E (Telescoping Box, Figure 2.6)

The telescoping box design is a series of progressively smaller cell covered boxes telescoping into each other. The deployment sequence requires an initial 90° rotation before the boxes can be extended. The drive is an inflatable bag within the structure.

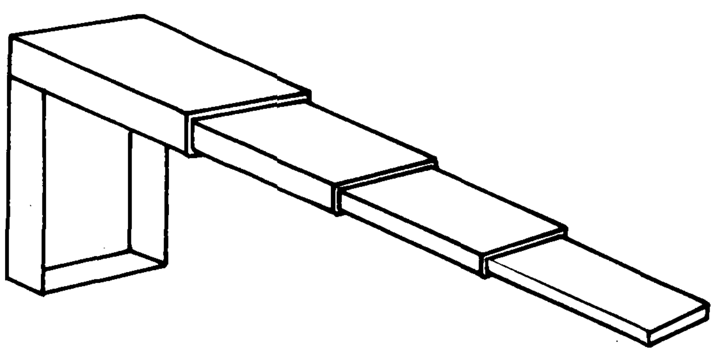

FIGURE 2.6 CONFIGURATION E (TELESCOPING BOX)

2.3.2 Flexible Substrates

2.3.2.1 Configuration F (Integrally Stiffened Substrate, Figure 2.7)

The stiffening of the substrate for this design is accomplished by preformed sheet metal tubes fastened to the back of a semi-flexible substrate. In the stowed condition, the tubes are flattened and wound on a roller with the cells and substrate. When deployed, the rods resume their original shape and stiffen the panel. Two substrates are required for this system and are attached to each other by a plate at their deployed ends. The rotation of the rollers is synchronized to insure uniform motion.

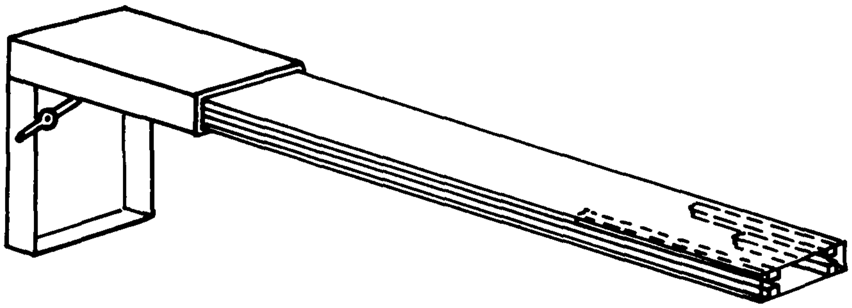

FIGURE 2.7 CONFIGURATION F (INTEGRALLY STIFFENED SUB-STRATE)

2.3.2.2 Configuration G (Sawtooth, Figure 2.8)

The sawtooth arrangement is a variation on the stiffener principle of the previous device. It consists of two preformed, curved, metallic substrates joined to each other at their edges by a series of interlocking tabs. In the undeployed configuration, the cells and substrates are wound on parallel, synchronized rollers. During deployment, a latching mechanism is employed to fasten the sheets to each other. This concept must first undergo a 90° positioning motion.

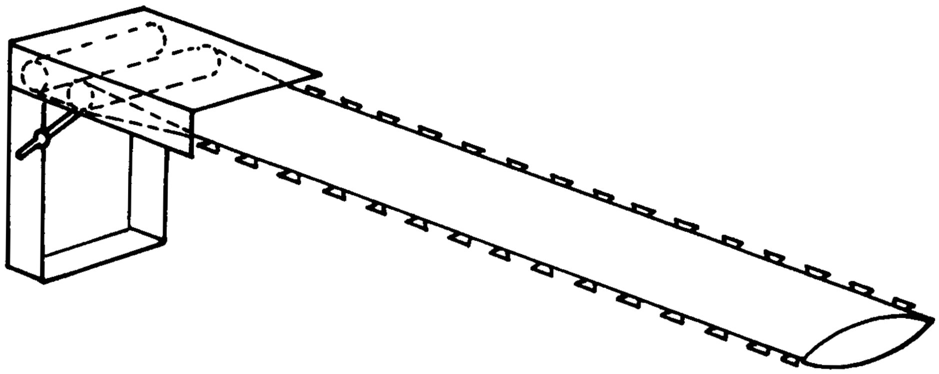

FIGURE 2.8 FIGURE 2.8 CONFIGURATION G (SAWTOOTH)

2.3.2.3 Configuration H (Scissor-Flexible Substrate, Figure 2.9)

This system employs a linkage similar to Configuration B to guide a set of flexible substrates from the rolls. It requires twice the number of links, because it is packaged within a space half as long.

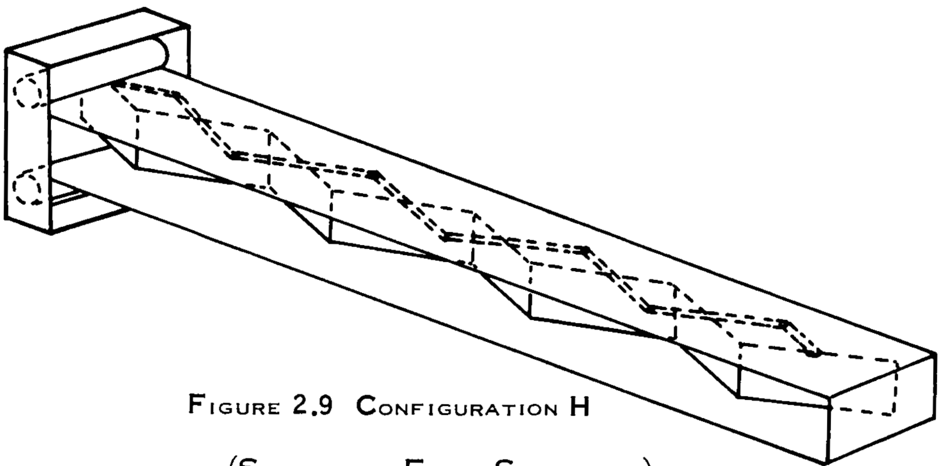

FIGURE 2.9 CONFIGURATION H

(SCISSORS - FLEX SUBSTRATE)

2.3.2.4 Configuration I (Telescoping Rod, Figure 2.10)

This method of deploying a set of rolled flexible panels uses a telescoping rod ejected from the end of a package initially rotated into position. The telescope lends itself well to a pneumatic erection system.

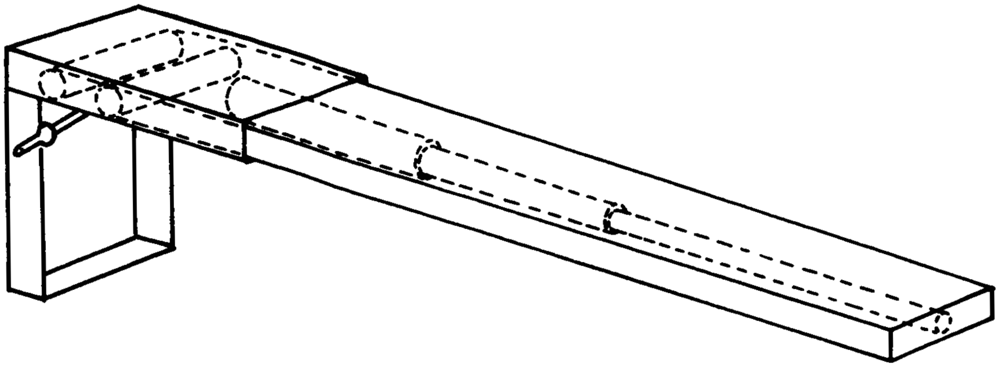

Figure 2.10 Configuration I (Telescoping Tube)

2.3.2.5 Configuration J (Telescoping Rail, Figure 2.11)

The telescoping rail system consists of two parallel sets of sliding rails joined by a cross member to make them an integral unit. In the stowed condition the rails nest inside each other. The package is rotated into position prior to deployment and then the rails are deployed, pulling the substrate with them.

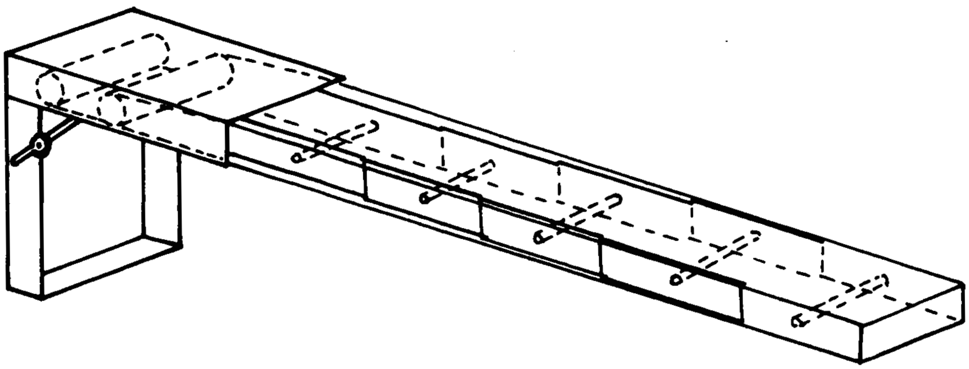

Figure 2.11 Configuration J (Telescoping Rail)

2.4 REDUCTION OF CONCEPTS

Since it was not practical to look at all of these concepts in detail, each design was considered for:

- Structural soundness
- Simplicity of the deployment mechanism
- Adaptability to possible drive/damper systems
- Compactness
- Vibration capability
- Reliability
- Ease of manufacture.

The concepts selected for further study were Configurations A, B, H,and I.

2.5 MECHANISMS

Only simple mechanisms were used in this study because of the requirements of state-of-the-art, high reliability, simplicity of operation, moderate cost, etc. It was also considered desirable to use devices previously proven successful for similar applications since this obviously cuts qualification and development time.

The deployable solar array mechanical system is made up of the following set of mechanisms shown in the sequence of utilization:

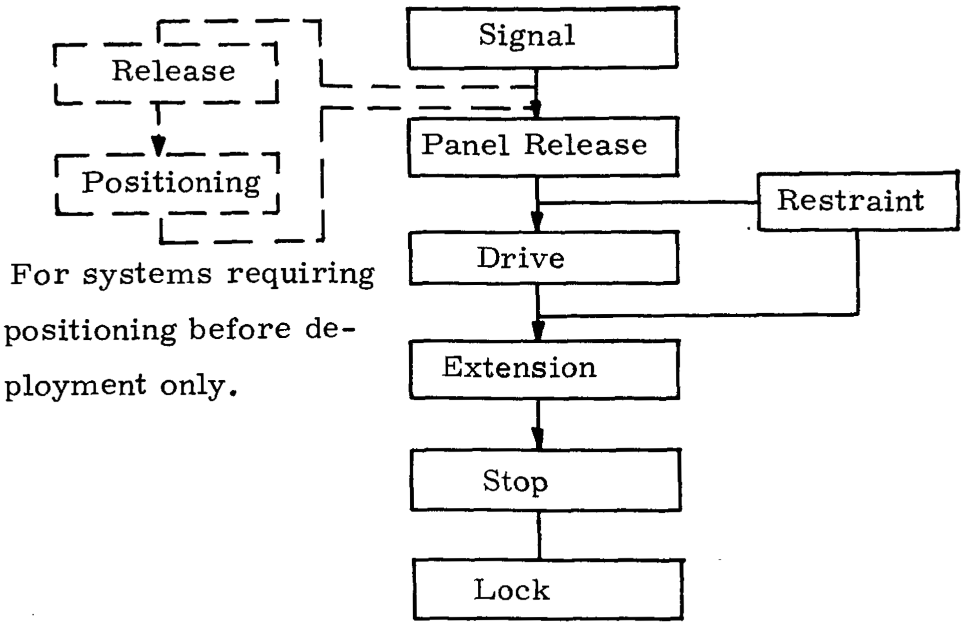

For systems initially rotated into position before deployment, an additional release and a positioning mechanism is required.

2.5.1 Release Systems

The requirements for a release system are compactness, fast reaction time, and production of high forces through a short distance. Since the input release signal from the spacecraft can be assumed to be electrical, the search can be limited to either a pyrotechnic device or an electrically driven motor or solenoid. The latter can be eliminated because of the non-magnetic material requirement imposed on the design. (It may be advisable however, to incorporate a re-usable solenoid or a motor for the proof-of-principle model). Some of the common pyrotechnics available are:

1. Pin pullers
2. Pin pushers
3. Cable cutters
4. Bolt cutters

5. Explosive nuts
6. Explosive bolts
7. Shaped charges
8. Pyrofuse

When dealing with solar cells and other delicate electronic equipment it is considered wise to stay away from those systems that tend to contaminate adjacent components. Therefore, all but self-contained reactions were eliminated. The weight and volume of release systems are generally a small percentage of the overall design. For that reason the design of this subsystem was delayed until the major systems were firm. The technique chosen was a redundant set of cable cutters that release the drive linkage and allow the substrate rollers to turn.

2.5.2 Drive System

The input signal to the drive system is mechanical, provided by the release system. The energy for deployment will be mainly kinetic energy resulting from spacecraft rotation. A survey of existing state-of-the-art driving systems points to storing the remaining required energy as a compressed gas, a gas generator, or in a mechanical spring. For deployment concepts chosen for further study, three are of a scissors or similar linkage system and will require a long straight motion for deployment. Of the energy storage methods discussed, only a piston or a tension spring can provide this type of motion directly. A motor spring or air motor will provide rotational motion which must be transformed into linear motion. This can be done with 1) a motor spring or air motor combined with a screwjack, or 2) a motor spring or air motor combined with a shaft upon which a slider is driven by a chain or cable system.

A similar driving motion is needed for the telescope arrangement, the difference between the two being that the motion of the telescope is perpendicular to the linkage drive and must be of a considerably longer stroke. A trade-off matrix of the selected deployment concepts and the drive mechanisms mentioned above is shown in Table 2.1.

From this matrix study, it was concluded that the motor spring/jackscrew drive system is most desirable for Configurations A, B, and H. The disadvantages of this system are 1) the low torque available, 2) the side loads on the screws and the gearing, and 3) the requirement for synchronizing mechanisms. Although it is not possible to eliminate these disadvantages completely, they can be overcome. The only need for torque on the screws is during static ground deployment tests since the rotation of the spacecraft provides the bulk of deployment energy. This will, however, produce slow deployment velocity during a non-spin condition. Side loading of screws in most cases is undesirable but since the loads are low, it was felt the selection is justified. Gearing and synchronizing devices are necessary for all the linkage concepts and, because they are compact, cannot be considered disadvantageous.

The pneumatic cylinder was the drive system chosen for Configuration I. Although this system requires extra components for gas storage, system control, and leakage, the required stored volume does not compromise the design. This is true because the telescoping rod does not package very efficiently and ample volume is available in the structure. The control subsystem will use highly reliable and redundant components. Leakage can be made acceptable by using an inert gas.

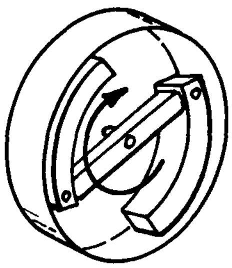 CENTRIFICAL BRAKE	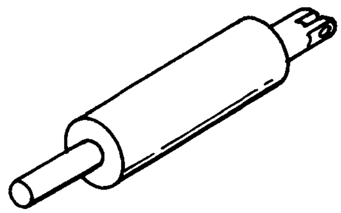 HYDRAULIC OR GAS CYLINDER	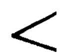
● MAY NEED GEAR TRAIN FOR SPEED INCREASE ● WIDE CHOICE OF ADJUSTMENTS AVAILABLE ● ADJUSTMENT SIMPLE ● WIDE SPEED RANGE ● OPERATING CHARACTERISTICS MAY CHANGE WITH ENVIRONMENTS ● REPEATABILITY PROBABLY GOOD FOR SAME OPERATING CONDITIONS ● SIMPLE PROVEN PRINCIPLE ● SMALL CONTAMINATION ● FORCE / VELOCITY RATIO IS GOOD ● SHORT DEVELOPMENT TIME ● COST SEEMS REASONABLE	● LEAKAGE MAY BE A PROBLEM ● RESIDUAL DRAG DUE TO CLOSE FITTINGS AND 'O' RINGS ● ADJUSTMENT DIFFICULT ● OPERATING CHARACTERISTICS MAY CHANGE WITH TEMP ● FOR ANY REASONABLE STROKE CYLINDER IS HEAVY ● SIMPLE AND PROVEN PRINCIPLE ● IT HAS DESIRABLE FORCE / VELOCITY RATIO ● DEVELOPMENT AND TEST MAY TAKE CONSIDERABLE TIME ● MODERATE COST ● NOT EASILY PACKAGED	● IF U SUB. OF (WIS ● REP USE ● OPE VAR ● ADJU OF T ● MAY OBT. ● APPI WEI ● HIGH ● NEE MEN ● FOR TOO ● MAT INEX

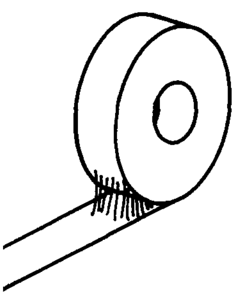

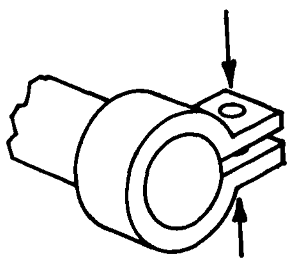

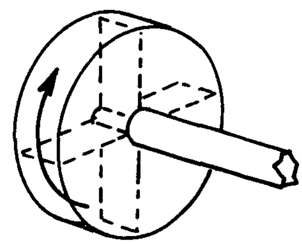

STICKTION TAPE	FRICTION BRAKE	FLUID COUPLING
SED AS PART OF ;TRATE WILL USE PART :OLLECTOR AREA, OTHER- : VERY COMPACT :ATABILITY AFTER LONG QUESTIONABLE RATION CHARACTERISTICS WITH ENVIRONMENT ISTMENT BY REPLACEMENT 'APE NOT BE ABLE TO AIN SUFFICIENT RESTRAINT :ARS TO BE VERY LIGHT 3HT STARTING LOADS) CONSIDERABLE DEVELOP- T TIME :E / VELOCITY RATIO NOT ATTRACTIVE ERIALS MAY NOT BE PENSIVE	● CHARACTERISTICS CAN VARY GREATLY WITH ENVIRONMENT ● VERY SENSITIVE TO CLAMPING FORCE ● HIGH STARTING TORQUE ● LOW WEIGHT ● REPEATABILITY MAY VARY DUE TO WEAR OR TEMPERATURE ● PROVEN SIMPLE DESIGN ● LOW CONTAMINATION ● MAY NEED GEARING FOR SPEED ● FORCE/VELOCITY CHARACTERISTICS NOT DESIRABLE ● SHORT DEVELOPMENT AND TEST SCHEDULE ● LOW COST ● COMPACT	● LEAKAGE MAY BE A PROBLEM ● DRAG OF SHAFT SEAL CAUSES HIGH INITIAL LOAD ● MAY NEED GEARING FOR SPEED INCREASE ● POSSIBLY TEMPERATURE SENSITI' ● DIFFICULT TO ADJUST ● REPEATABILITY MAY CHANGE WITI TEMPERATURE OF FLUID ● WOULD NEED CONSIDERABLE DEVE ● DESIRABLE FORCE / VELOCITY RATIO ● RELATIVELY HIGH WEIGHT ● STRAIGHTFORWARD DESIGN ● CONSIDERABLE DEVELOPMENT AND TEST TIME REQUIRED ● RELATIVE HIGH COST ● SATISFACTORY PACKAGING

TABLE 2.1

	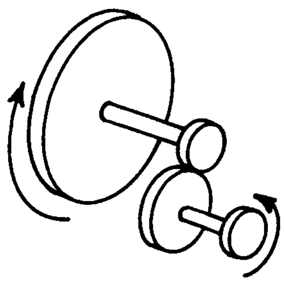 MOMENTUM WHEEL	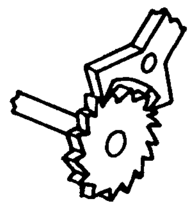 ESCAPEMENT
'E I -OPMENT	● MAY INTERFERE WITH THE DYNAMICS OF THE VEHICLE ● WILL NEED SPEED INCREASE ● WEIGHT MAY BE EXCESSIVE ● NEEDS BRAKE TO STOP WHEEL AFTER DEPLOYMENT ● ADJUSTMENT POSSIBLE ● LOW STARTING LOAD ● REPEATS ITSELF FOR ALL CONDITIONS ● WIDE SPEED RANGE ● SIMPLE, PROVEN DESIGN ● NO CONTAMINATION ● UNDESIREABLE FORCE / VELOCITY RATIO ● SHORT DEVELOPMENT AND TEST REQUIREMENTS ● LOW COST ● SATISFACTORY PACKAGING	● ONLY SLOW DEPLOYMENTS POSSIBLE ● EASY TO ADJUST SPEED ● INITIAL MOTION REQUIRED TO START THE BALANCE WEIGHT ● GENERALLY USED FOR LOW LOADS ● STRENGTH MAY BE A PROBLEM ● INTERMITTENT MOTION ● WEIGHT SHOULD BE COMPETITIVE ● PROVEN DESIGN ● VERY GOOD REPEATABILITY UNDER ALL CONDITIONS ● NO CONTAMINATION ● REASONABLE FORCE / VELOCITY RATIO ● DEVELOPMENT TIME COULD BE LENGTHY, TEST TIME PROBABLY SHORT ● MODERATE COST ● REASONABLE SPACE REQUIREMENTS

2.5.3 Damping System

The damping system controls the rate at which the solar panel deploys. The initiation of this system is mechanical and occurs when the drive system begins to function. Unlike the drive system, the damper system must dissipate energy rather than use it. This dissipation of energy can be achieved in several ways. It can be accomplished through friction, viscous flow, "stiction", or material damping.

For all of the deployment concepts selected for further study, the damper installation requirements were found to be quite similar. On the rigid type, the damper will be attached to the screwjack because of packaging considerations and will be a rotary damper. On the flexible concepts it is necessary to fasten the damper to the substrate roller to prevent the substrate from billowing outward during deployment. This also will require a rotary damper.

The advantages and disadvantages of each damper considered have been tabulated in Table 2.2. From this table, a damper was chosen based on the following desirable characteristics:

- Strength to take load
- Wide operating range
- Operating characteristics independent of environment
- Ease of adjustment
- Minimum weight
- Simplicity of design
- Reliability
- Proven principle of operation
- Non-contamination of adjacent mechanisms

DRIVE SYSTEM / EXTENSION CONCEPT	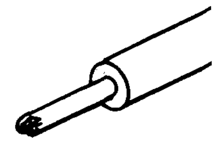 PNEUMATIC C
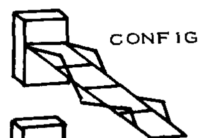 CONFIGURATION A 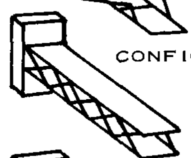 CONFIGURATION B 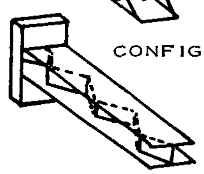 CONFIGURATION H	● CYLINDER NEEDS N 100% EXTENSION (T CYLINDER REQUIRE ● HIGH FORCE AVAIL ● WEIGHT HIGH DUE OF CYLINDER ● CYLINDER NOT A S ● DOES NOT PACKAGE ● DEVELOPMENT TIM ● COST MAY BE HIGH COMPLEX DESIGN A DEVELOPMENT TIM ● ADEQUATE REPEAT
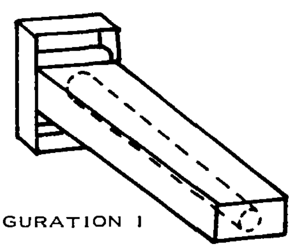 CONFIGURATION I	● TELESCOPE STRUCT USED AS THE CYLIN ● LARGE TENSION FOR APPLIED TO SUBSTR ● NO ADDITIONAL COS THAT FOR TELESCOP ● ONLY ADDITIONAL W IS FOR AUXILIARY S
GENERAL CONSIDERATIONS	● REQUIRES GAS STOR ● REQUIRES PLUMBIN AND CONTROLS ● MAY BE ENVIRONME (ESPECIALLY PRESS ● LEAKAGE MAY BE A ESPECIALLY IF PYR USED ● ADJUSTMENT EASY

 YLINDER	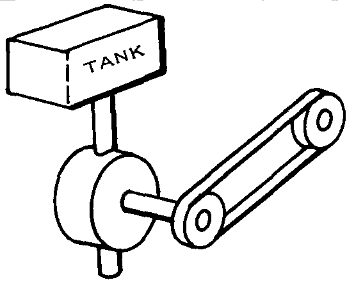 PNEUMATIC MOTOR - PULLEY AND CABLE SYSTEM (OR CHAIN AND SPROCKET)	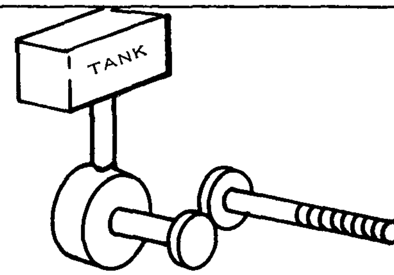 PNEUMATIC MOTOR - JACKSCREW	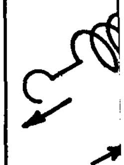
IORE THAN ELESCOPING D) ABLE O COMPLEXITY TANDARD ITEM WELL E MAY BE LONG DUE TO ND LONG E ABILITY	● MOTOR DOES NOT PACKAGE WELL ● RIGGING DIFFICULT TO PROVIDE SYNCHRONUS DRIVE ● CABLE SYSTEM NOT POSITIVE DRIVE ● HIGH TORQUE AVAILABLE ● GEAR REDUCTION MAY BE REQUIRED	● TWO SYNCHRONIZED SCREWS REQUIRED FOR ALL CONFIGURATIONS. ● GEAR REDUCTIONS MAY BE REQUIRED. ● JACK SCREWS MUST TAKE SIDE LOADS. ● MOTOR DOES NOT PACKAGE WELL. ● HIGH TORQUE AVAILABLE	● EXTE COMF TOO FAVO ● DOES ● NEED LINKA FOR AND ● NOT ● TENS NOT ● MODE
URE MAY BE DER CE CAN BE ATE T ABOVE IC STRUCTURE EIGHT REQUIRED UB-SYSTEMS	● DIFFICULT TO RIG CABLES AND PULLEYS IN SPACE AVAILABLE ● CHAIN SYSTEM NOT PRACTICAL ● MAY NOT REQUIRE SPEED REDUCER	● WOULD REQUIRE SEGMENTED JACKSCREW ● HIGH WEIGHT WOULD PACKAGE WELL ● FORCE LIMITED TO COLUMN STRENGTH OF SCREW.	● ADE PRO HEA ● CON
AGE , VALVES, NT SENSITIVE JRE) PROBLEM TECHNIC IS	● ADJUSTABLE ● OPERATING CHARACTERISTICS NOT INDEPENDENT OF ENVIRONMENT ● REPEATABILITY ADEQUATE ● PROVEN HARDWARE ● REQUIRES GAS STORAGE ● REQUIRES PLUMBING AND CONTROLS ● LEAKAGE AND EXHAUST MAY CONTAMINATE ● REASONABLE COST FOR MOTOR ● HIGH FORCE AVAILABLE ● LIGHTEST MOTOR AVAILABLE APPROXIMATELY .6LB. ● HIGH FRICTION IN SYSTEM	● ADJUSTABLE ● OPERATING CHARACTERISTICS NOT INDEPENDENT OF ENVIRONMENT ● REPEATABILITY ADEQUATE ● PROVEN HARDWARE ● REQUIRES GAS STORAGE ● REQUIRES PLUMBING AND CONTROLS ● LEAKAGE AND EXHAUST MAY CONTAMINATE REASONABLE COST FOR MOTOR ● HIGH FORCE AVAILABLE ● LIGHTEST MOTOR AVAILABLE APPROX. .6 LB.	● COMP HIGHL ● NO CO ● LOW ● ADJUS ● OPERA OF EN ● GOOD ● NON - ARE N EFFIC MODU

TABLE 2.2

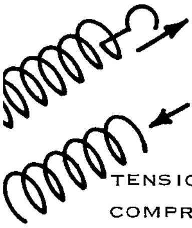 TENSION OR COMPRESSION SPRING	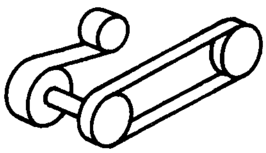 MOTOR SPRING – PULLEY AND CABLE (OR CHAIN AND SPROCKET)	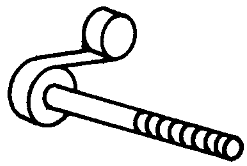 MOTOR SPRING– JACKSCREW
NDED LENGTH VS. RESSED LENGTH .ARGE FOR RABLE LOADS NOT PACKAGE WELL 3 ADDITIONAL .GE AND STRUCTURE YNCHRONIZATION .INK STABILITY. INIFORM LOAD. ON SPRINGS 'AIL SAFE RATE WEIGHT	● SPRING PACKAGES WELL ● CABLE RIGGING DIFFICULT TO PROVIDE SYNCHRONUS DRIVE. ● CABLE SYSTEM NOT A POSITIVE DRIVE	● SYNCHRONIZING MECHANISM REQUIRED. ● GEARING MAY BE REQUIRED ● JACKSCREWS MUST TAKE SIDE LOADS ● PACKAGES WELL
JATE SPRING TO JCE LOAD VERY (ENENT PACKAGING	● DIFFICULT TO RIG CABLES AND PULLEYS IN SPACE AVAILABLE ● CHAIN SYSTEM NOT PRACTICAL	● WOULD REQUIRE SEGMENTED JACKSCREW ● HIGH WEIGHT ● WOULD PACKAGE WELL ● FORCE LIMITED TO COLUMN STRENGTH OF SCREW. ● POSSIBLY LIMITED BY SCREW REVOLUTIONS REQUIRED ● HIGH FRICTION
RESSION SPRINGS Y RELIABLE NTAMINATION :OST TMENT DIFFICULT .TION INDEPENDANT VIORNMENT. REPEATABILITY MAGNETIC SPRINGS OT USUALLY AS IENT DUE TO LOW .ES.	● LOW TORQUE, WOULD PROBABLY NEED GEARING ● LIMITED ADJUSTABILITY ● LOW COST ● OPERATING CHARACTERISTICS INDEPENDANT OF ENVIORNMENT ● NO CONTAMINATION ● GOOD REPEATABILITY ● NON – MAGNETIC SPRINGS HURT EFFICIENCY. ● HIGH FRICTION IN SYSTEM	● LOW TORQUE, WOULD PROBABLY NEED GEARING ● LIMITED ADJUSTABILITY ● LOW COST ● OPERATING CHARACTERISTICS INDEPENDANT OF ENVIRONMENT ● NO CONTAMINATION ● GOOD REPEATABILITY ● NON – MAGNETIC SPRINGS HURT EFFICIENCY. ● HIGH FRICTION IN SYSTEM

- Unlimited angular motion
- Force at least proportional to velocity
- Non-Magnetic materials
- Short development and test time
- Reasonable cost
- Compactness

Except for uniform performance under different environmental conditions, especially vacuum, the centrifugal brake is the obvious choice. It is felt, however, that through testing, the performance of the device can be predicted with sufficient accuracy to insure its reliable use.

2.5.4 Stop and Locking Mechanism

Stop and locking mechanisms are generally very simple and their nature depends upon the individual configurations with which they are used. It was felt, therefore, that the detail design would be best covered on the final recommended design configuration on which it would be used, rather than perform multiple design efforts on the several possible configurations.

2.6 STRUCTURE

The purpose of the housing on the deployable solar array is to support the mechanisms and the substrate for vibration, spin, launch, and handling loads. The structure must be rigid enough to provide for deployment without binding of the mechanisms. The structure selected should be lightweight, state-of-the-art design that is relatively easy to manufacture. A minimum of dissimilar metals must be used to alleviate the problems of galvanic action and differential expansion. Materials for the structure must be non-magnetic, compatible with the space flight environment, and should possess a high strength-to-weight ratio. The most likely types of construction for the housing are sheet metal, machined parts, honeycomb, trussworks, laminated metals and plastics, or combinations of these methods. The following paragraphs list the considerations for selecting methods of fabrication.

Flat sheet metal spans are inadequate for vibration environments unless stiffeners are added. Machine bulkheads are made lightweight by elimination of overlap of webs and fittings and can be stiffened with intragal machined stiffeners. They are, however, relatively expensive. Honeycomb structure is generally light, but is sometimes difficult to attach to adjacent parts. As the housing of the array, it also consumes a great amount of space. Problems with truss works are usually found in lightweight joint design. The laminated structures require more expensive tooling.

The methods of fastening include: welding, which may cause distortion; bonding, which requires expensive tooling, but gives a uniform joint and is ideal for thin sheets; and mechanical fasteners, which include screws, bolts, rivets, and similar devices.

Considering these aspects of construction, structures for the four configurations studied were chosen. For Configurations A and B (four inches by thirteen inches), the ends of the structure will be machined parts or sheet metal with attached fittings. The sides will be honeycomb or stiffened sheet metal with lightening holes or truss type cutouts. The back will be cutout honeycomb or possibly a sheet metal stamping. A hold-down plate partially across the open front will be required as part of the release system. This will be a honeycomb or stamped sheet metal panel.

Construction of Configuration H employs machined end plates similar to A and B. Material for the sides and back are stamped sheet metal stiffened with lightening holes and/or beads. The hold-down strap or plate across the front of the box will be also a stiffened sheet.

For Configuration I, the construction chosen was machine parts in the area of the rollers and gears with the rest of the side panels of stiffened sheet metal. The 25 inch x 13 inch dimension on the box will be stiffened sheet metal or fiberglass reinforced plastic. The end cap of the box which attaches to the telescope will be sheet metal. The preliminary weights and volume for these four configurations were used for the trade-off study and are tabulated in Table 2.3.

2.7 SUBSTRATE DEVELOPMENT

As noted in Figure 1.1, the design of cell attachment follows two courses; attachment to rigid substrate, and attachments to flexible substrate. Work on the rigid type will be discussed first.

2.7.1 The stated objective of the study is to arrive at a general series-parallel cell connection. From previous development, FHC has found the "Z" bar concept shown in Figure 2.12 to be the most satisfactory design and therefore the study was limited to this concept. The gaps between cells are in the 0.01 to 0.02 range.

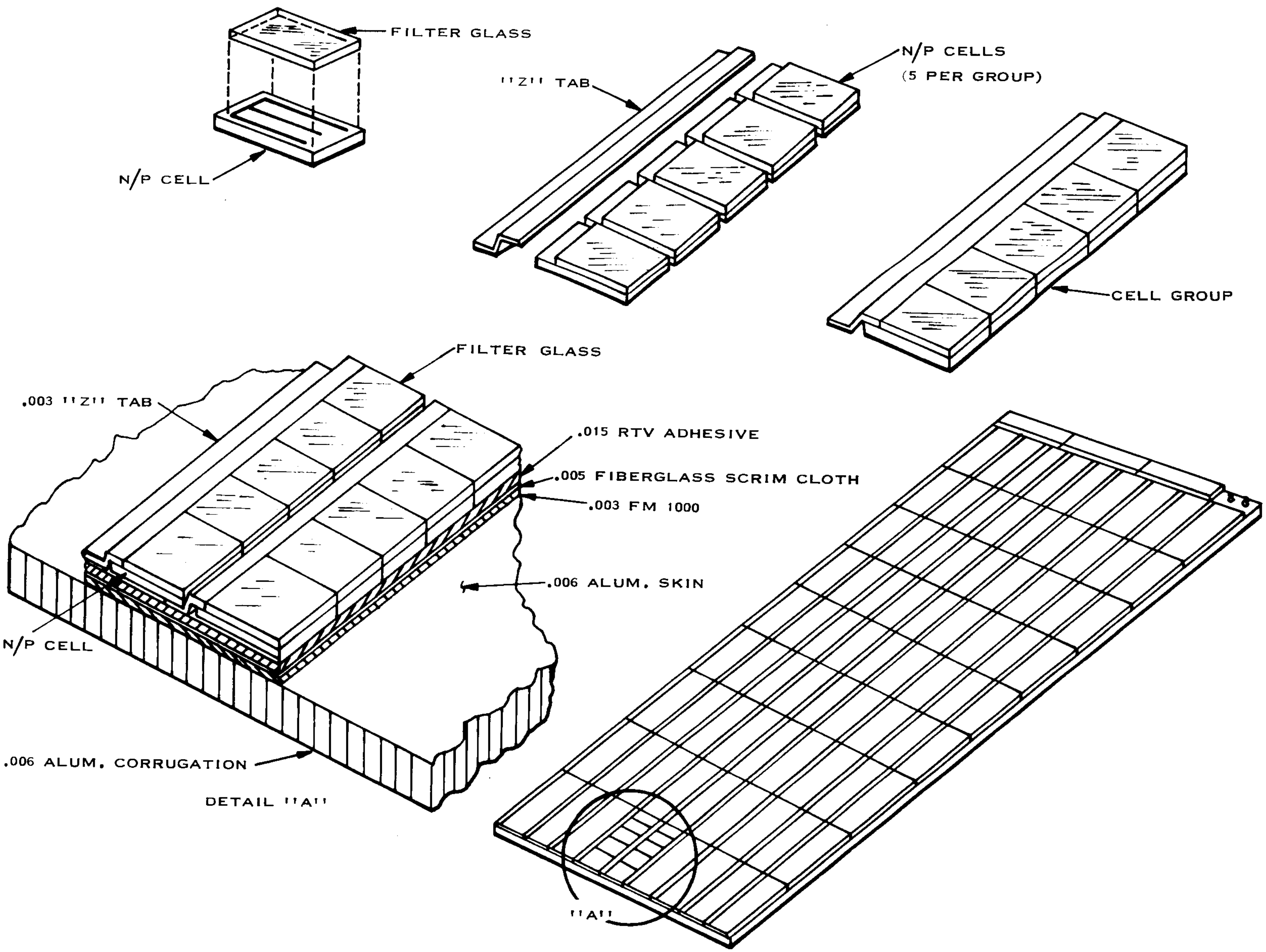

FIGURE 2.12 SOLAR CELL GROUP LAY DOWN

Materials examined for the Z bars have been thin metal foil of 2% silver content, pure silver, and brass. To date the 100% silver has proved most favorable. The solder found to give the best results is a lead-tin-silver (2%-5%) alloy.

A fabrication technique developed for the rigid substrate has been abstracted from our previous in-house work and is described in the following paragraphs.

Groups of solar cells, selected in accordance with dimensional tolerance requirements for a specific cell grouping, are placed in a locating and soldering fixture. A preformed, pre-cut photo etched 0.003 inch silver "Z" tab and a 0.003 inch silver ribbon conductor are located in the fixture in position for soldering to the bottom surface terminals of the solar cells. The ribbon conductor and the "Z" tabs are soldered to the solar cells, using a lead-tin-silver (2%-5% silver) solder.

The resulting cell grouping (Figure 2.12) is the fundamental element used in application of the solar cells to the module substrate. The "Z" tab acts as the common terminal for subsequent electrical connection of the cell grouping to other similar elements. The ribbon conductor lends mechanical stability to the grouping and also provides the means of electrical connection between the end elements in adjacent rows of elements. As part of the fabrication procedure for the module structural substrate, a 0.030 lb/ft^2 film of FM-1000 adhesive (including scrim cloth) is bonded to the skin of the substrate to provide a dielectric and mechanical barrier between the solar cells and the substrate. This approach entirely eliminates the necessity for a subsequent dielectric/mechanical coating sequence and greatly reduces the probability of damage to the bonded substrate.

The module structural substrate is then mounted in the bonding fixture. The FM-1000 coated surface is cleaned (solvent wipe) and primed (A4004) for silicone adhesive. Catalyzed RTV-40 silicone adhesive is then applied onto the primed surface to the prescribed depth. A 0.005 inch glass fabric scrim cloth, impregnated with RTV-40 silicone adhesive is then laminated onto the uncured adhesive layer previously applied. The scrim cloth serves as an additional barrier to short circuiting between solar cells and substrate and improves the silicone adhesive tear resistance.

Final adjustment of the now reinforced adhesive layer is performed to remove any trapped air and to achieve the desired adhesive thickness. Cell groupings, which have been checked for adequacy of functional performance, are ultrasonically cleaned preparatory to bonding. Using a locating and aligning fixture, the cell groupings are placed in position on the adhesive coated surface of the module substrate and seated in the adhesive by application of modest pressure. The adhesive is allowed to cure at room temperature under this pressure to assure positive bond surface contact. Upon completion of adhesive cure, any excess is removed mechanically. Electrical connection between cell groupings is made via the "Z" tabs or ribbon conductors as appropriate, employing the same soldering procedures used in fabricating the cell groupings. The assembly is now checked for adequacy of functional performance.

Cover glasses for the solar cells are ultrasonically cleaned and the surfaces of the solar cells are cleaned by means of a light solvent wipe. Cover glasses are prefitted and then applied to the solar cells and held under modest pressure until the adhesive is cured. The entire assembly is then carefully wrapped with polyethylene sheeting to protect all surfaces prior to final assembly. Figure 2.13 is a photograph of this development.

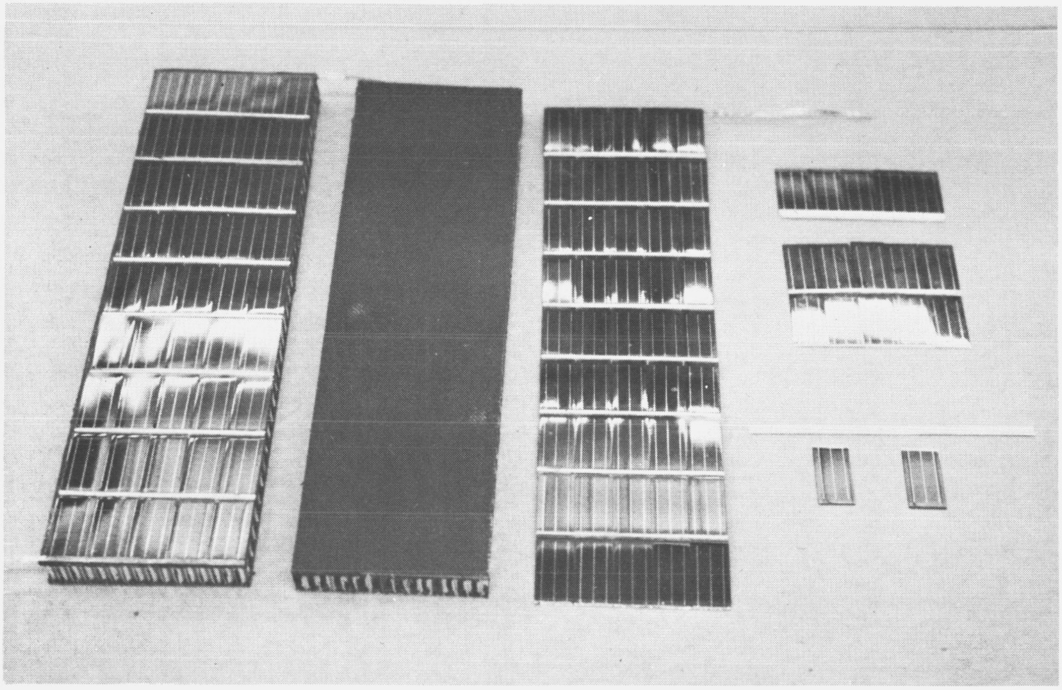

Figure 2.13 Rigid Substrate Development

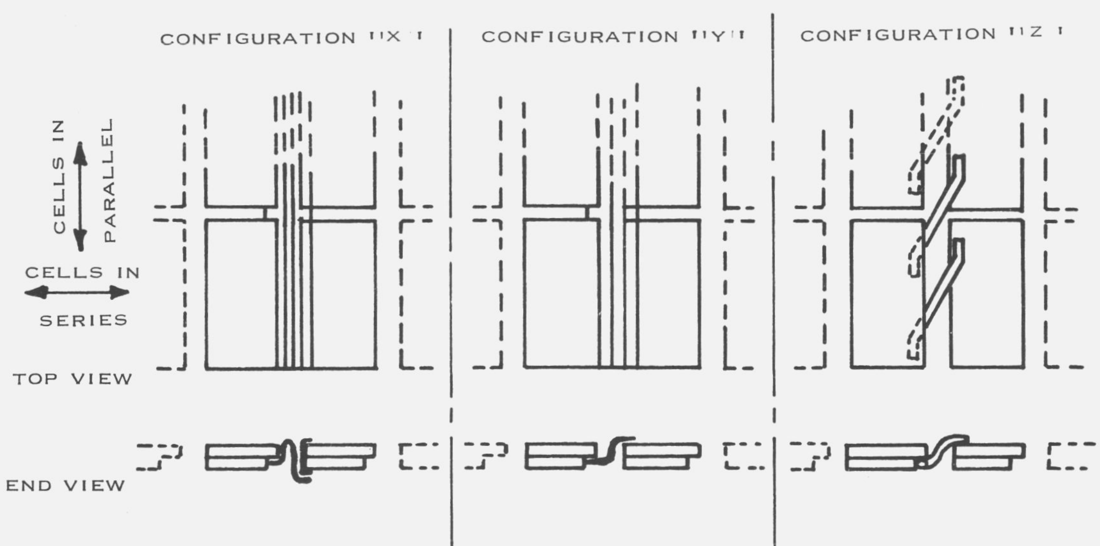

Figure 2.14 Three Experimental Configurations For Inter-cell Connection in a Series - Parallel Arrangement

2.7.2 Development of Flexible Arrays

It has been determined that in addition to those requirements of Section 1.0, a practical flexible solar cell array must be flexible only in one direction, and possess tensile strength sufficient to sustain the necessary loads during deployment. In addition, the electrical interconnection of the cells (in the deployment direction) must be capable of flexing through an angle of approximately 45° and permit the closest feasible spacing of solar cells. To satisfy these requirements, consideration has been given during the development effort to the details of design, materials selection, fabrication feasibility, and functional reliability of a practical flexible solar cell array for spacecraft. These studies are described in succeeding paragraphs.

In order to assess some of the practical manufacturing aspects of the flexible solar cell array, development work was undertaken which resulted in the fabrication of several small arrays. These items have served to demonstrate clearly the feasibility of the selected design concepts as well as to provide information for materials selection and fabrication methods.

Various design configurations were considered, each of which met, to some degree, the basic requirements. From the fabrication standpoint, the most important design concept proved to be the inter-cell electrical connection. Three configurations were selected for trial. Small arrays were then made using two of them. Soldered inter-cell connections were made in each case. The three designs are shown in Figure 2.14.

2.7.2.1 Substrate Concepts

Configuration X employs a hat-section made of 0.001 inch brass or 0.0015 inch beryllium - copper foil, which was termed a hinge strip. Both of these materials were used successfully. The photograph of Figure 2.15 shows the detail parts and the completed sample solar cell array made using

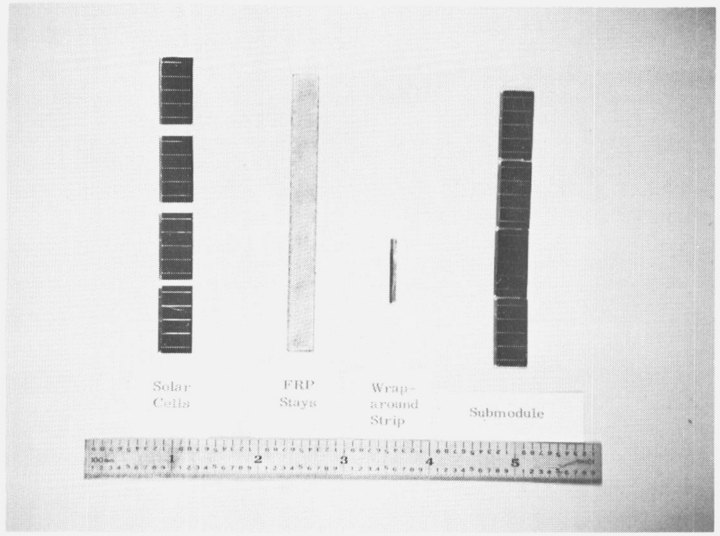

(A) Components of Submodule

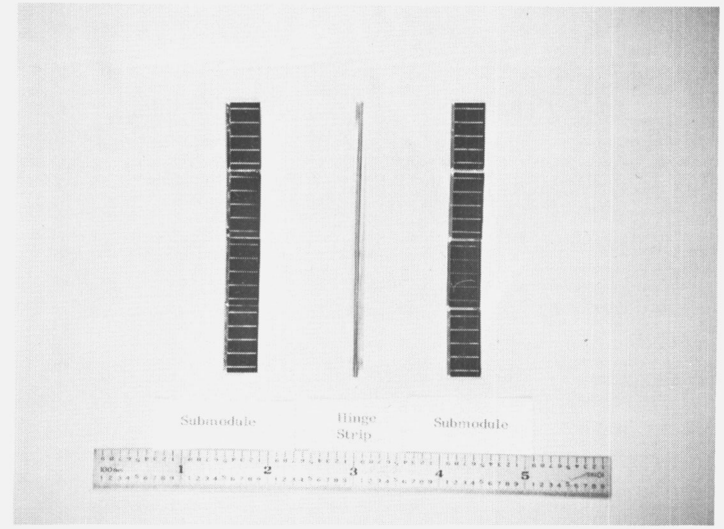

(B) Interconnection Parts

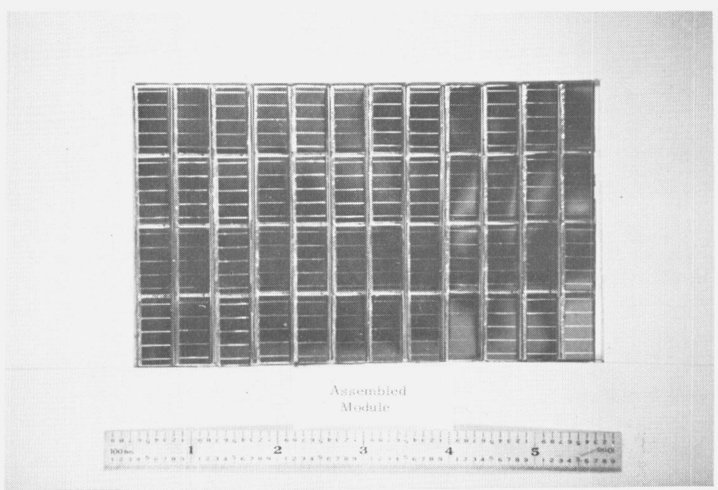

(C) Assembled Module

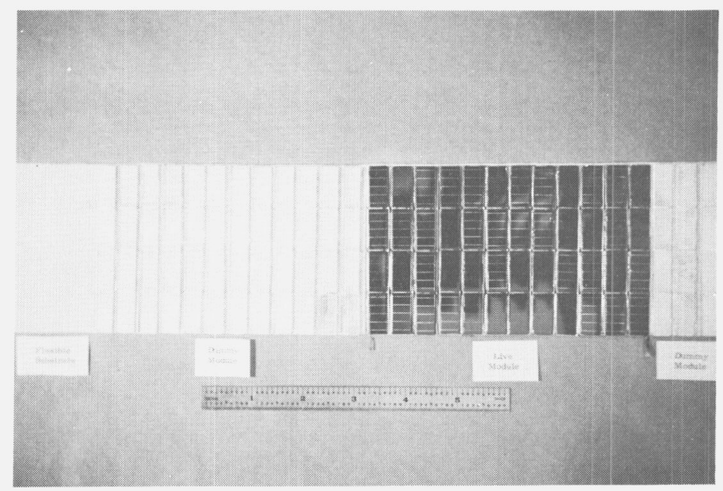

(D) Completed Sample Array

Figure 2.15 Photographs Illustrating Steps in Fabrication of Sample Solar Array

Configuration X. Each row contains four cells connected in parallel by the hat section hinge strips; the latter also connects adjacent rows in series.

Two flexible substrate materials were used in combination with the hat section hinge strip. These are silicone rubber impregntaed fiberglass fabric and mylar film. Both substrates were functionally satisfactory.

Since solar cells having both terminals on the bottom face were not available a brass "wrap-around" strip was soldered to each cell. This is shown by the sketch in Figure 2.16.

Configuration Y consists of a "Z" section strip made from fine-weave brass wire cloth. This material is flexible and the strips are bias cut in order that the action on the individual wires during roll-up and deployment will consist of torsion, in part, rather than bending only. This concept proved to be useless because the fine weave of the cloth prevents the individual wires from twisting. The very fine mesh wire cloth was most difficult to solder properly because it acted as a wick to the liquid metal, decreasing its flexibility. After experimenting with two sizes of wire cloth (60 mesh and 200 mesh), this configuration was abandoned.

Configuration Z proved easy to fabricate. It consists of wire connections between cells. The small soldered wires connect the N terminal of a given cell to the P terminal of a cell in the adjacent row, as shown in Figure 2.14. An unsuccessful attempt was made to use soft-temper flexible stranded wire, but wicking of the liquid solder occurred. The short pieces of the wire also tended to become unstranded during handling. Two kinds of wire, solid 0.020 inch diameter silver coated soft copper wire and 0.016 inch diameter cupro-nickel wire (Driver Co. Alloy 180), were used successfully.

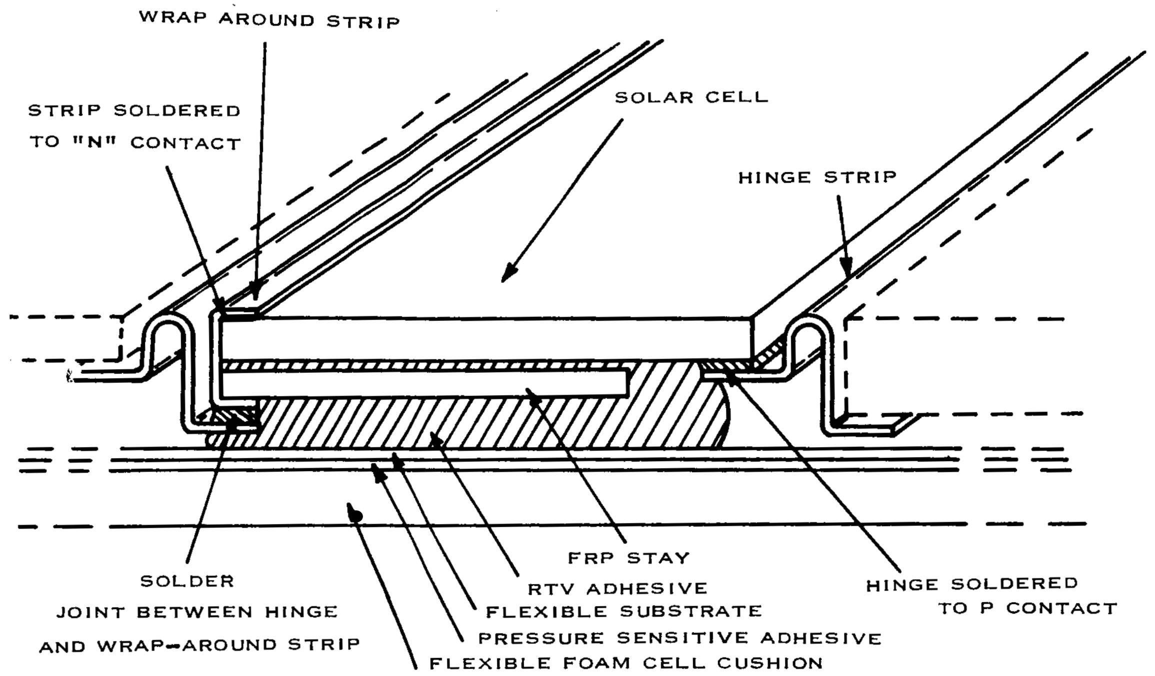

FIGURE 2.16 CONFIGURATION FOR ATTACHING SOLAR CELLS TO SUBSTRATE

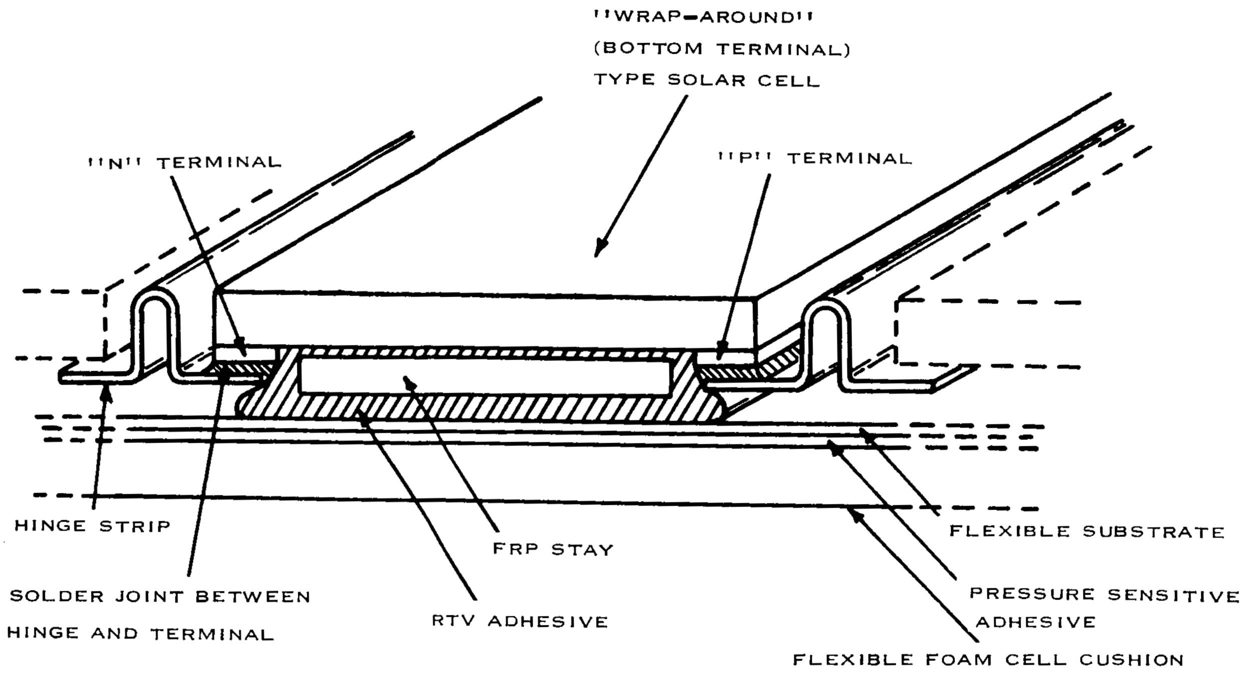

FIGURE 2.17 CONFIGURATION FOR ATTACHING WRAP-AROUND TYPE (BOTH TERMINAL CONTACTS ON BOTTOM) SOLAR CELLS TO SUBSTRATE

A sample-size solar cell array, similar to that shown in Figure 2.15 was constructed by using the wire-type inter-cell connection, but appears to be less desirable than hinge strip connection in at least two significant respects. Configuration Z array is not as flexible, will not bend around the roller as readily, and the wires are yielded by the rolling-up action causing possible fatigue. Less cell-to-cell spacing was found to be required for Configuration Z. It was concluded that Configuration X was the most desirable of those investigated.

2.7.2.2 Description of Configuration

The configuration selected for additional studies is an arrangement of solar cells bonded to an epoxy-fiberglass laminate which is in turn bonded to a mylar film substrate (Figures 2.15 and 2.16). "Wrap-around" cells shall be used on this design. The terminal for the N layer is brought down over the edge and onto the bottom of the cell, producing both an N and a P terminal on the bottom. If this cell is not available, a conventional cell can be converted by means of a brass channel soldered to the top terminal strip, wrapped over the edge of the cell and the fiberglass stiffening member, and then bonded to the bottom of the fiberglass laminate. The electrical connections use a beryllium - copper "hinge" strip connecting the P layer of one row of cells to the N layer of the adjacent row. This hinge makes a parallel connection between cells in a row and makes a series connection between rows. In addition to providing electrical contact between rows, the beryllium copper hat sections supplements the stiffness provided by the epoxy-fiberglass strips. The hat section shape was also chosen to provide the flexibility necessary to wrap the array onto a small diameter roller.

A thin sheet of flexible foam is attached to the side of the flexible substrate opposite the solar cells. This foam has a pressure sensitive adhesive film on one side which allows attachment to the substrate.

2.7.2.3 Flexible Substrate Material Selection

Three materials were considered for this application: Silicone rubber coated glass fabric, mylar, and a polyimide film (H-film). All give good service in the space environment because the outer surface of the flexible substrate will be covered with the solar cells and their supports. Sample arrays were fabricated using both the mylar and the silicone rubber. The silicone rubber coated fabric is much heavier than either the mylar or the H-film. Although the H-film is slightly more stable in the space environment than the mylar, it was not available to be used in the sample substrates during Phase I of the program.

2.7.2.4 Solar Cell Stiffener

It was determined that the solar cells should be supported normal to the direction of the array deployment and in the plane of the array by a rigid member approximately the width of a solar cell to decrease the bending stress in the cell while rolled. The material used for this member must be non-magnetic and preferably non-conductive.

The various metallic materials investigated included aluminum, magnesium, beryllium copper, beryllium, and titanium. The beryllium stiffener is the lightest structure for a given thickness. However, its cost and toxicity were considered to be too undesirable to allow practical application to the design.

Although metallic materials result in the lightest weight for the stiffeners, it was tentatively decided that epoxy-fiberglass should be used for these members. This decision was based on the non-conductive properties of the material as well as Fairchild Hiller's experience in the fabrication of thin glass laminates. The use of the non-conductive material reduces considerably the possibility of shorting and eliminates the necessity for the additional insulation barrier normally provided. The use of the fiberglass laminate permits direct bonding of the cell to the stiffener without the rubber impregnated fabric generally used.

Figure 2.16 shows the relationship of these stiffeners to the solar cell array.

Figure 2.15 (a) shows the solar cells about to be bonded to the stiffener.

2.7.2.5 Solar Cell Interconnects

Intercell connection is accomplished with beryllium copper foil formed into a hat section. One sample array was fabricated using brass foil and another using beryllium copper foil. Although the former performed satisfactorily, beryllium copper was a slightly better selection because of bending stiffness and fatigue life.

Figure 2.16 shows the configuration of these solar hinge strip interconnects.

Figure 2.15(b) shows the hinge strip about to be attached to two solar cell submodules.

2.7.2.6 Solar Cell Cushion

In order to protect the individual layers of the cells from vibration damage and abrasion when in the stowed condition on the roller, a thin layer of flexible urethane foam is interleaved between layers. The flexible foam is obtained with a pressure sensitive adhesive backing for attachment to the flexible substrate. See Figure 2.16 for descriptions of this installation. Figure 2.15(d) shows the solar cell array with the flexible foam attached to the substrate.

2.7.2.8 Manufacturing Plan - Solar Cell Array

The solar cell stiffeners are fabricated using epoxy resin (MIL-R-9300) and 181 glass fabric (MIL-P-9084). The laminate is cured in an autoclave at approximately 100 psi and 350^{O}F. After cure the laminate is cut into strips approximately one cm wide and twelve inches long.

The solar cells are then bonded to the fiberglass stiffeners using General Electric RTV-40 silicone rubber adhesive. The fiberglass stiffeners and the bottom surface of the solar cells are primed with SS-4004 silicone primer prior to application of the RTV-40.

If wrap-around solar cells are not available, standard solar cells shall be reworked per Section 2.7.2.2.

Cover glass is bonded to the solar cells using LTV 602 adhesive. When this adhesive has cured, the cover glass is then coated with a stripable coating for protection during the following assembly operations.

Hat section solar cell interconnects are formed from pretinned beryllium copper 0.001" strip and soldered to the bottom terminals of the solar cells using 60/40 solder. The cells are positioned such that the interconnect joins N and P layers of adjacent rows of cells - thus affording a series connection between rows - and a parallel connection of cells in the same row.

The row of cells is then bonded to the flexible substrate using RTV-40. The under surfaces of the row and the substrate are primed with SS-4004 silicone primer before application of the RTV-40.

When the joint between the row and the substrate has cured, the flexible foam is attached to the inner surface of the substrate.

After assembly of the completed solar cell array onto the take up roller and attachment of the extension mechanism, the stripable coating is removed from the cover glass and an isopropyl alcohol wash given the entire array.

2.7.2.9 Test Performed on Experimental Arrays

A test apparatus was constructed which permitted a simulated deployment test to be performed on the three experimental arrays. This apparatus is shown in Figure 2.18. It consists of a 1.5 inch diameter roller onto which

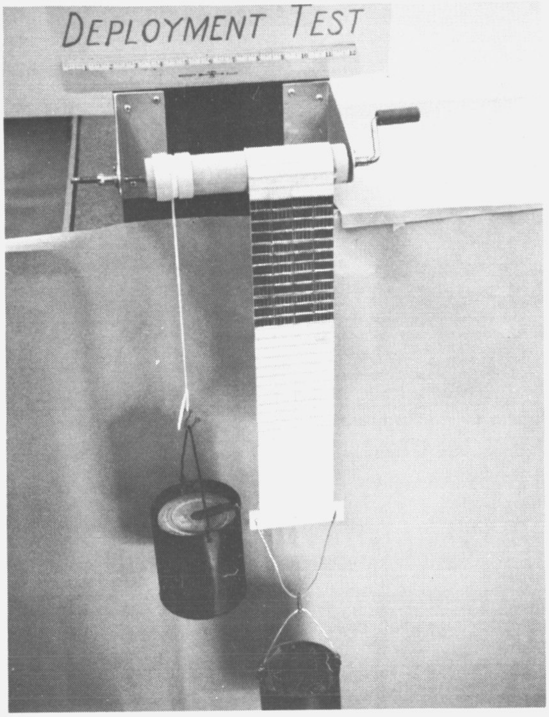

FIGURE 6(A) UNROLLED POSITION

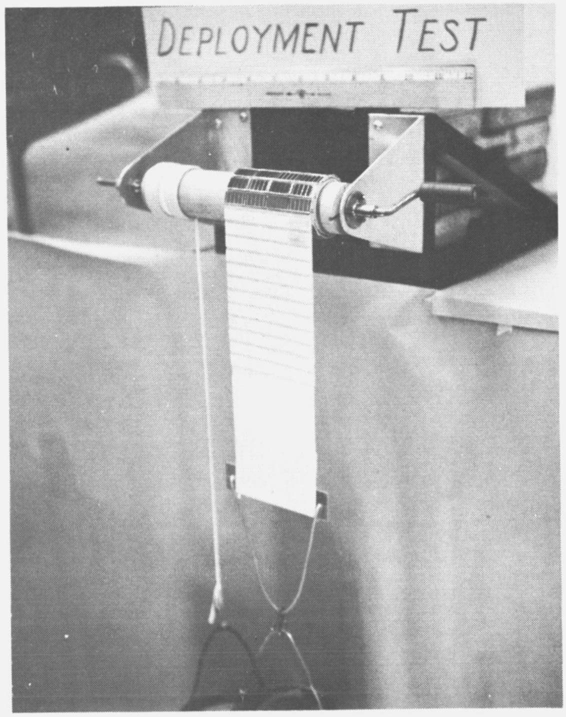

FIGURE 6(B) ROLLED UP POSITION

FIGURE 2.18 PHOTOGRAPHS OF SIMULATED DEPLOYMENT TEST APPARATUS FOR EXPERIMENTAL SOLAR CELL ARRAY

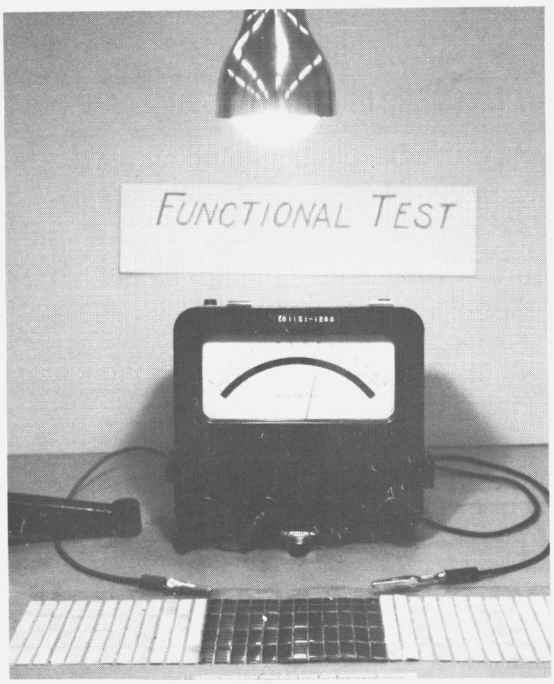

FIGURE 2.19 PHOTOGRAPH OF TEST APPARATUS USED TO DEMONSTRATE THE FUNCTIONAL CAPABILITY OF THE EXPERIMENTAL SOLAR CELL ARRAY

the array was repeatedly wound and unwound. The substrate was made to support a 10 pound static load throughout the simulated deployment. The additional weighted container shown in Figure 2.18 was used to counter-balance the rotational force. A digital counter was used to indicate automatically the number of simulated deployment cycles.

The simulated deployment test was performed 500 times on each of the three experimental solar cell arrays fabricated. All three arrays withstood the 500 cycles of deployment without serious physical effects caused by the test itself. Certain defects which were already present on the cell inter-connectors appeared to be accentuated by the flexing. Because the brass hinge strips were hand formed, they sustained some damage where efforts were made to produce sharp radii in the hat section with sharp-edged tools. These defects were noted beforehand. Nevertheless, it was deemed advisable to proceed with the cyclic deployment test since the cell modules functioned quite satisfactorily. Two small cracks were noted on the beryllium-copper hinge strips in the array fabricated with that material. These defects appeared to be slightly aggravated by the deployment test. A third crack appeared after 100 cycles in the test. However, it may be expected that either brass or beryllium-copper may be formed with the aid of more suitable tools into hinge strips that will be free of cracks and will perform satisfactorily in repeated deployment tests. The wire connectors in the third array were not damaged in the test. In spite of the apparent relative inflexibility of this array, the 10 pound force on the 3.25 inch wide substrate was quite adequate to straighten the array completely during each deployment cycle.

There appeared to be no significant difference in the performance of the two substrates used, 0.002 inch thick mylar film and 0.010 inch thick silicone rubber impregnated fiberglass. Both were quite satisfactory.

A simple test was devised to demonstrate that the solar cell arrays functioned properly both before and after the cyclic deployment test. It consisted of a light source and a d-c output voltmeter as shown in Figure 2.19. In each case the position and distance from the light remained fixed. A light meter was used to ascertain that the incident energy remained substantially constant. In all cases the experimental solar cell arrays functioned equally well after sustaining 500 cycles of deployment as they did before the latter test.

2.8 TRADE-OFF DISCUSSION

Following the outline of Figure 1.1 the trade-off will first select a flexible substrate design and then a rigid substrate design. A selection will then be made between the flexible and rigid substrate.

For this trade-off, only weight, occupied volume, reliability, cost and power-weight ratio need be considered since all of the configurations meet the specifications stated in Section 1.0. The rigid substrate has arbitrarily been taken for evaluation first. These are configuration A and configuration B.

For configuration A the power-weight ratio is affected by the total weight of the structure, the packaging efficiency of the cells and a shadowing factor due to the drive links. This shadowing factor has been determined as 3% for the worst shadowing condition. The same factors, except shadowing, affect configuration B. In addition, configuration B has twice the number of substrate hinges which cut down the total cell area. This amounts to approximately 1%. The packing efficiency of cells for both are .93 (based on cell geometry only). The power-weight trade-off can be made as follows:

$$R_A = \frac{A_A}{W_A}$$

A = Total area of substrate

A_A = Usable area of configuration A substrate $= (.93)(.97)A$

$$R_B = \frac{A_B}{W_B}$$

A_B = Usable area of configuration B substrate $= (.93)(.99)A$

R_A = Power-weight ratio of configuration A

R_B = Power-weight ratio of configuration B

W_A = Weight of configuration A = 13.83 lb.

W_B = Weight of configuration B = 14.83

$$\frac{R_A}{R_B} = \frac{.97A\,(14.51)(.93)}{.99A\,(13.83)(.93)}$$

$$= 1.03$$

This shows configuration A to be 3% more efficient. The difference in reliability between configurations A and B is difficult to assess. The only determination that can be made is that B is slightly less reliable because of the greater number of parts in the system. The volumes of both configurations are identical. The cost of B may be slightly more because there are more parts. The selection of the rigid substrate of configuration A is made on the basis of a slightly better power-weight ratio, better reliability factor, and possibly, a slight reduction in the total cost.

Selection in the flexible substrate category is between configurations H and I. Since both configurations have the same area and the same method of attaching cells, the power-weight ratio of configuration H is more desirable because of the smaller overall weight of the system. The selection for occupied volume is obviously configuration H because its volume is half that of configuration I. The reliability trade-off is a gray area, but favors configuration H. This is due chiefly to the added positioning mechanism and the pneumatic system that must be installed. Configurations H and I will have approximately the same cost. The selection made for the flexible system is configuration H, made on the basis of smaller packaged volume and a higher power-weight ratio.

For the final selection between flexible versus rigid substrate, the arguments will be limited to the same considerations as the preceding selections.

Power-weight ratio has to take into account several things: the shadowing effect of the scissors link on the rigid substrate, the packaging efficiency of the cells on the flexible substrate, and the total weights of both configurations. This trade-off is presented below:

$$R_A = \frac{A_A}{W_A} \qquad A_A = .97\,(.93)A$$

$$A_H = .87\,A$$

$$R_H = \frac{A_H}{W_H} \qquad W_A = 13.83$$

$$W_H = 12.86$$

$$\frac{R_H}{R_A} = \frac{.87\,(13.83)}{(.93)(.97)(12.86)} = 1.04$$

The configuration H is shown to be 4% more desirable than configuration A. For reliability, the rigid system is believed to be better. Lack of test data on the substrate made analysis impractical. The unknown area is the interconnection between the cells. The mechanisms for both concepts have almost identical reliability numbers because each have the same number of parts and the same type of drive and damper systems. The occupied volumes of the systems vary by a large percentage, with the flexible concept being much more desirable. This is shown in Table 2.3. The cost will be about equal for the deployment mechanism. If the substrate development is included, configuration H will be more expensive. The selection for the final design was chosen as configuration H. It is a trade-off of packaged volume and a slight increase in power-weight ratio versus cost. Fairchild Hiller believes that the flexible substrate has a greater potential than shown in this design study. The confining depth dimension and the deployment requirements have greatly limited the end design.

TABLE 2.3

CONFIGURATION	PRELIMINARY WEIGHT AND VOLUME DATA			
	RIGID		FLEXIBLE	
	A	B	H	I
Extension Mechanism	2.15	2.15	1.89	2.36
Substrate	1.57	2.25	2.05	2.05
Cells Bond & Cover Glass	4.50	4.50	4.50	4.50
Drive Mechanism	1.89	1.89	1.25	.55
Release Mechanism	.40	.40	.30	.30
Damper Mechanism	.60	.60	.60	.60
Housing Structure	2.26	2.26	1.75	3.30
Wiring, etc.	.46	.46	.52	.52
Positioning Mechanism	N/A	N/A	N/A	.69
TOTAL WEIGHT	13.83	14.51	12.86	14.87
Required Volume (Inches ^{3})	1300	1300	630	1300

2.9 DESCRIPTION OF FINAL CONFIGURATION

The final configuration of the deployable solar array is shown in Figure 2.20. The end plates are machined magnesium upon which are mounted the substrate rollers and the screw jack drive system. The top and bottom are magnesium webs stiffened by beads and flanged lightning holes. The back, or 25 inch x 13 inch dimension, of the structure is constructed of stamped magnesium sheet forming a truss like pattern. The entire structure is mounted to the spacecraft by four bolts in the corners of the back face of the box and four additional bolts in the middle of the back face. The later mounting holes are attached to the skin of the structure and provide support for screw jacks when they are fully deployed.

The release system is activated by a signal from the spacecraft (assumed to be electrical). This electrical signal activates a dual set of redundant cable cutters. Severing of the cable does two things; it releases the substrate rollers from the fixed position and releases the front plate of the structure. The rollers are restrained during vibration to prevent unrolling during launch.

The release of the front plate activates the drive system. The system is designed to allow either one of the cable cutters to perform the release function. The drive system for the deployable array consists of a neg'ator spring driving a gear train which turns the screw jacks. The bearing-mounted gears are fabricated of aluminum and coated with dry lubricant. The spools for reeling and unreeling the spring are plastic.

The screw jacks are titanium and are of the ball bearing type screw. Both screws work together and are synchronized by the gear train previously mentioned. The screw jacks are half left-handed and half right-handed threads arranged so that the slider blocks on each end of the screw will proceed toward each other for the rotation caused by the spring. These slider blocks are attached to the scissors links by the hinge pins. The drive system becomes activated upon initiation of the release system.

The extension mechanism consists of 2 sets of eight and one-half scissors links which when stowed fold into each other, packaging two links in the space of one.

The channel type drive link is machined aluminum and the box type link is of aluminum honeycomb construction. They are joined by non-magnetic stainless steel hinge pins. The drive links are attached to the substrate through the end plate. The substrate has been described in detail in Section 2.7. Its rollers are magnesium tubing with plates on the end to prevent lateral shifting of the substrate during vibration. The rollers are synchronized through a gear train to insure their uniform deployment. Upon deployment, the rotational energy of the vehicle pulls the substrate and the links from the structure. This motion is resisted by a centrifugal brake mounted through a gear train to the substrate rollers. The centrifugal brake drum is aluminum. The weights are beryllium-copper to which aluminum friction pads are attached. The brake can be adjusted several ways since the friction pad can be varied in position and composition. The weights may be changed by either shortening or changing materials. During deployment the brake is driven by the substrate.

The brake system contains an over-running clutch so that at the end of deployment the inertia of the brake does not tend to rewind the substrate. The stopping mechanism is simply letting the substrate "bottom out" on the roller when full deployment is reached. This caused a slight amount of shock in the substrate but, since the radial velocity at the full deployment is low, the loads were negligible. Locking of the system is accomplished by maintaining the spring load on the scissors links.

Figure 2.21 is a drawing tree of the design.

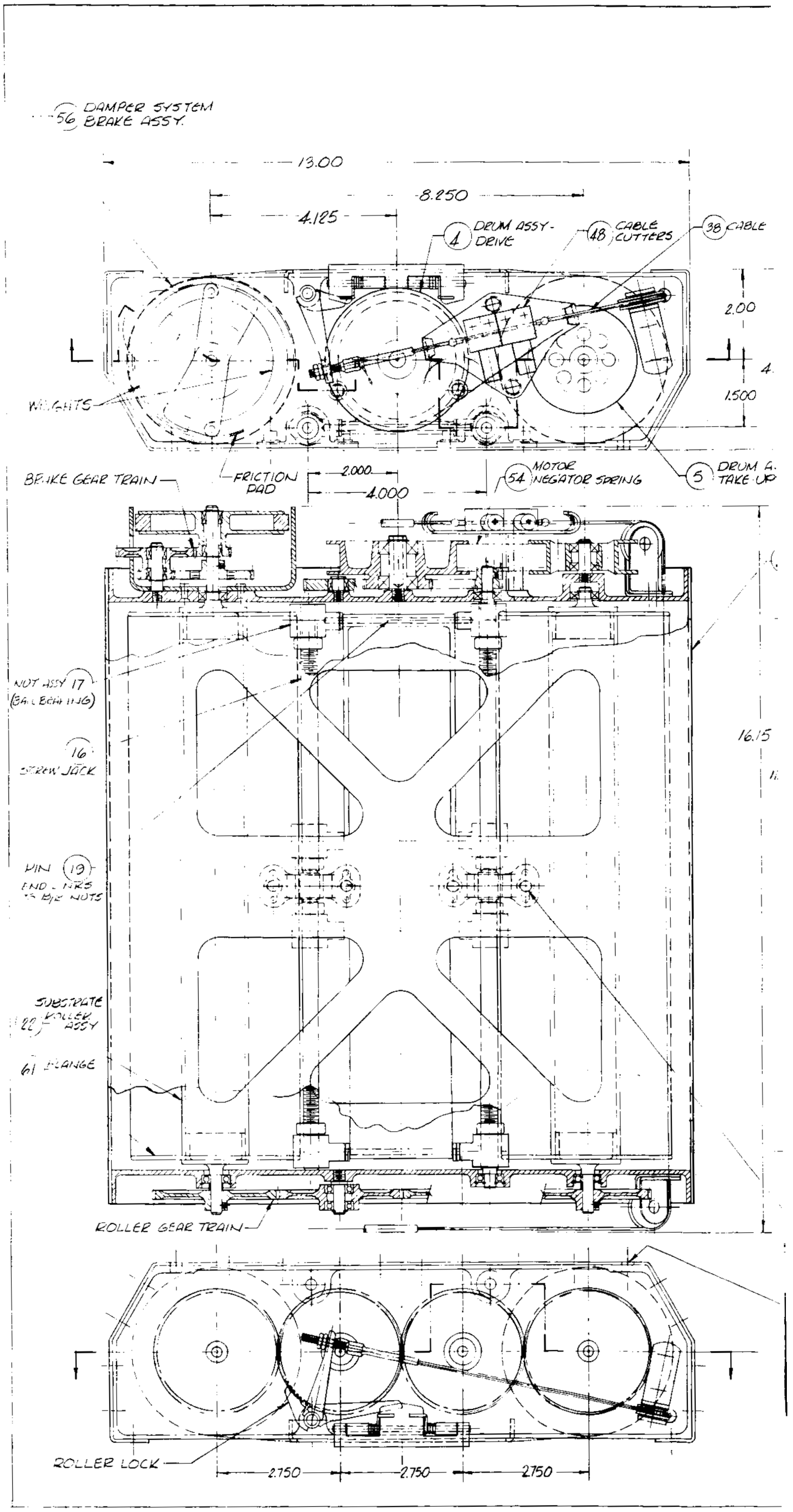
56 DAMPER SYSTEM BRAKE ASSY.
13.00
8.250
4.125
4 DRUM ASSY-DRIVE
48 CABLE CUTTERS
38 CABLE
2.00
1.500
WEIGHTS
BRAKE GEAR TRAIN
FRICTION PAD
2.000
4.000
54 MOTOR NEGATOR SPRING
5 DRUM A. TAKE UP
NUT ASSY 17 (BALL BEARING)
16 SCREW JACK
16.15
PIN 19
SUBSTRATE ROLLER ASSY
61 FLANGE
ROLLER GEAR TRAIN
ROLLER LOCK
2.750
2.750
2750

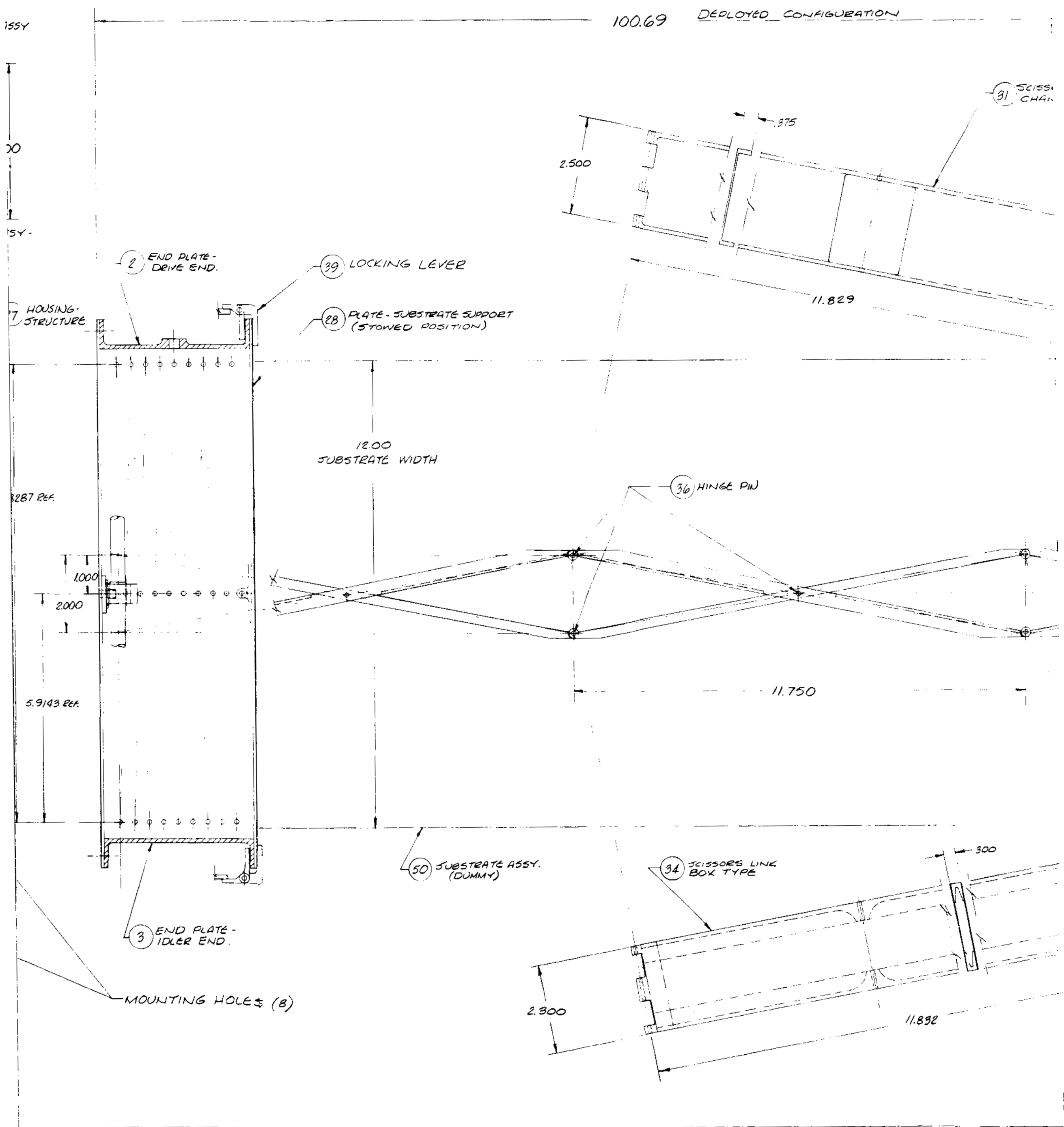
100.69 DEPLOYED CONFIGURATION
31 SCISS CHA
.375
2.500
11.829
2 END PLATE - DRIVE END.
39 LOCKING LEVER
HOUSING STRUCTURE
28 PLATE - SUBSTRATE SUPPORT (STOWED POSITION)
12.00 SUBSTRATE WIDTH
36 HINGE PIN
1.000
2.000
5.9143 REF.
11.750
50 SUBSTRATE ASSY. (DUMMY)
34 SCISSORS LINK BOX TYPE
.300
3 END PLATE - IDLER END.
MOUNTING HOLES (8)
2.300
11.892

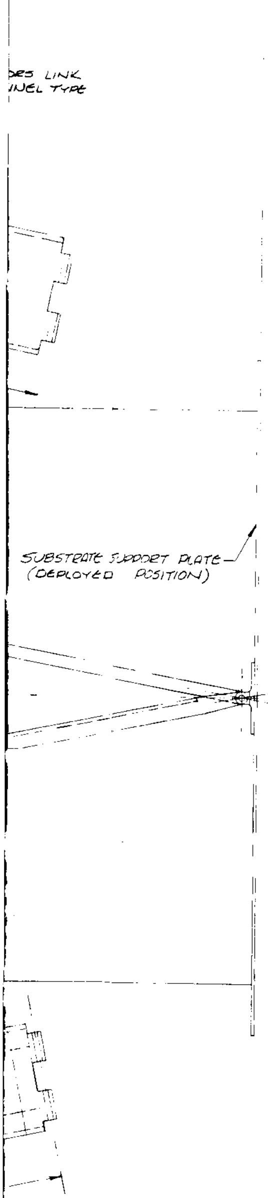

REVISIONS			
SYM	DESCRIPTION	DATE	APPROVED

NOTE:
SEE LIST OF MATERIALS FOR ITEMS SHOWN IN FIELD OF DRAWING BUT NOT DESIGNATED INDIVIDUALLY.

29	22	15	59	57	56	37	ITEM	NO REQD (1)	PART NO	DESCRIPTION	MATERIAL	SPECIFICATION
2	2						61		XXX-32030	FLANGE		
1	1						60		XXX-32029	ROLLER		
							59	1	XXX-00000-59	DRIVE & DEPLOYMENT SYSTEM		
						1	58	1	XXX-31013	CABLE RETAINER		
							57	1	XXX-00000-57	STRUCTURE		
							56	1	XXX-00000-56	DAMPER SYSTEM		
							55	18	XXX-00000-55	ANTI-FRICTION BEARINGS		
			1				54		XXX-32010	MOTOR-NEGATOR SPRING		
					1		53		XXX-33004	CLUTCH ASSY		
					1		52		XXX-33006	SHAFT		
							51	1	XXX-43000	ELECTRICAL SYSTEM		
							50	1	XXX 70000	SUBSTRATE ASSY (DUMMY)		
						1	49		XXX-31012	PULLEY BRKT INSTAL.		
						2	48		XXX-31011	CABLE CUTTER		
						2	47		XXX-31010	PIN LOCKING LEVER HINGE		
						1	46		XXX-31009	STUD - RELEASE LEVER		
						1	45		XXX-31008	STUD - RELEASE LEVER		
						1	44		XXX-31007	RELEASE LEVER		
						2	43		XXX-31006	SPRING - TENSION		
						1	42		XXX-31005	RELEASE LEVER		
						4	41		XXX-31004	SPRING TENSION		
						2	40		XXX-31003	HINGE FITTING		
						2	39		XXX-31002	LOCKING LEVER		
						1	38		XXX-31001	CABLE ASSY		
							37	1	XXX-31000	RELEASE MECHANISM INSTAL.		
			25				36		XXX-32026	HINGE PIN - SCISSORS		
			1				35		XXX-32028	SCISSORS HALF LINK ASSY - BOX TYPE		
			7				34		XXX-32027	SCISSORS LINK ASSY - BOX TYPE		
			1				33		XXX-32025	SCISSORS LINK ASSY (END) - BOX TYPE		
			1				32		XXX-32024	SCISSORS HALF LINK CHANNEL		
			7				31		XXX-32023	SCISSORS LINK - CHANNEL		
			1				30		XXX-32022	SCISSORS LINK (END) - CHANNEL		
			1				29		XXX-32021	FITTING - SUPPORT PLATE		
				1			28		XXX-32020	PLATE - SUBSTRATE SUPPORT		
				1			27		XXX-11002	HOUSING - STRUCTURE		
1							26		XXX-32019	STUB SHAFT		
	1						25		XXX-32017	STUB SHAFT		
1	1						24		XXX-32016	STUB SHAFT		
			1				23		XXX-32018	ROLLER ASSY (SUBSTRATE STORAGE)		
			1				22		XXX-32015	ROLLER ASSY (SUBSTRATE STORAGE)		
			2				21		XXX-32013	GEAR - IDLER		
			2				20		XXX-32014	GEAR ASSY - IDLER		
			2				19		XXX-32012	PIN (END LINKS TO B/B NUTS)		
		1					18		XXX-32011	BEARING BLOCK ASSY		
		11 12					17		XXX-32009	NUT ASSY (BALL BEARING)		
		1					16		XXX-32008	SCREW JACK		
			2				15		XXX-32007	SCREW ASSY (BALL BRG.)		
					1		14		XXX-33003	BRAKE LEVER & GEAR ASSY		
					1		13		XXX-33005	GEAR ASSY - INTERMEDIATE		
					2		12		XXX-33001	BRAKE SHOE ASSY		
					1		11		XXX-33000	BRAKE DRUM		
			2				10		XXX-32006	SHAFT - IDLER GEAR		
			1				9		XXX-32005	SHAFT TAKE UP DRUM		
			1				8		XXX-32004	SHAFT DRIVING DRUM		
			2				7		XXX-32003	GEAR - PINION		
			2				6		XXX-32002	GEAR ASSY - IDLER		
			1				5		XXX-32001	DRUM ASSY - TAKE UP		
			1				4		XXX-32000	DRUM ASSY - DRIVE		
				1			3		XXX-11001	END PLATE - IDLER END		
				1			2		XXX-11000	END PLATE - DRIVE END		
							1		XXX-00000-1	DEPLOYABLE SOLAR ARRAY - ASSY.		

← ITEM NO. — LIST OF MATERIALS

NEXT ASSY	USED ON	QTY
APPLICATION		

MATERIAL

HEAT TREATMENT

FINISH

UNLESS OTHERWISE SPECIFIED
DIMENSIONS ARE IN INCHES AND INCLUDE CHEMICALLY APPLIED OR PLATED FINISHES
ALL TOLERANCES ±

BASIC DIMENSION	DECIMALS .XX	DECIMALS .XXX	FRACTIONS	ANGLES
UNDER 12	.02	.010	1/64	0°30'
12-24 INCL	.03	.015	1/32	
24-48	.04	.020	1/16	
OVER 48	.06	.030	1/8	

STOCK SIZE TOL CONF OR MIL AS APPLICABLE
MACHINE SURFACES RMS 125 MAX.
BREAK ALL SHARP EDGES

APPROVAL		DATE
DR	G. DELANEY	0-16-64
CHK		
APPD		
APPD		
APPD		
APPD		
APPROVAL		
APPROVAL		

FAIRCHILD STRATOS — ROCKVILLE, MARYLAND

LAYOUT
POSITIVE DEPLOYABLE SOLAR ARRAY
FLEXIBLE SUBSTRATE

CODE IDENT NO	SIZE	DRAWING NO.
17232	E	XXX-00000

SCALE 1/1 | WT | SHEET

[XXX-00000]

FIGURE 2.20 POSITIVE DEPLOYABLE SOLAR ARRAY FLEXIBLE SUBSTRATE.

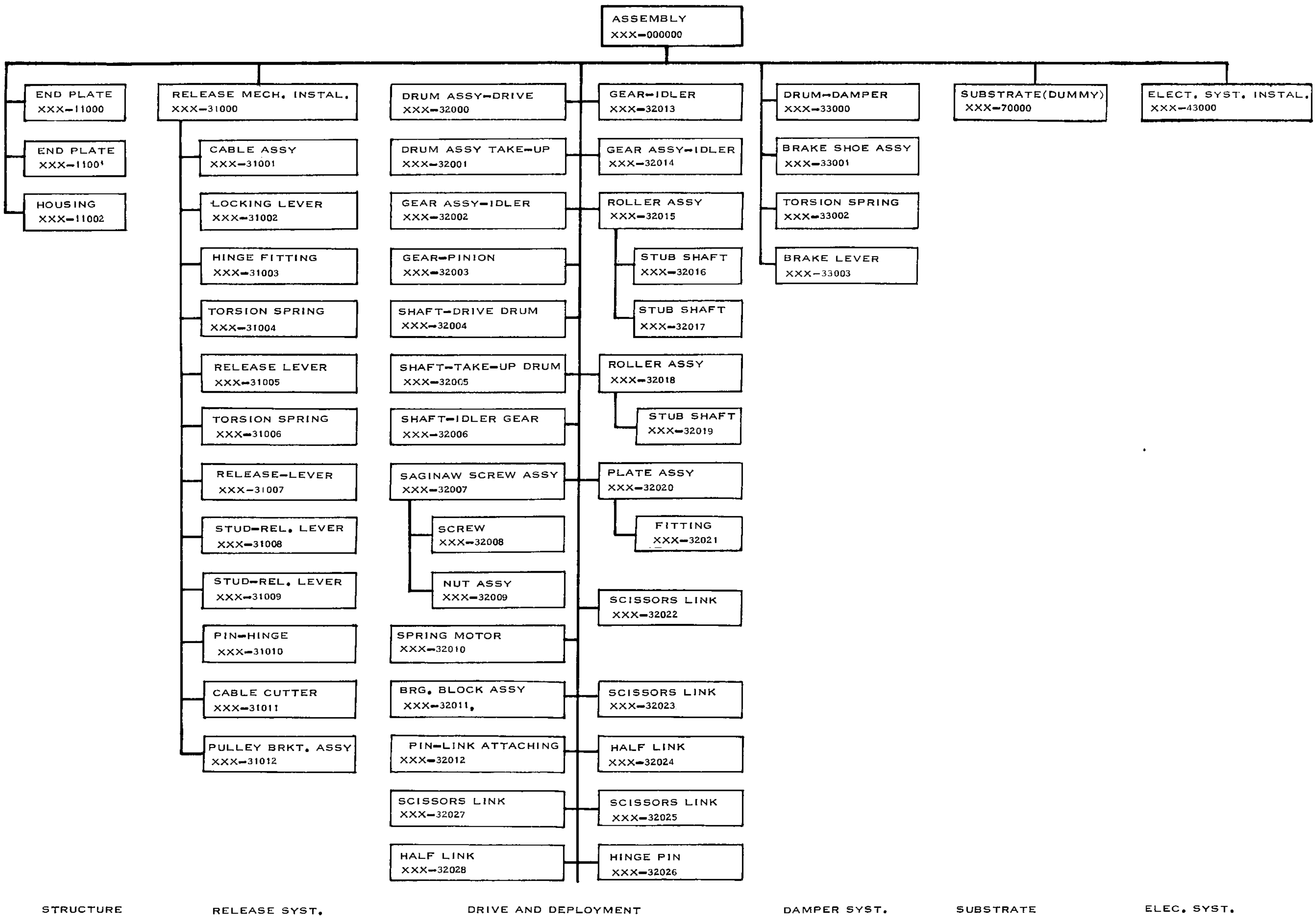

FIGURE 2.21 DRAWING TREE

3.0 ANALYSIS

3.1 DYNAMIC ANALYSIS

3.1.1 Introduction

This section presents the analysis developed in support of the Deployable Solar Array program. The analyses are presented in the order by which they effect the detail design decisions.

Computer programs have been used extensively to economize on time and cost. The detail results are presented in Appendix I.

3.1.2 Vibration Analysis

The packaged solar array was analyzed to determine the vibration environment of the cells. The lateral natural frequency, magnification factor and response of the roller-cell package was determined by analyzing a mathematical lumped mass-spring model. The roller was idealized as a pin-pin beam reflecting the proper stiffness and mass. It was assumed the stiffness supplied by the substrate and cells was negligible compared to the stiffness of the roller and thus not included. The mass of the roller, cells and substrate were lumped into two masses as shown in Figure 3.1.

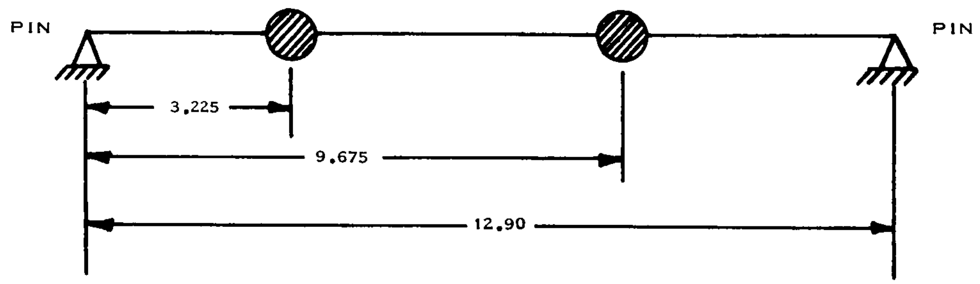

FIGURE 3.1
VIBRATION ANALYSIS LUMP MASS MODEL

It was further assumed the input to the packaged cells is sinusoidal and of the magnitude specified in the deployable solar array sinusoidal test specification. These inputs were multiplied by four to include the response of the spacecraft structure.

The analysis was performed by initially deriving a set of deflection influence coefficients for the two lumped mass model. The lateral natural frequency was obtained from the mathematical model by matrix iteration of the equation:

$$\left\{ x_i \right\} = \omega^2 \left[\delta_{ij} \right] \left\lceil m_i \right\rfloor \left\{ x_i \right\}$$

Where: x_i = Column matrix of normalized mode shape, in/in

δ_{ij} = Matrix of deflection influence coefficients, in/lb

m_i = Matrix of lumped mass, lb-sec^2/in

ω = Frequency, rad/sec

Structural magnification factors for a 1 g input were calculated from the equation:

$$\left\{ M.F. \right\} = (1 + iq) \left[\lceil 1 \rfloor - \omega^2 [\delta] \lceil m \rfloor + i \lceil q \rfloor \right]^{-1} \left\{ 1 \right\}$$

Where: M.F. = Column matrix of magnification factors

q = Structural damping coefficient

The fundamental lateral mode of the roller-cell package was determined to be:

$$f_n = 287 \text{ cps}$$

Using a conservative structural damping of $q = .05$ the magnification factor from the roller pin was calculated to be

$$M.F. = 20.0$$

For an input to the rollers of 8.4 g's, determined as previously explained, a response of 168 g's will be experienced by the packaged cells.

The vibration analysis of the packaged array included only the substrate and cells stowed on the roller. A more complete Phase II study would include a response calculation of the stowed scissor links to determine excessive vibratory loads. In addition, the analysis would be furthered by utilizing a more sophisticated model.

3.1.3 Mechanical System Analysis

3.1.3.1 Introduction

In this section the equations of motion necessary to describe the deployment dynamics of the Deployable Solar Array are developed.

The assumptions used in this analysis are:

- Rigid body dynamics
- The deployment occurs in a zero gravity field
- Aerodynamic phenomena do not exist
- The angular velocity vector remains coincident with the spin axis
- The dynamic system is symmetric about the spin axis.

3.1.3.2 Description of System

The system consists of a 3 foot diameter solid, homogeneous, cylindrical centerbody around whose perifery are four equally spaced solar array assemblies. Each assembly consists of a fixed housing structure, a flexible substrate stowed on rollers and a set of scissors deployment links. When released, the four solar panels are uniformly extended by centrifugal force and the force of the spring driven linkage. Self energizing centrifugal brakes geared to the substrates limit the deployment speed. Deployment ceases when the substrates have been extended 9.5 feet from the center of rotation.

A diagramatic sketch, dimensional nomenclature and a list of symbols and definitions used in this analysis appears at the end of this section.

3.1.3.3 Equations of Motion

Angular velocity and angular acceleration of the complete spacecraft about the spin axis can be described using conservation of momentum principles.

Denoting the total angular momentum of the system before deployment as

$$C = \omega_{c_o} I_o \tag{1}$$

it follows that the instantaneous angular velocity at any time during deployment is

$$\omega_c = C/I \tag{2}$$

and

$$\dot{\omega}_c = -C\dot{I}/I^2 \tag{3}$$

where

$$I = \left\{ \left[\frac{W_c}{2} + 4 W_b + \frac{4}{3} W_p + 4 W_r + \frac{8}{3} \mu R_c \right] R_c^{\,2} + \frac{4}{3} W_p X_e^{\,2} + \frac{4}{3} W_p X_e R_c - 4 \mu X_e R_c^{\,2} + \frac{4}{3} \mu X_e^{\,3} \right\} \Big/ g \tag{4}$$

and is a function of only the masses in the system and the deployment length. Knowing the total momentum (C) from the initial conditions and substituting equation (4) into equation (2), the angular velocity can be found for any length of paddle. This is given in Figure 3.2.

$$\dot{I} = 4 \left[\mu \left(X_e^{\,2} - R_c^{\,2} \right) + \frac{W_p}{3} \left(2X_e + R_c \right) \right] \dot{X}_e \Big/ g \tag{5}$$

The development of Equations (4) and (5) are found in Appendix I.

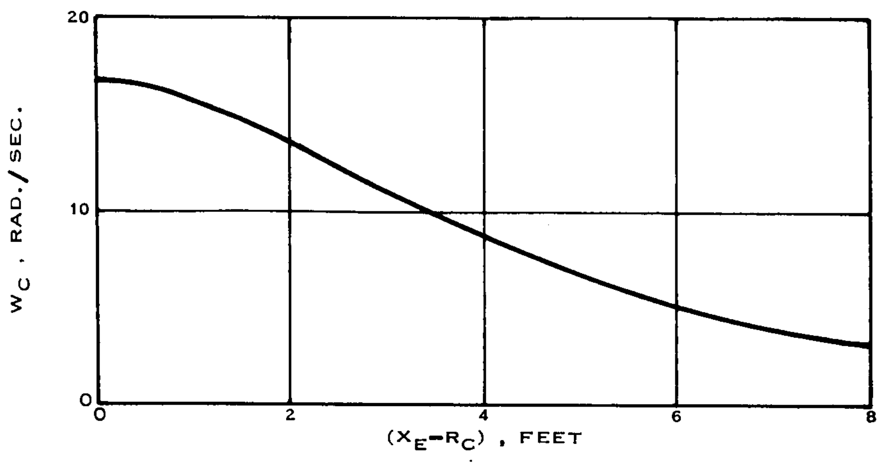

FIGURE 3.2
W_c VERSUS $(X_e - R_c)$

Having described the angular motion of the entire unit, the equilibrium equation for each deploying panel can now be defined.

The centripetal acceleration at any point on the deployed panels is:

$$a_n = -X \omega_c^2$$

Integrating this acceleration times the scissors mass from R_c to X_e gives the total instantaneous contrifugal force of the scissors unit.

$$F_{n_p} = W_p \left(X_e + R_c \right) \omega_c^2 \Big/ 2g \qquad (7)$$

Integration of this acceleration times the mass of the deployed substrate from R_c to X_e gives the total instantaneous centrifugal force of the deployed portion of the substrate.

$$F_{n_r} = \mu\left(X_e^2 - R_c^2\right)\omega_c^2 \Big/ 2g \tag{8}$$

The radial force exerted by the scissors unit, which aids in the deployment is as follows:

$$F_p = (X_e - R_c)\, F_{y_s} \Big/ N\sqrt{N^2 R_p^2 - (X_e - R_c)^2} \tag{9}$$

where

F_{y_s} = Force which activates the scissors unit, pound

R_p = Length of one link in the scissors unit, feet

There are four (4) inertia forces restricting deployment due to the linear radial acceleration, $\ddot{X}$,

(1) Scissors

$$F_{I_p} = - W_p \ddot{X}_e / 2g \tag{10}$$

(2) Substrate (Rolled plus deployed portion)

This inertia force acts in the plane of the deployed substrate.

$$F_{I_r} = -\left[W_r + \mu(X_e - R_c)\right]\ddot{X}_e \Big/ 2g \tag{11}$$

(3) Brake Unit

This inertia force acts in the plane of the deployed substrate.

$$F_{I_f} = -S^2 W_f R_f^2 \ddot{X}_e \Big/ g R_r^2 \tag{12}$$

The braking force resisting deployment of the panels is derived in Appendix I and acts in the plane of the deployed panels.

$$F_f = - \frac{C_f S^3 W_f R_1 R_f^2 \dot{X}_e^2 \sin \Theta_2}{g \left[R_f \sin \Theta_1 - C_f (R_1 - R_f \cos \Theta_1) \right] R_r^3} \tag{13}$$

The equation of motion for the radial motion of the deploying panels, then, can be written by summing equations (7) through (13).

$$F_{I_p} + F_{I_r} + F_{I_f} + F_p + F_{n_r} + F_{n_p} \quad F_f = 0$$

or

$$\left[\frac{W_p + W_r + \mu (X_e - R_c) + (2S^2 W_f R_f^2 / R_r^2)}{2g} \right] \ddot{X}_e - \left[\frac{F_f}{\dot{X}_e^2} \right] \dot{X}_e^2 - F_p - F_{n_r} - F_{n_p} = 0 \tag{14}$$

Since equation (14) is a non-linear differential equation involving variable coefficients, a digital solution using iteration techniques taken over small time intervals is required.

Solving equation (14) for $\ddot{X}_e$ and integrating twice to obtain $\ddot{X}_e$ and X_e gives the following equations.

$$\ddot{X}_e = \frac{2g \left(\dfrac{F_{y_s} \tan \emptyset}{N} + F_{n_r} + F_{n_p} + F_f \right)}{\left[W_p + W + \mu (X_e - R_c) + \dfrac{2S^2 W_f R_f^2}{R_r^2} \right]} \tag{15}$$

$$\dot{X}_e = \int_0^t \ddot{X}_e \, dt + \dot{X}_{e_o} \tag{16}$$

$$X_e = \int_0^t \dot{X}_e \, dt + X_{e_o} \tag{17}$$

Where

$$\tan \phi = (X_e - R_c) \Big/ \sqrt{N^2 R_p^2 - (X_e - R_c)^2} \tag{18}$$

$$R_r = \sqrt{R_{r_e}^{\ 2} + \frac{t_r (L_p - X_e + R_c)}{\pi}} \tag{19}$$

R_{r_e} = Radius of spool on which the stubstrate is rolled.

Iterating these equations with equations (2) and (4) produces the following results describing deployment of the Deployable Solar Array. Figures 3.3 and 3.4 present curves of deployed length vs time and radial velocity vs time.

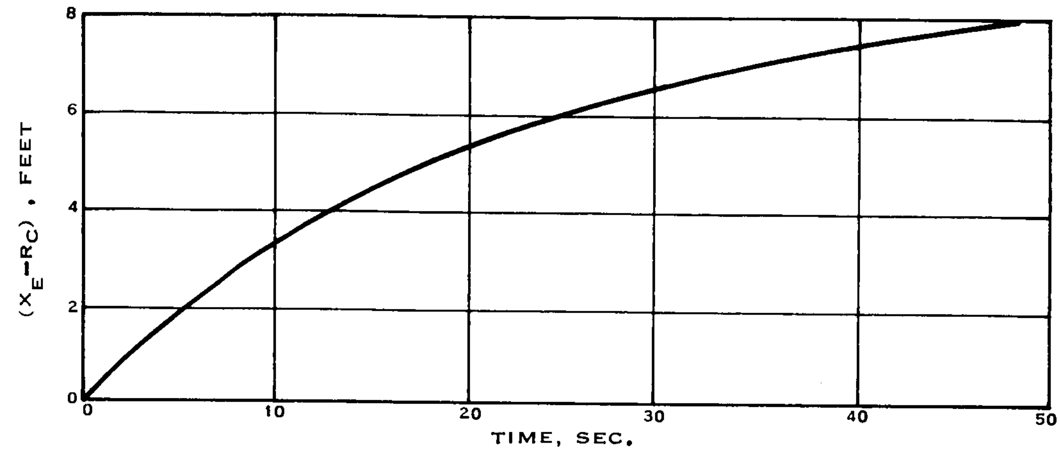

FIGURE 3.3 $(X_e - R_c)$ VERSUS TIME

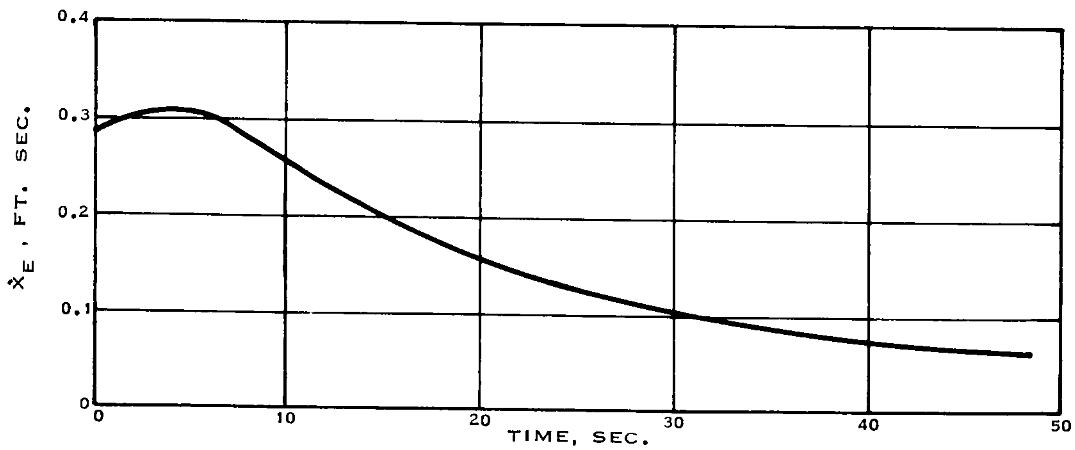

FIGURE 3.4 $\dot{X}_e$ VERSUS TIME

3.1.3.4 Results

The angular acceleration ($\dot{\omega}_c$) occurs when (X_e - R_c) equals 2.19 feet. This maximum value is -0.754 rad./sec.^{2}. The minimum angular acceleration occurs when (X_e -R_c) equals 8 feet (full deployment), its value is -0.047 rad./sec.^{2}.

Figures 3.3 and 3.4 show deployment distance and deployment velocity versus time. It is evident from Figure 3.3 that the speed brake is very adequate as presently designed since complete deployment takes nearly 50 seconds to accomplish. Figure 3.4 is somewhat deceptive in that it appears to show an initial velocity at the instant of panel release. In actuality, the panels accelerate to the velocity shown in approximately 0.01 seconds making the plotting of this acceleration impractical with the scale used. The maximum acceleration, $\ddot{X}_e$, occurs at time zero and is approximately 90 ft./sec.^{2}. Peak deceleration occurs at 10.2 seconds and has a value of -0.012 ft./sec.^{2} indicating inertia forces due to linear acceleration are practically non-existent following t = 0.01 seconds.

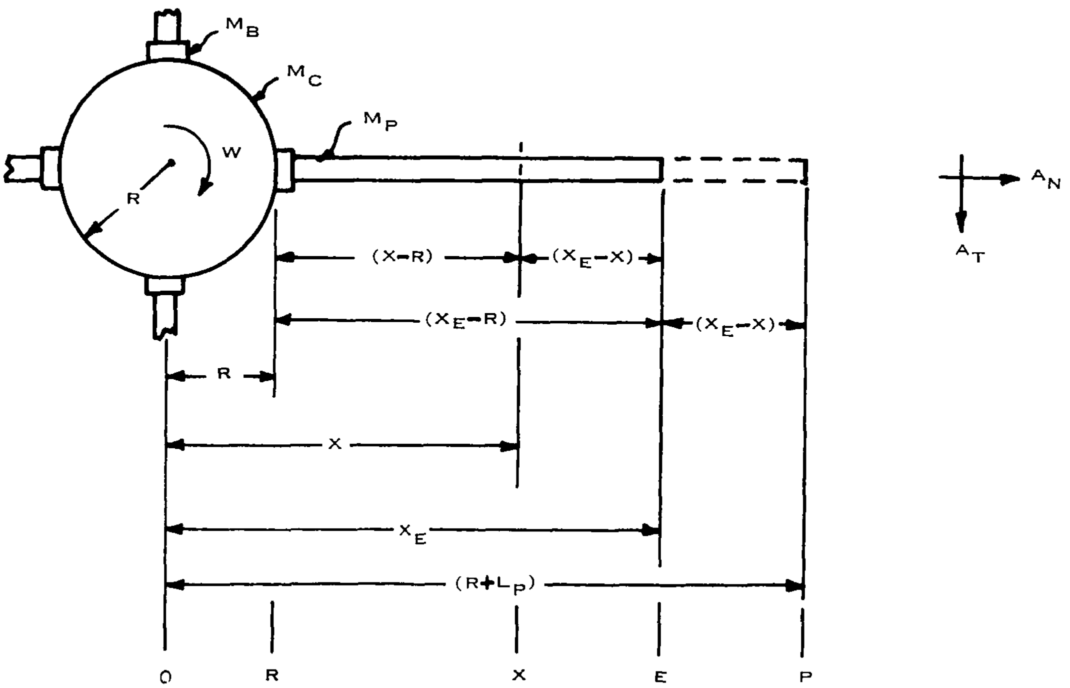

FIGURE 3.5 DESCRIPTIVE DIAGRAM

a	Linear acceleration, ft./sec.^{2}
C	Total angular momentum, ft. lb. sec.
C_f	Friction coefficient, lb./lb.
F	Force, lb.
g	Gravity acceleration, 32.2 ft./sec.^{2}
I	Mass moment of inertia about spin axis, ft. lb. sec.^{2}
L_p	Total length of substrate, ft.
N	Number of scissors links
R	Radius, ft.
S	Gear ratio, Brake speed/substrate roller speed
t	Time, sec.
W	Weight, lb.
X	Radial station measured from spin axis, ft.
X_e	Distance of outermost point on deploying panel from spin axis, ft.
Θ_1	Radial angle between speed brake mass hinge and friction point
Θ_2	Radial angle between speed brake mass hinge and mass C.G.
μ	Substrate weight per linear foot, lb./ft.
ω	Angular velocity, rad./sec.

Subscripts

b	Refers to stationary housing boxes
c	Refers to cylindrical centerbody
e	Refers to outermost point on deploying panel
f	Refers to speed brake friction device
n	Refers to normal or radial direction
p	Refers to scissors
r	Refers to substrate (rolled and/or extended portion)
t	Refers to tangential direction
l	Refers to length

3.1.4 Loading Analysis

3.1.4.1 Introduction

The purpose of this section is to develop the equations and present the component loads for the deploying panels of the Deployable Solar Array. The same assumptions and nomenclature are used in this analysis as are used in the section describing deployment dynamics. The loading curves shown i ι the results were produced during the digital iteration solution of the equations of motion discussed previously.

3.1.4.2 Loading Equations

The loads of primary interest in the deploying panels are the tangential (in-plane) shear and bending moments, and the tension in the flexible substrate material.

The in-plane loadings are a result of local tangential accelerations caused by the angular acceleration of the entire unit about the spin axis (equation 3) as well as Coriolis acceleration caused by the instantaneous deployment velocity $\dot{X}$. The total tangential acceleration at any point on the panel is:

$$a_t = \dot{\omega}_c X + 2\,\omega_c \dot{X} \tag{20}$$

Since the scissors unit is fixed to the centerbody at a point which does not move radially, it is seen that

$$\dot{X}_p = \left(\frac{X - R_c}{X_e - R_c} \right) \dot{X}_e \tag{21}$$

The substrate, however, will deploy with a constant velocity since it is being unwound from a roll.

$$\dot{X}_r = \dot{X}_e \tag{22}$$

The assumption that the total tangential acceleration, a_t, varies linearly from zero at the spin axis to a maximum at X_e is conservative regarding the scissors linkage inertia force but unconservative regarding the in-plane substrate inertia force. It is evident from Figure 3. 6 that Coriolis acceleration is very small near the completion of deployment and that the assumption that a_t is linear from the spin axis to the panel tip would serve to develop adequate loads for design purposes.

The shear at a point X on the deployed panel can then be found by integrating the inertia forces outboard of that point.

$$a_t = \left(\frac{X}{X_e} \right) a_{t_e}$$

$$dV = -a_t \, dm = -\left(\frac{X}{X_e} \right) a_{t_e} \left[\frac{W_p}{X_e - R_c} + \mu \right] \frac{dX}{g}$$

$$V = - \frac{a_{t_e} \left[W_p + \mu (X_e - R_c) \right]}{X_e (X_e - R_c) g} \int_X^{X_e} X \, dX$$

$$V = - \frac{a_{t_e} \left[W_p + \mu (X_e - R_c) \right] \left(X_e^2 - X^2 \right)}{2 X_e (X_e - R_c) g} \qquad (23)$$

Integrating equation (23) from X to X_e yields the following equation for the in-plane bending moment at a point X.

$$M = - \frac{a_{t_e} \left[W_p + \mu (X_e - R_c) \right] \left(2X_e^3 - 3 X X_e^2 + X^3 \right)}{6 X_e (X_e - R_c) g} \qquad (24)$$

for both equations (23) and (24)

$$R_c \leq X \leq X_e$$

It is assumed that the substrate material will not reach tangential loads and that it will have to withstand only the tension loads imposed by the speed brake and inertia loads caused by $\ddot{X}_e$. The inertia loads of interest are that of the speed brake, expressed by equation (12), and that of the undeployed (rolled) portion of the substrate, expressed as follows:

$$F'_{i_r} = -\left[W_r - \mu (X_e - R_c)\right] \ddot{X}_e \Big/ 2g \qquad (25)$$

Combining the speed brake force, expressed in equation (13) with the inertia forces, all considered to be acting in the plane of the substrate and at the instantaneous position R_c, the tension in the substrate can be expressed as follows for one thickness of substrate.

$$p_r = \frac{F_f}{2} + \left\{ \frac{W_r - \mu (X_e - R_c)}{4g} + \frac{S^2 \; W_f \; R_f^2}{2 g R_r^2} \right\} \ddot{X}_e \qquad (26)$$

Figures 3.6, 3.7, and 3.8 show the results of the loading analysis.

3.1.5 Results

Figure 3.2 shows the variation in the angular velocity about the spin axis versus panel deployment distance. The angular acceleration, ($\dot{\omega}_c$), occurs when $(X_e - R_c)$ equals 2.19 feet. This maximum value is -0.754 rad./sec.^{2}. The minimum angular acceleration occurs when $(X_e - R_c)$ equals 8 feet (full deployment and has a value of -0.047 rad./sec.^{2}.

Figures 3.3 and 3.4 show deployment distance and deployment velocity versus time. It is evident from Figure 3.3 that the speed brake is very adequate as presently designed since complete deployment takes nearly 50 seconds to

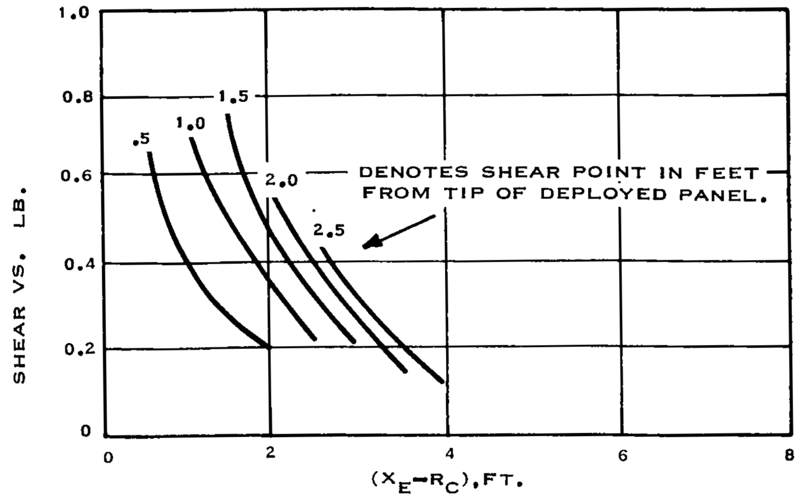

FIGURE 3.6 SHEAR VS. $(X_E - R_C)$

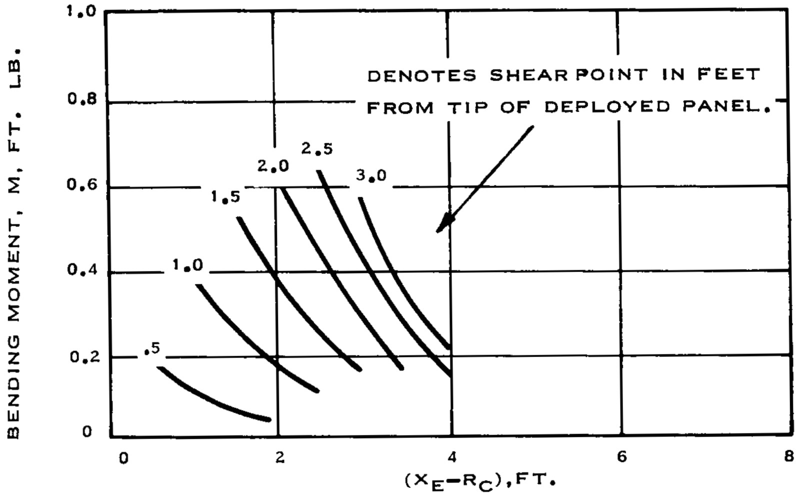

FIGURE 3.7 BENDING MOMENT VS. $(X_E - R_C)$

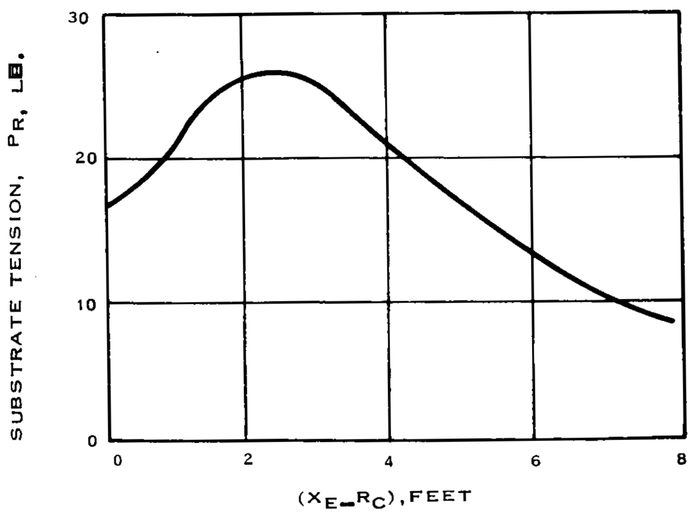

FIGURE 3.8 SUBSTRATE TENSION VS. $(X_E - R_C)$

accomplish. Figure 3.4 is somewhat deceptive in that it appears to show an initial velocity at the instant of panel release. In actuality the panels accelerate to the velocity shown in approximately 0.01 seconds making the plotting of this acceleration impractical with the scale used. The maximum acceleration, $\ddot{X}_e$, occurs at time zero and is approximately 90 ft./sec.^{2}. Peak deceleration occurs at 10.2 seconds and has a value of -0.012 ft./sec.^{2}. indicating inertia forces due to linear acceleration are practically non-existent following t = 0.01 seconds.

3.2.3 Structural Analysis

A structural analysis was performed to establish the structural integrity of the Deployable Solar Array. Margins of safety obtained by the analysis are summarized in Table 3.1. Supporting calculations are presented in Appendix II.

Table 3.1 - Summary of Minimum Ultimate Margins of Safety

Item	Load Condition	Mode of Failure	Allowable Stress psi	Actual Stress psi	Calc. M.S.
Scissor linkage					
Channel link	1 g static deploy.	Shear due to torsion, bending, comp.	48,000	35,000	+0.37
Box beam link	1 g static deploy.	Shear due to torsion bending, comp.	48,000	9,000	+4.3
Hinge Pins	1 g static deploy.	Bending and Shear	100,000	53,000	+ .89
Screw Jacks	1 g static deploy.	Bending and Shear	70,000	68,000	+0.03
End Plate	1 g static deploy.	Bending	37,000	10,000	+2.7
Substrate Rollers	Vibration Stowed	Bending	38,000	11,000	+2.4
Housing	Vibration Stowed	Local buckling due to shaft loads	P_{CR}=408 lbs.	P=330	0.23

Item	Load Condition	Mode of Failure	Allowable Stress PSA	Actual Stress PSA	Calc. M.S.
Housing Attachments	Vibration Stowed	Tension and Shear in bolt	50,000	26,000	0.92
Substrate	1 g static deploy.	Tension	140 lbs/in	2.1 lb/in	High

3.2.3.1 Design Loads

The entire system was analyzed for three loading conditions

a) Static deployment under 1 g conditions was a load factor of 2 to account for any random vibrations and disturbances which may occur during deployment.

b) Dynamic deployment under 1 g condition with a load factor of 2.0.

c) Vibration of the system in the stowed condition.

3.2.3.2 Static 1 g Deployment

The condition of maximum loading in the scissor linkage was obtained by equating to zero the derivative of the torsional and bending moments with respect to angle of deployment. Maximum torsion exists for an angle of deployment of 38.5^{o} and maximum bending for the linkage fully deployed. Maximum torsion resulted in the most critical combination of loads for the linkage. The screw jacks were studied for bending stresses and deflections during deployment. The housing was examined for its ability to react the loads delivered to it by the shafts of the substrate rollers and screw jacks. The hinge pins of the linkage were analyzed for the fully deployed condition and the substrate was checked for tension during dynamic deployment.

Deflections of the scissor linkage during deployment was studied also and the analysis indicated a considerable torsional deflection of the channel section of the scissor linkage may result during deployment. The linkage will, however, retain its integrity and function as required. If the deflection of the deploying structure is considered a problem, additional study of the deflections would be warranted.

3.2.3.3 Dynamic 1 g Deployment

The dynamic analysis of the deploying panel has determined maximum bending, shear, tensile and axial loads in the scissor linkage caused by deployment. Forces and moments in the scissor links due to dynamic deployment were small for deployment rate chosen and the resulting stresses were negligible. Maximum tension in the substrate was very low compared to the allowable.

3.2.3.4 Stowed Dynamic Loads

The dynamic analysis of the Deployable Solar Array in the stowed configuration produced magnification factors for the rollers, the scissor linkage, and the housing. Those responses are shown below.

	Response (g)	
Element	Limit	Ultimate
Roller & Substrate	168	252
Scissor linkage	100	150
Housing	15	22.5

Dynamic Response for Stowed Configuration Ultimate Load = 1.5 x limit load

3.2.3.5 Stress Analysis

The linkage supports itself and the flexible substrate as a cantilever beam during 1 g deployment. The most inboard link of the scissor linkage is, therefore, the most highly loaded member for any degree of deployment. The total moment applied to this member is a function of the angle of deployment and expressed as follows:

$$\overline{M} = 334\ WR_P^{\ 2}\ \mathrm{Cos}^2\,\Theta + 72.5\ qR_P\ \mathrm{Cos}\,\Theta, \quad \text{ft-lbs.}$$

where: $\overline{M}$ = is total moment about an axis perpendicular to longitudinal axis of scissor mechanism.

R_P = length of scissor link

μ = weight of substrate per foot

q = weights of scissor link per foot of link

Θ = angle between link and longitudinal axis

The total moment $\overline{M}$ is carried partially by bending and partially by torsion of the links. Expressions for the torsional component of the moment M_T and the bending component M_b are:

$$M_T = \overline{M}\ \mathrm{Sin}\,\Theta$$

$$M_b = \overline{M}\ \mathrm{Cos}\,\Theta$$

As the angle Θ decreases during deployment, the bending component increases continuously but the torsional component increases to a maximum and then deteriorates. The value of Θ corresponding to the maximum value of M_T can be obtained by solving the equation;

$$\frac{dM_T}{d\,\Theta} = 0$$

This occurs at $\Theta = 38.5^{\circ}$. Since the channel and box links are connected at points where they cross, they deflect vertically by an equal amount. Thus the moment carried by each is proportional to its bending stiffness. The amount of bending and torsion in each member of the linkage was determined and the stresses produced in each was calculated.

The scissor mechanism was also analyzed for axial and transverse loads resulting from rotational forces. The stresses due to these loads were negligible.

The substrate rollers were checked in the stowed position under the loads produced by the vibration environment. Buckling under combined bending and shear was checked. The screw jacks of the deploying mechanism were studied for stresses and deflections due to bending. Each screw was analyzed as a two span continuous beam and influence lines were used to determine the absolute maximum value of the moments and deflections. The sides of the housing act as a bracket to carry the roller and screw jack shaft loads to the vehicle. The bracket is subjected to concentrated loads in the plane of the web. These loads act in such a way as to cause bending and shear. The buckling strength of the box was determined and the ability of the box to carry all applied loads was established.

3.3 RELIABILITY ANALYSIS

3.3.1 Introduction

During the Phase I study, a preliminary reliability analysis of the scissors mechanism with flexible substrate was performed. Based on studies (Ref. 9) made in the field of mechanical and electro-mechanical devices, predictions have been made for selected components. Those studies were based on the fact that mechanical devices exhibit a wear-out characteristic. As the device approaches its wear-life the probability of a catastrophic failure becomes progressively greater. Where the ratio of operating time (t_{op}) to wear out life (t_{wo}) is low, the failures are essentially random. With an estimate of (t_{wo}) random failure rate can be determined.

For this analysis, the wear-life is calculated for the bearings, gears and clutch. The mission time for the Deployable Solar Array is such that the component parts will never realize their calculated life; therefore, only the effect of random failures are considered for these components.

The prediction for the spring motor is based on life data presented by Hunter Spring Company (Ref. 8).

No data is available for substrates and flexing conductors; therefore, the life of each of these items has been estimated.

3.3.2 Assumptions

The analysis assumes that the following conditions exist:

Mission time	-	25 cycles at one minute per cycle for a total time of 25 minutes (24 cycles for ground check and one cycle for flight.
Duty cycle	-	one minute per hour at 32 PRM

Degradation factor	-	100 for mechanical parts due to launch environment.

It is also assumed that the designer has selected and specified materials adequate for their intended use and the manufacturer has used these materials as specified, employing workmanlike methods.

3.3.3 Model for Solar Cell Deployment

The reliability block diagram is shown below with the mathematical model of the system.

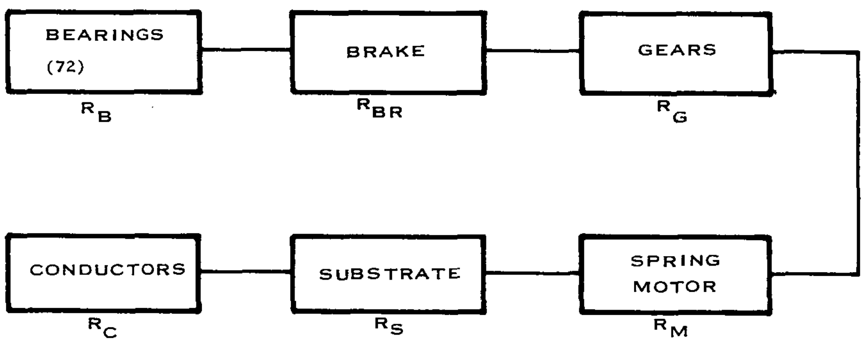

FIGURE 3.9 RELIABILITY BLOCK DIAGRAM

3.3.4 Failure Rate Estimate

The calculations of the individual terms of the reliability mathematical model and the estimating method is contained in Appendix III. Table 3.2 is a summary of the analysis results.

Making use of the mathematical model above the system reliability (R_{SYS}) is predicted to be approximately 0.9448.

Part	Failure Rate $X 10^{-6}$	Reliability of Part
Bearing	288	0.999712
Brake	8	0.999992
Gears	501	0.999500
Motor	992	0.999008
Substrate	5000	0.995013
Conductors	50000	0.951229
System	56789	0.9448

Failure Rate Summary

Table 3.2

3.4 THERMAL ANALYSIS

3.4.1 Introduction

This section of the final report presents a thermodynamic analysis of the final configuration of the deployable solar array. The configuration for this analysis is shown in Figure 2.20. A parametric configuration factor analysis was also performed using parameters of substrate separation distance, and angle of the solar flux.

This analysis also shows the effect of the radient interchange between the substrates on the operating temperature of the solar cells.

A steady state heat transfer mode was assumed with the maximum orbital heat fluxes, since an orbit had not been selected for the configuration. Results of the steady state analysis show that the efficient operating temperature of the solar cells was exceeded for the worst case conditions chosen, but were acceptable for a spin stabilized vehicle.

3.4.2 Assumptions

The assumptions for the preliminary analysis were:

- The sun could be at any angle to the solar array so that incident albedo, earth, and solar flux could be "seen" by the substrates.
- The orbital heat fluxes assumed were for the maximum value encountered.
- The steady-state condition was assumed because the orbit parameters were unknown.
- The material properties of the solar cells were lumped together and an effective value determined for simplicity.

This was also done for the substrates.

- The value of the solar absorptance and emissivity of the flexible foam were assumed to be 1.0 and 0.9, respectively. These are the maximum possible values for each.

- The effect of the configuration or view factor was assumed to vary as the distance between the substrates and angle of incidence.

3.4.3 Method of Analysis

The configuration factors were determined in parametric form. Their effect is on the radiant interchange between the substrates. Two cases were analyzed: 1) The sun was perpendicular to the solar cells and the total area of the substrates was not subjected to any orbital heat flux and 2) The angle of the sun to the substrate, at some point in the orbit allows the substrates to "see" solar, albedo and earth heat fluxes. An IBM 7090 computer program was utilized to determine these factors. This program computes the configuration factor given the spatial co-ordinates of emitter and of the receiver.

The problem of radiant interchange between the substrates has a definite effect on the temperature of the solar cell. In the first case mentioned above, total area of the substrates are at different temperatures so that the radiation can be given by:

$$q\,RAD = \sigma\, F_A F_\epsilon (A_1 T_1^4 - A_2 T_2^4)$$

where:

σ = stefan - boltzmann constant

F_A = configuration factor

F_ϵ = emissivity factor

A_1 & A_2 = areas of substrate

T_1 & T_2 = temperatures of each substrate

When the angle of the substrate or solar flux is such that the substrates "see" this flux, a slightly different problem occurs. The area of the substrate seeing this flux is now at a different temperature than the area adjacent to it. The radiant interchange is therefore different because: 1) The areas are at different temperatures and therefore different values of the radiant heat flux exist, 2) With these non-isothermal adjacent areas different, the configuration factor between these areas and the substrate parallel to it is also different. It could occur that this deployable array was at some angle in the orbit where the substrates not only "see" solar flux but also albedo and earth heat flux. This problem was assumed in the heat transfer analysis.

A steady-state heat transfer analysis was performed on the deployable solar array. The "worst" conditions of heat flux and angle of incidence were assumed to exist. This gave the maximum temperature to which the solar cells would be subjected. The array was allowed to be at some angle to the orbit plane in order that the total area of the substrates would "see" solar, albedo and earth heat fluxes. This is shown in Figure 3.10 and the angle assumed is 36^{o}. The corresponding incident fluxes were computed according to the cosine of the angle and are also shown in Figure 3.10. The material properties of density, specific heat and thermal conductivity are shown in Figure 3.11. These properties were lumped into an effective value for simplicity and identified as nodes 1 and 4 for the solar cells and nodes 2 and 3 for the substrate. The steady-state analysis was performed utilizing a two-dimensional heat transfer program. This was set up using the thermal model shown in Figures 3.10 and 3.11. The effective emissivity of the **nodes** 2 and 3 is given by

$$F_{\epsilon} = \frac{1}{\frac{1}{\epsilon_1} + \frac{1}{\epsilon_2} - 1} \quad \text{for parallel plates}$$

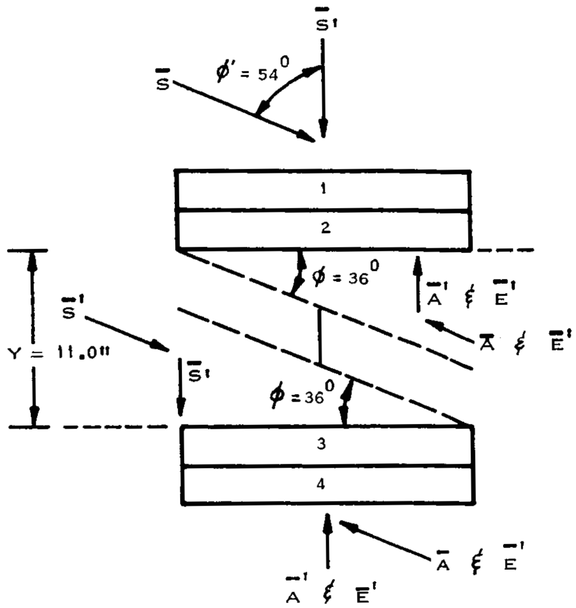

CALCULATION OF SOLAR, ALBEDO AND EARTH FLUXES

$$\bar{S}' = \bar{S} \cos \phi'$$
$$\bar{S}' = 453.2 \cos 54^0$$
$$\bar{S}' = 266.4 \text{ BTU HR-FT}^2$$

$$\bar{A}' = \bar{A} \cos \phi'$$
$$\bar{A}' = 0.52 \cos 54^0$$
$$\bar{A}' = 0.03056 \text{ BTU HR-FT}^2$$

$$\bar{E}' = \bar{E} \cos \phi'$$
$$\bar{E}' = 88.02 \cos 54^0$$
$$\bar{E}' = 51.74 \text{ BTU HR-FT}^2$$

NODES 1 & 4 SOLAR CELL AREA
NODES 2 & 3 SUBSTRATE AREA

FIGURE 3.10 THERMAL MODEL AND GEOMETRY FOR STEADY— STATE HEAT TRANSFER CALCULATIONS

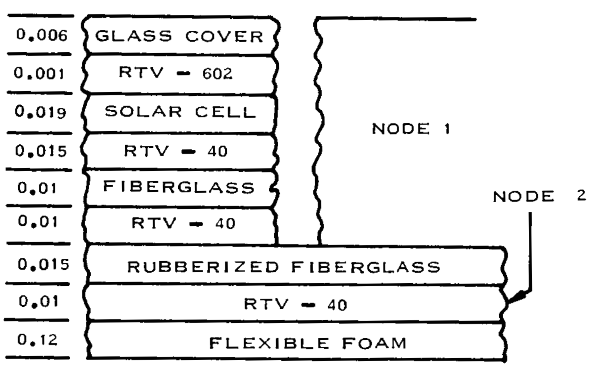

NOMENCLATURE

ρ = DENSITY = LB FT^3

C_P - SPECIFIC HEAT = BTU/LB-^{0}F

K - THERMAL CONDUCTIVITY = BTU/HR-FT-^{0}F

ALL DIMENSIONS IN INCHES

$\frac{\alpha}{\epsilon}$ OF SOLAR CELL = 0.78 0.82 (NODE 1)

$\frac{\alpha}{\epsilon}$ OF FLEXIBLE FOAM = 1.0 0.9 (NODE 2)

QUARTZ GLASS COVER
ρ = 137.346
C_p = 0.10 0.19
k = 0.8

SOLAR CELL
ρ = 145.2
C_p = 0.162
k = NEGILIGBLE

RTV — 602
ρ = 62.1
C_p = 0.365
k = 0.1

RTV — 40
ρ = 60.0
C_p = 0.5
k = 0.18

FIBERGLASS LAMINATE
ρ = 1.0886
C_p = 0.25
k = 0.01668

FLEXIBLE FOAM
ρ = 2.0
C_p = 0.2
k = 0.0111

RUBBERIZED FIBERGLASS—SILICONE
ρ = 60.0
C_p = 0.25
k = 0.1668

FIGURE 3.11 MATERIAL PROPERTIES AND DIMENSIONS FOR STEADY — STATE HEAT TRANSFER ANALYSIS

3.4.4 Results

The results of the configuration factor analysis are shown in Figures 3.12 and 3.13. In Figure 3.12 the results are for the first case, i.e., the sun perpendicular to substrate 1. This curve shows that the increasing distance between the substrates decreases the configuration factor. As the distance increases substrate 1 "sees" less of substrate 2's area. Figures 3.13a 3.13b show the results when substrate 2 "sees" the solar flux directly and the two adjacent non-isothermal areas exist. From Figure 3.13a, the configuration factor increases as the amount of substrate 2 "seeing" the heat flux increases. Then from Figure 3.13 the distance between the substrates increasing the configuration factor decreases. The steady-state temperature was calculated to be 197°F.

A less conservative analysis, using a spinning vehicle gave a maximum substrate temperature of 120° F. This analysis also assumed the transient mode rather than the highly conservative steady-state mode. In addition,

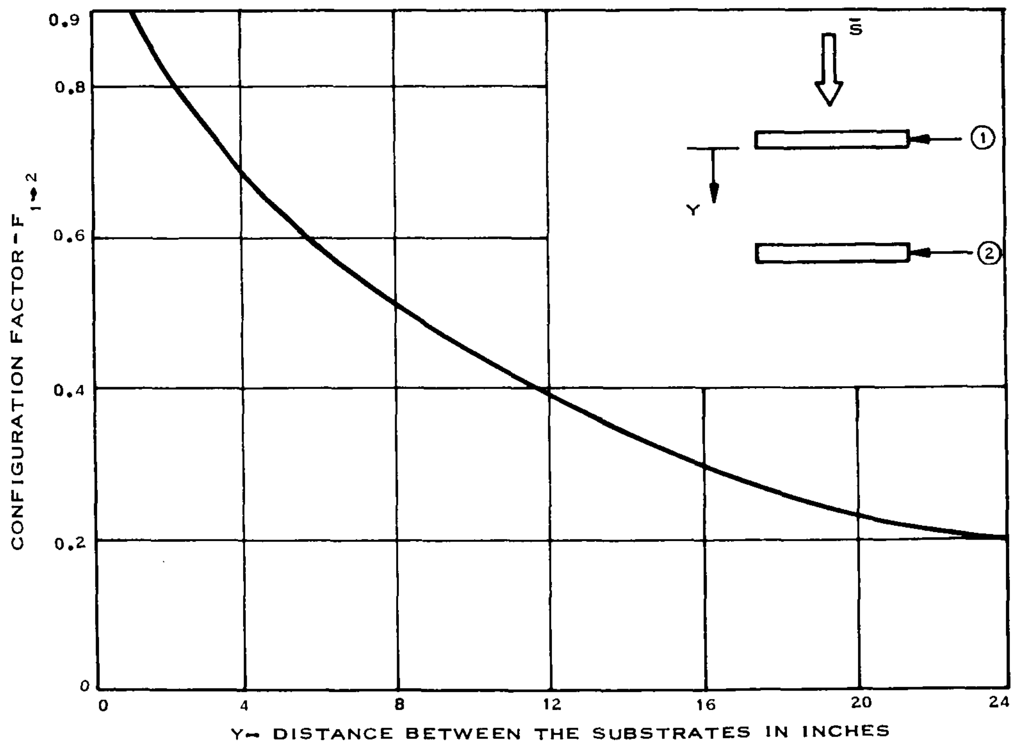

FIGURE 3.12 CONFIGURATION FACTOR BETWEEN SUBSTRATES WHEN THE SUN IS PERPENDICULAR TO ONE OF THE SUBSTRATES

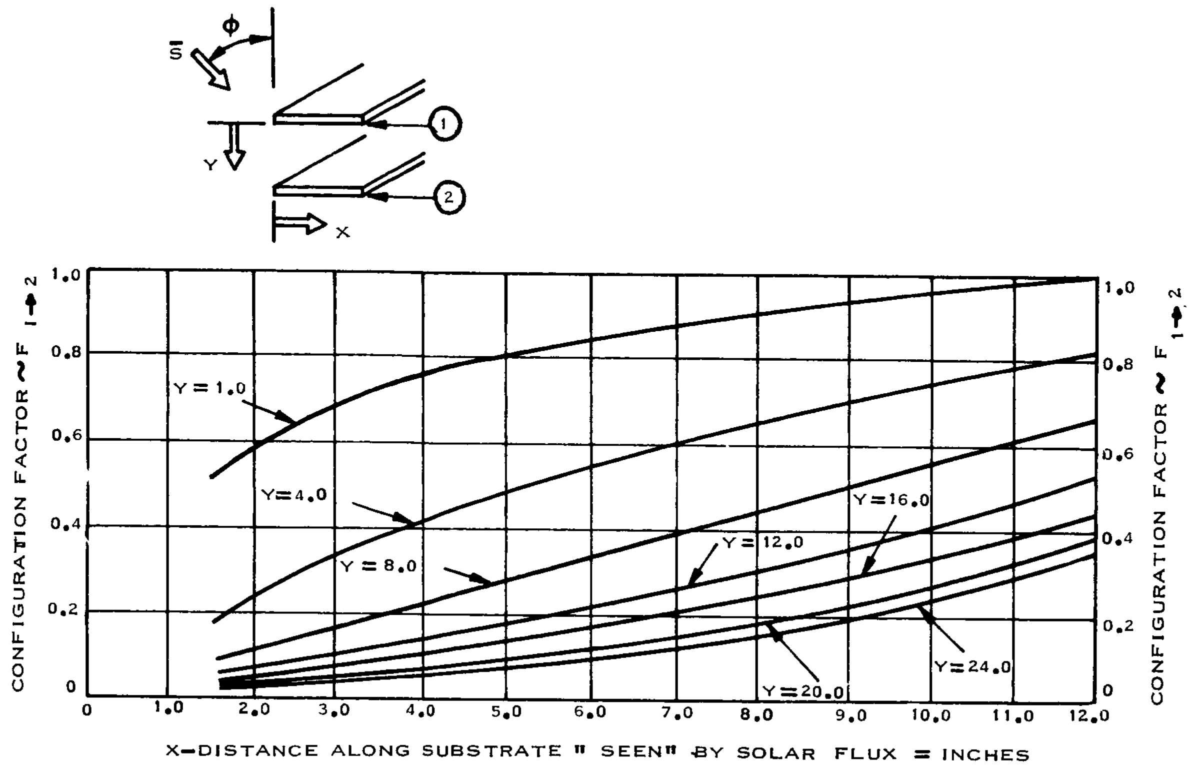

FIGURE 3.13A CONFIGURATION FACTORS FOR VARIOUS DISTANCES BETWEEN THE SUBSTRATES AT VARYING EXPOSED LENGTH OF SUBSTRATE 2.

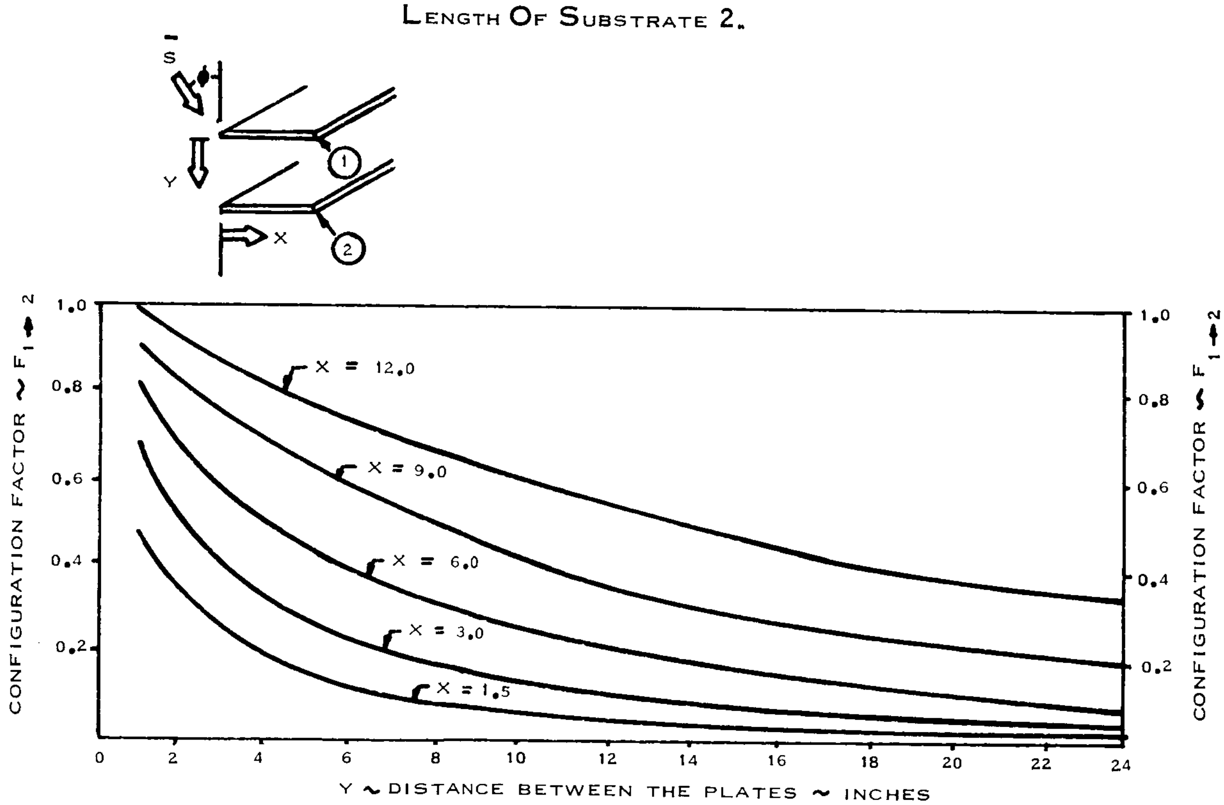

FIGURE 3.13B CONFIGURATION FACTORS FOR VARIOUS EXPOSED LENGTHS OF SUBSTRATE 2 AT VARYING DISTANCE BETWEEN THE SUBSTRATES.

this analysis approximated the three dimensional thermal system instead of using the one dimensional analysis used in the detail preliminary analysis.

3.4.5 Conclusions and Recommendations

The two analyses performed indicate a wide possible variation in temperature. For example, the assumed orbital parameters (a spinning vehicle versus a fixed vehicle in space), had the greatest influence on maximum calculated temperatures.

It is therefore recommended that specific orbital parameters (apogee, perigee, inclination) be defined. In addition, the limits on vehicle rotation and the array orientation with respect to body axis should be assessed. With these design criteria a detail thermal analysis may be performed and the operating efficiency of the arrays in space may be calculated.

3.5 WEIGHT SUMMARY

Table 3.3 presents a detailed weight summary of Configuration H. This table does not reflect exactly Table 2.3 preliminary data but is close enough to lend confidence that trade-off decisions are valid.

The item number appearing in the left hand column refers to item number on the layout (Figure 2.20).

TABLE 3.3

DEPLOYABLE SUBSTRATE SYSTEM

WEIGHT SUMMARY

Item No.	Nomenclature	Quantity	Total Weight
	Structure		
2	End Plate (Drive End)	1	.30
3	End Plate	1	.30
27	Housing	1	.35
28	Plate Assembly (Substrate Support)	1	.15
	SUB TOTAL		1.10
	Drive and Deployment Mechanisms		
54	Spring Motor	1	.10
4	Drum and Gear Assembly (Drive)	1	.11
5	Drum Assembly (Take Up)	1	.05
6	Gear Assembly (Idler)	2	.06
7	Gear (Pinion)	2	.02
8	Shaft (For Item 4)	1	.04
9	Shaft (For Item 5)	1	.015
10	Shaft (For Item 6)	2	.015
15	Ball Bearing Screw Assembly	2	.75
18	Bearing Block Assembly (Scr. Support)	2	.06
19	Pin (Scissors Links to B/B Nuts)	2	.02
30	Scissors Link (End Link)	1	.15
31	Scissors Links	7	.91
32	Scissors Half Link	1	.05
33	Scissors Link Assembly (End Link)	1	.23
34	Scissors Link Assembly	7	1.25
35	Scissors Half Link Assembly	1	.06

TABLE 3.3 (Cont'd)

Item No.	Nomenclature	Quantity	Total Weight
36	Scissors Hinge Pins	25	.08
29	Fitting - Support Plate Attach	1	.04
	SUB TOTAL		4.01
	Damper Mechanism		
11	Brake Drum	1	.16
12	Brake Shoe Assembly (Wt. & Friction Pad)	2	.20
13	Intermediate Gear	1	.05
14	Brake Lever and Gear	1	.05
52	Shaft (For Item 13)	1	.07
53	Gear and Clutch Assembly	1	.07
	SUB TOTAL		.60
37	Release System	1	.30
	SUB TOTAL		.30
50	Substrate	2	
	Membrane		.21
	Stiffners		1.11
	Adhesive		.50
	SUB TOTAL		1.82
	Electrical System		
	Cells Bond and Cover Glass		4.50
	Wiring and Interconnections		.52
	SUB TOTAL		5.02
	Miscellaneous		
	Bearings		.18
	Fasteners		.15
	SUB TOTAL		.33
		TOTAL	13.18

4.0 RECOMMENDATIONS AND CONCLUSIONS

This final report presents the results of a study to select an optimum design for a compact storable solar array system for use with stabilized satellites. The study has culminated in a final design using a flexible substrate with a scissors type extension mechanism. The scissors are driven by constant torque spring driven screw jacks and controlled during deployment by a centrifugal brake mechanism. Fairchild Hiller believes that for the conditions stipulated in the contract, the design submitted is near optimum. It is a trade-off of packaged volume, and power/weight versus cost.

All of the contract requirements have been met or bettered except the requirement for a 12 lb. package. The design as submitted, is 1.18 lbs. overweight. This is due to the design requirements of static deployment under 1 g and also the package depth of 4 inches. The first imposes higher loads than are necessary to fulfill the mission in space and the latter makes it necessary to use thin inefficient structural members to take these loads. A considerable weight saving could be made by the use of a deployment fixture for static test or by deploying the substrate downward. This would also help simulate the loads incountered during the spin condition. A further weight saving may also be made by the use of lighter weight cells now under development and close control of the substrate manufacture especially in the area of bond thicknesses.

During this study an investigation was made to determine the parameters for the box depth. Figure 4.1 shows these parameters. For the investigation a .10 inch thick substrate was assumed. The two cases plotted are for mechanisms composed of a 12-inch linkage with .38-inch thick members and a 24-inch linkage with .50-inch thick members. The 12-inch linkage design is similar to the one submitted. The 24-inch linkage would be a system rotated 90° from the orientation of the specified system. It was found that for the present packaging with 12-inch links, the panel length is "substrate limited" up to 6.7 feet and thereafter is "link limited". For the 24-inch links the panel length is limited to 16.7 feet by the substrate and thereafter is also "link limited". If the rotated system could be adopted, the full packaged volume would be used. From Figure 4.1 it is seen that if the depth of the box were increased to approximately 5.50 inch and a 24-inch wide substrate used, four times the area could be deployed from only slightly more than twice the present package size. It is also possible that a more efficient packaging of the array could be made if the relationship between spacecraft and fairing were known. Figure 4.2 is an investigation of the effect of substrate thickness on package depth. Note in Figure 4.1 and 4.2 that for packages less than 1.25-inches no length of substrate is obtained. This is due to the excessive bending of the solar cells on a small diameter roller.

For Phase II it is recommended the requirement for tilting the package relative to the spacecraft be included. This requirement was not made in Phase I. Four flat panels on a spinning vehicle will not provide power throughout a one year mission.

Another recommendation for the design is a central drive and synchronizing system to deploy all panels at a uniform rate.

The feasibility of a flexible system has been proven through fabrication and test of several sample substrates. Additional effort is needed: 1) for developing manufacturing processes to reduce the cost of assembly, 2) for testing to obtain high confidence levels of reliability, 3) for developing methods of replacing cells on the substrate after manufacture, and 4) for obtaining higher cell packaging efficiencies.

During the study it was found that the temperature for the solar cells arrived at through our generalized analysis is very marginal. For a more refined analysis, the specific orbital parameters are needed.

In the dynamic analysis it was found that the angular velocity of the spacecraft system is reduced to approximately 40 RPM after full deployment of all panels. This could possibly eliminate the need for a despin system onboard the spacecraft, thereby reducing weight of the overall system.

The reliability of the system is high and results from a conservative design using proven parts.

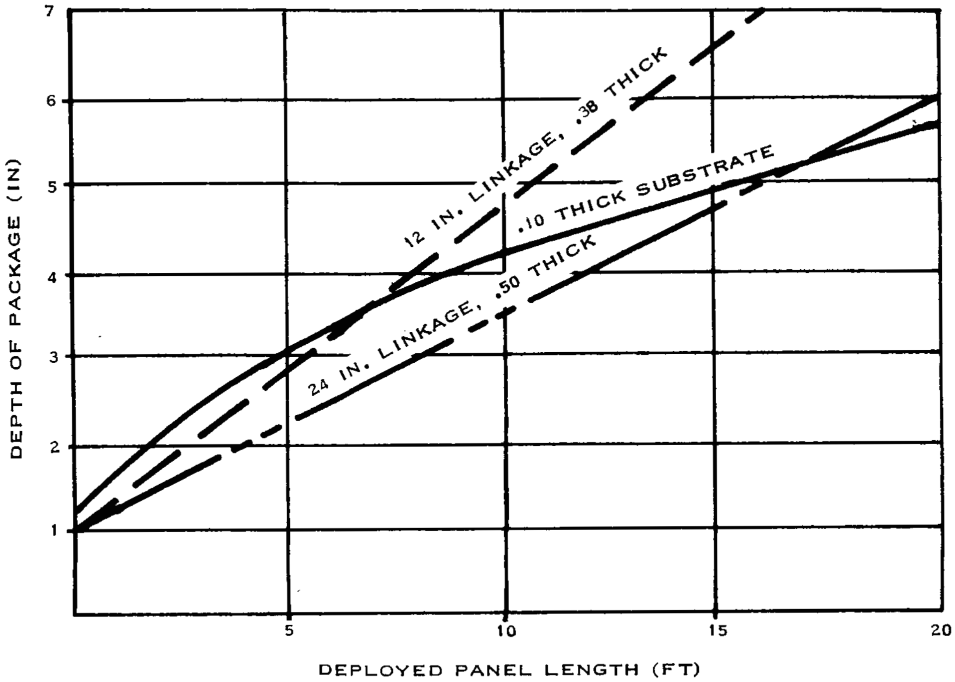

FIG. 4.1 STUDY OF PANEL LENGTH LIMITING PARAMETERS

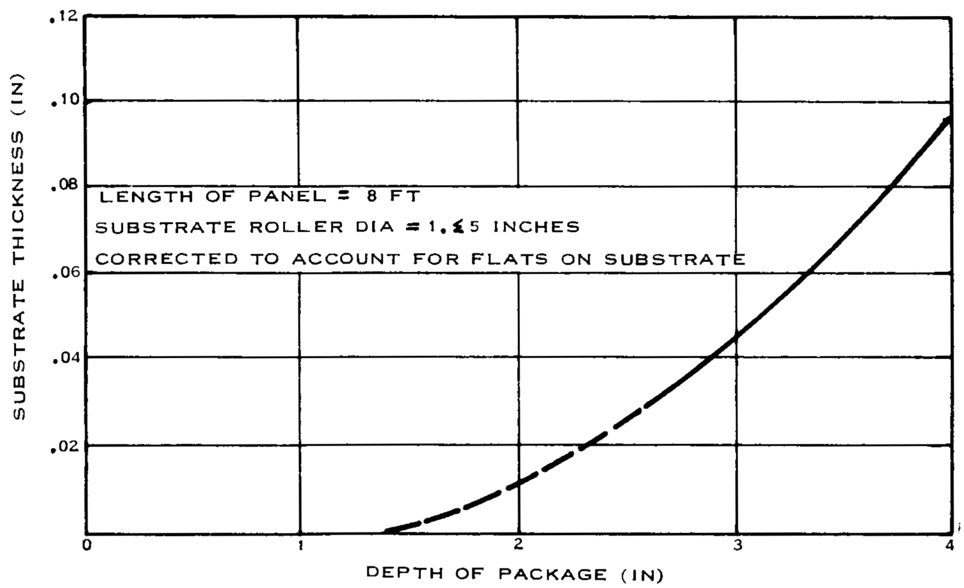

FIG 4.2 SUBSTRATE THICKNESS VS. PACKAGE DEPTH

5.0 PHASE II AND III PROGRAM PLAN

5.1 INTRODUCTION

Phase II will consist of design refinement of the structural-mechanical system followed by a final analysis of the detailed parts and a re-analysis of the complete solar cell array. This final analysis will cover structural, dynamic, thermal, and reliability areas. The manufacture of the proof of principle model for Phase II and the flight type articles of Phase III will be manufactured in the model shop of Fairchild Hiller. A test plan has been written for Phase II and Phase III and is presented in this section. The Q. C. and reliability plans are also submitted in this section.

5.2 DESIGN

A refinement of the design will be made to take into account any new operating requirements and to reduce the cost and weight of the system. Upon completion, detailed drawings will be made to Fairchild Hiller Corporation standards. These drawings will start with the long lead time items which are the centrifugal brake and the drive screw jacks. Orders for purchased parts for the Deployable Solar Array will be started as soon as the design refinement has been completed. Raw materials for the design will be purchased early in the program. The materials specified are plentiful and no difficulty is expected in obtaining the needed quantities. Liaison with the model shop will be provided by the design group and will extend for the full length of manufacture and test. Phase III liaison will be covered by the Project Engineer since only minor design changes are expected.

5.3 MANUFACTURING AND ASSEMBLY

The manufacturing and assembly for the mechanism will be in the model shop of Fairchild Hiller Corporation, Bladensburg, Maryland. This work will be monitored by the Project Engineer and the quality and reliability section of the corporation. Any further development of the substrate will be at Fairchild Hiller Corporation's facility in Hagerstown, Maryland.

5.4 ANALYSIS

The stress calculations presented in the Phase I report will be revised as design changes are made. Any other areas deemed necessary will also be analyzed in Phase II. Detailed drawings will be checked by the stress group, who will, in addition, provide drawing change coverage during the manufacture and test period. The stress group will also make an analysis of all test fixtures. The Phase III task of this group will be material review action and drawing change coverage necessary to complete the flight worthy articles.

The Dynamics group support during Phase II and III will include recommendations on new parameters to be used for the centrifugal brake, a revision of the vibration analysis to take into account the spacecraft stiffness, and analytical backup during spin testing of the complete system.

A further thermal analysis is necessary for this system. This analysis should include detailed orbital information and will also attempt to put in more precise values for material properties. The latter may require some test.

5.5 TEST PROGRAM

A two part test program is contemplated to support and evaluate Phase II of the Deployable Solar Array Program. The first will include engineering development tests of components of the Proof of the Principle Model. The second part of the test program will accomplish an environmental test program of the Proof of the Principle Model utilizing a dummy flexible substrate. Figure 5.1 presents a flow diagram of the proposed tests program program.

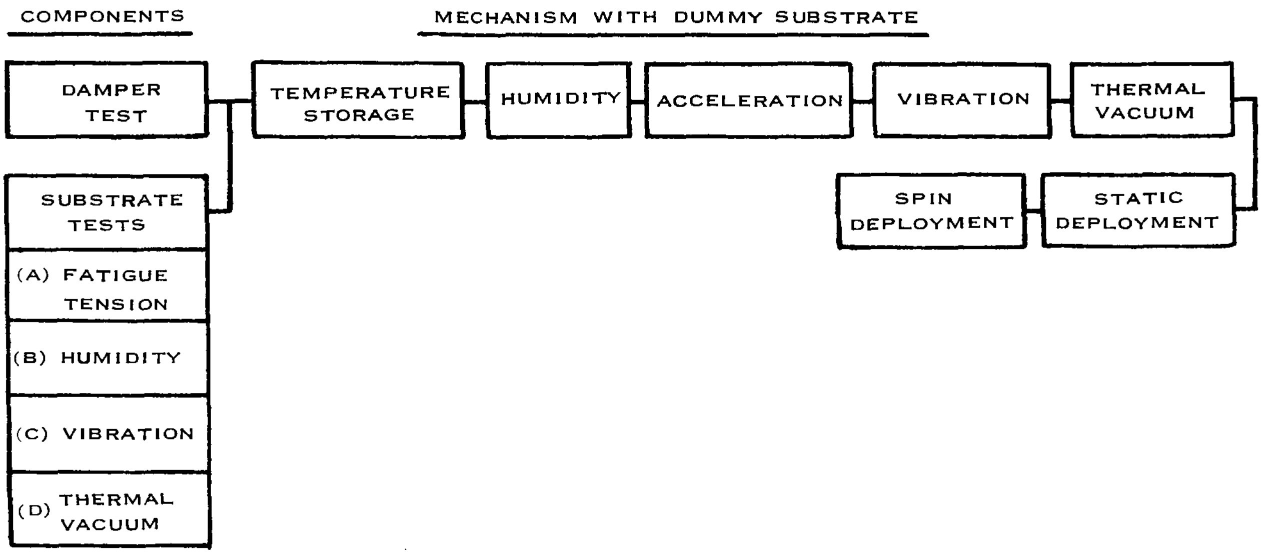

FIGURE 5.1 DEPLOYABLE SOLAR ARRAY TEST PROGRAM BLOCK DIAGRAM

5.5.1 Development Tests

The first part of the test program will be concerned with engineering development tests to demonstrate the operational capability of the mechanical components and subsystems. The damper component shall be the first subsystem tested. Since it was not originally proposed to test live solar cells on the Proof of Principle Model, it is recommended a sample substrate of live and simulated cells be subjected to a limited number of developmental tests. In order to obtain representative and realistic load environments during these tests, the total mass of solar cells must be included on the array. However, to prevent excessive costs, Fairchild Hiller proposes to simulate the cell mass with a combination of actual cells and mass-size simulated aluminum strips. A pattern and distribution of the actual cells will be selected to provide representative conditions throughout the panel array. Visual and electrical examination of the test specimens will be conducted at least before and after its exposure to each test environment. The following outline constitutes a basic plan describing the suggested environments to be experienced by the developmental units.

5.5.1.1 Substrate Developmental Tests

Fairchild Hiller is suggesting that in addition to testing the Proof of Principle Model, a sample substrate containing an arrangement of actual and simulated cells be subjected to the following environments to investigate the structural integrity of the flexible substrate concept. The substrate shall be rolled on a drum in the same manner as the actual deployment array during these tests.

- Fatigue - Tension Test
  The substrate shall be subjected to a tension and fatigue test by cycling the test unit on a spring loaded drum. The fatigue shall be experienced by repeated flexures around the drum and the tension load is applied by the spring loaded drum when the substrate is in an extended position. See Figure 5.2.

- Humidity Tests
  The substrate will be rolled on the drum and suspended or mounted in a Bowser Humidity Chamber and subsequently subjected to a high humid atmosphere. Test Criteria: 24 hrs @ 30° C and 95% R.H. A visual examination of the specimen will be performed before and after exposure to the environment. Principal environmental effects of the test unit to be investigated are:
    a. corrosion
    b. swelling
    c. deterioration

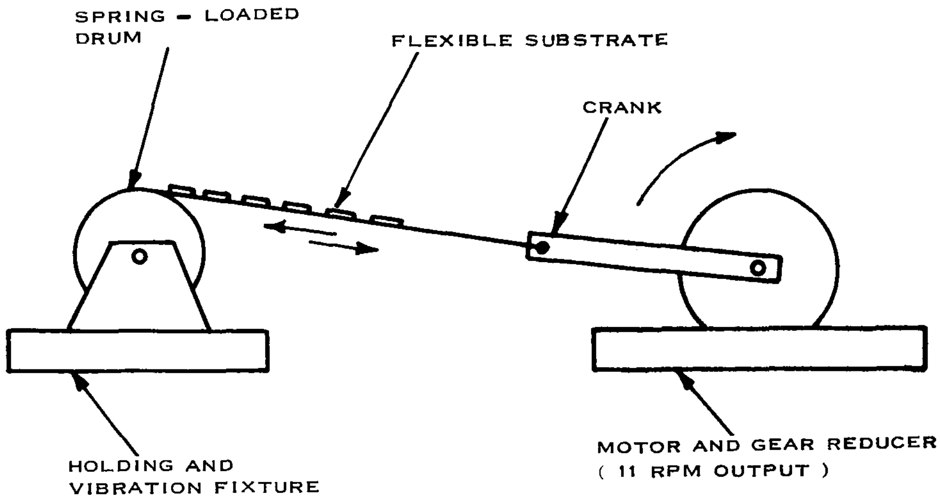

FIGURE 5.2 TENSION-FATIGUE TEST SCHEMATIC

d. loss of strength
e. other changes in mechanical properties
f. adhesive degradation

- Vibration Test

  Part of the suggested evaluation of the proposed deployment solar array will consist of a development vibrations test of a sample substrate containing an arrangement of live and dummy solar cells. Since live cells were not proposed on the Proof of the Principle Model, Fairchild Hiller is suggesting an additional vibration test to cover the concept of the live cells attached to a flexible substrate. For developmental testing the frequency range of 5 to 3000 cps shall be used, however, since the sample substrate is smaller than the actual substrate, the input levels shall be determined by analysis and subjected to a constant sweep rate of 2 octaves/minutes. Major resonant frequencies of the specimen will be determined during each axis of excitation and for each critical frequency noted. A 5-minute resonant dwell will be performed at that frequency. Test levels for the resonant dwell will be one-half the levels used for the sinusoidal sweep test.

- Thermal Vacuum Tests

  The substrate test unit will be mounted or suspended within a space chamber and the chamber pressure reduced to 10^{-7} Torr. The specimen will be heated (using heating blankets) to a temperature of $+70^{o}$ C until stabilization of it is realized. Temperature to the specimen will then be lowered to -70^{o} C until stabilization is reached. While maintaining the specified chamber pressure level, three complete temperature cycles shall be completed.

  A visual examination of the test unit will be performed before and after exposure to the environment to evaluate any changes to physical and chemical properties of specimen materials.

5.5.1.2 Damper Developmental Tests

A mock-up of the centrifugal brake will be fabricated and tested utilizing a calculated load which will be expected from the drive mechanism. The damper will be static tested at this time to demonstrate its operation characteristics and capability. This information is required for adjustments during the static and spin deployments.

5.5.2 Environmental Test

The second part of the test program will consist of a carefully planned and executed sequence of environmental tests conducted on the Proof of the Principle assembly deployable solar array. The proposed test environments are designed to simulate the array aerospace environments experienced on a typical spacecraft during shipping, ground handling, and storage, power flight and space exposure. The sequence of test environments will be performed, as nearly as possible, to an actual operational sequence so as not to impose unrealistic environmental interaction effects on the test unit. Overall test results will be used to substantiate the structural integrity of the Proof of the Principle unit and to conclusively demonstrate the operability of the solar array deployment system.

In order to obtain representative and realistic load environments during these tests, the total mass of solar cells must be included on the array of the selected configuration. The cost of simulating this mass with actual cells would be prohibitive. Therefore, Fairchild Hiller proposes to simulate the cell mass with mass-size simulated aluminum slips.

During its acceleration and vibration environment, the test specimen will be adequately instrumented to effectively measure its static and dynamic characteristics. Stress levels and dynamic responses determined from the test data will be compared to the design analysis to conclusively substantiate the structural integrity of the deployable solar array design configuration. Visual examination of the test specimen will be conducted at least before and after its exposure to each test environment. The following outline constitutes a basic test plan describing the minimum environments the Proof of the Principle unit will experience. It is understood that a spacecraft has not been established to carry a deployable solar array payload. Typical aerospace test criteria are presented as test environments for this program where ever the environment was not specified in the RFP. All the test conditions described in this proposal are in accordance with portions of the following documentation:

a. Guidelines for research and development of deployable solar arrays (from GSFC).

b. Mil-STD-202B - Test Methods of Electronic and Electrical

Component Parts, 3/14/60.

c. Mil-STD-810 - Environmental Test Methods for Aerospace and Ground Equipment, 6/14/62.

5.5.2.1 Temperature Storage Test

To evaluate the effects of long term storage, the test unit (in its packaged configuration) will be suspended in a Bowser Test Chamber and subjected to the following temperature storage environment:

6 hours @ -20^{o} C

6 hours @ $+60^{o}$ C

The specimen will be visually inspected before and after each test condition to determine the effects of the temperature environment on the test unit.

5.5.2.2 Humidity Test

While in its folded configuration, the test unit will be suspended or mounted within a Bowser Humidity Chamber and subsequently subjected to a high humid atmosphere, such as encountered in tropical areas. Test Criteria:

24 hours @ 30^{o} C and 95% R.H.

A visual examination of the specimen will be performed before and after exposure to the environment. Principal environmental effects of the test unit to be investigated are:

a. Corrosion
b. Swelling
c. Deterioration
d. Loss of Strength
e. Other changes to mechanical properties
f. Adhesive degradation

5.5.2.3 Acceleration Test

To substantiate the structural integrity of the selected substrate for its anticipated steady-state powered flight loads, the test unit (in its in-flight rolled configuration) will be mounted to a rotary accelerator and subsequently subjected to three minutes of a combined axial thrust and radial (due to spin) acceleration. Actual test levels will be defined at the time of test. For proposal purposes, the following typical conditions are assumed: See Figure 5.3.

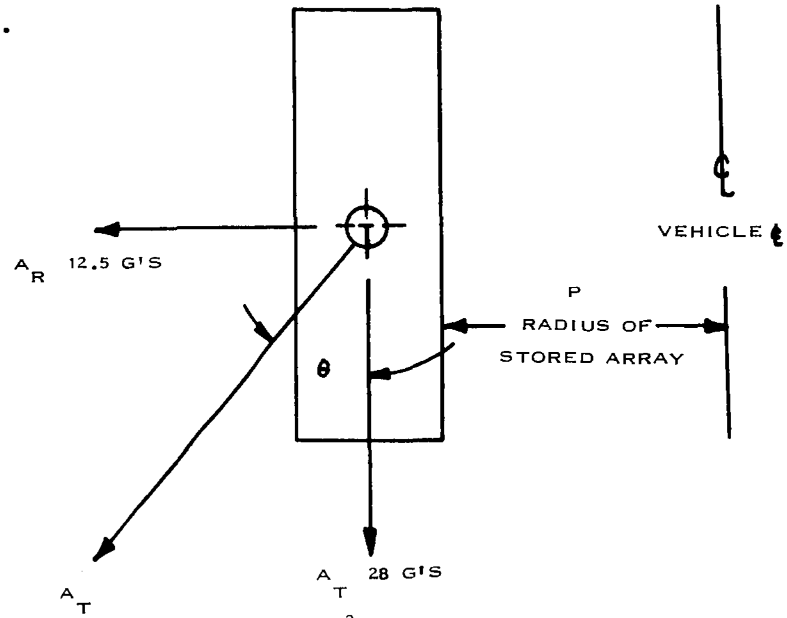

$$A_T = (12.5^2 + 28^2)^{1/2}$$

$$= 31 \text{ G'S}$$

$$\text{TAN } \theta = \frac{12.5}{28} = .445$$

$$\theta = 24^0$$

FIGURE 5.3 LOAD DIAGRAM FOR ACCELERATION TEST

Adequate strain gage instrumentation will be provided and continuously recorded during the test to conclusively evaluate the effects of the acceleration environment on the test unit structure.

5.5.2.4 Vibration Test

Part of the overall evaluation of the proposed deployable solar array substrate will consist of a development vibrations test. To perform the vibrations environment test, a versatile and flexible group of vibrations systems are available at both the Fairchild Hiller Bladensburg Test

Laboratory and its affiliated Aerotest Laboratories in Long Island, New York. The available systems are capable of performing sinusoidal, random or combined sine/random noise testing.

To provide the specified vibrations test levels to the prototype unit, a Ling A300-B Vibration System is proposed for this test. The system provides a 8000 pound sinusoidal force output with an automatic cycling frequency range of 5 - 3000 cps. Its 12 inch (bolt circle) table also provides 5000 lb. RMS random output force with half peak-to-peak displacement. Instrumentation available for this test includes two 7 Channel Sanborn Tape Recorders capable of simultaneously and continuously recording 12 channels of accelerometers. A narrowband analyzer and X-Y plotter are available for playback of the accelerometer data and its presentation as plots of accelerometer vs. frequency or power spectral density vs. frequency.

Approximately 6 accelerometer channels in each axis of excitation are contemplated to be continuously recorded. The test unit, while secured in its folded configuration, will be mounted to a shaker drive fixture and subsequently subjected to the following three major axis sine and random vibrations environment.

The input test levels specified in Table 5.1 are to the spacecraft interface. Past experience indicates that spacecraft amplifications of 4 to 1 are possible within the frequency range of 50 to 200 cps. Therefore, actual input levels to the test unit (for this program) will be determined at the time of tests and may be increased as much as 4 to 1 for the bandwidth of 50 to 200 cps.

TABLE 5.1 VIBRATION TEST LEVELS

A. Sinusoidal Tests

Frequency (cps)	Thrust Axis (z) (g's)	Transverse Axis (x&y) (g's)
5-50	2.3	0.9
50-500	10.7	2.1
500-2000	21.0	4.2
2000-3000	54.0	17

Constant sweep rate of 2 octaves/minute

B. Random Test (each axis)

Frequency Range (cps)	PSD Amplitude (g^2/cps)	(g-rms)	Duration Min.
20-2000	.07	11.5	4.0

Major resonant frequencies of the specimen will be determined during each axis of excitation and for each critical frequency noted. A 5-minute resonant dwell will be performed at that frequency. Test levels for the resonant dwell will be one-half the levels used for the sinusoidal sweep test.

An evaluation of the test results will be used to support the analysis performed and to substantiate the structural integrity of the substrate for its anticipated powered flight vibrations environment.

5.5.2.5 Thermal Vacuum Test

The Proof of the Principle unit will also be subjected to a thermal vacuum (cycling) test to determine if a typical orbital temperature/vacuum environment is detrimental.

The test unit will be mounted or suspended within a space chamber and the chamber pressure reduced to 10^{-7} Torr. The specimen will be heated (using heating blankets) to a temperature of $+70^{o}$ C until stabilization of it is realized. Temperature to the specimen will then be lowered to -70^{o} C until stabilization is reached. While maintaining the specified chamber pressure level, three complete temperature cycles shall be completed.

A visual examination of the test unit will be performed before and after exposure to the environment to evaluate any changes to physical and chemical properties of specimen materials.

5.5.2.6 Static Deployment Test

The Proof of the Principle Model shall be mounted on a fixture and deployed under a static environment and at this time, the release system, the drive mechanism, and the damper shall be adjusted and proven. These systems may require additional adjustment during the spin deployment and if so, the static deployment will have to be rechecked.

5.5.2.7 Spin Deployment Test

The spacecraft spin rate at deployment is estimated to be as high as 160 rpm. To demonstrate the performance of the solar array deployment system under a dynamic environment, the Proof of the Principle unit will be mounted to a rotating fixture and a limited deployment of the solar array will be performed. Should it be necessary to perform a full scale simulated satellite deployment, the dynamic vacuum chamber located at Goddard Space Flight Center should be considered.

5.6 PRODUCT ASSURANCE

Product Assurance is intrinsic to Fairchild Hiller's functional organization. Quality and reliability assurance activities are planned and time phased to provide assurance that contract requirements are satisfied starting in the design phase and continuing through to the use phase. To accomplish this,

- A quality system is maintained
- Reliability analysis is initiated during the conceptual stage
- The failure reporting and analysis system provides feedback to designers
- Inspections and test results are recorded to provide documented evidence of quality
- Product assurance tasks are planned in conjunction with the total program and experienced personnel are assigned to each task

5.6.1 Preliminary Inspection Plan

For Phase II and III of the Deployable Solar Array Program, an inspection plan will be prepared. The plan will be made available to GSFC upon request. A preliminary inspection plan consistent with Phase requirements has been prepared and is contained in Table 5.2. NASA Quality Publication NPC 200-3 has been used as a guide and for convenience, the preliminary plan has retained the paragraph numbering system of that specification. The Inspection Plan will provide further details for the implementation of each function and the controlling media.

Table 5.3 is the program reliability tasks for Phase II and III.

5.7 SCHEDULE

Figures 5.4 and 5.5 are the proposed schedule for Phase II and III respectively.

Table 5.2 PRELIMINARY INSPECTION PLAN - DEPLOYABLE SOLAR ARRAY

NPC 200-3 Paragraph Number and Requirement		Proposed Effort
2.2	Preparation and Submission of Inspection Plan	Prepare Phase II Detailed Inspection Plan for Deployable Solar Array including product flow chart and inspection stations.
2.3	Supplier's Obligation	Maintain surveillance over all inspection and test activity. Prepare and/or review procedures for inspection and test.
2.4	Drawing and Change Control	Review production drawings and changes. Provide configuration control sheets in inspection logs for test articles and the Proof of Principle model. Check log prior to unit acceptance for incorporation of all required changes.
3.1	Control of Procurement Sources	Review purchase requisitions for inclusion of requirement for source inspection, test criteria, test reports or other data. Review purchase orders and revisions to assure incorporation of requirements.

Table 5.2 - (cont'd)

NPC 200-3 Paragraph Number and Requirement		Proposed Effort
3.2	Government Source Inspection Requirements	In consonance with GSFC requirements, determine need for Government Source Inspection. Assure incorporation of appropriate statement on purchase order.
3.3	Government Furnished Property	There is no requirement for GFP. If at a later date, property is furnished by the Governement, appropriate controls will be initiated.
3.4	Identification, Handling and Storage of Material	Identify materials to be used for Phase II Deployable Solar Array at receiving inspection. Identification to remain with material through all subsequent inspection, storage and manufacturing activities. Apply other markings (i.e. material color code, markings for test, evaluation or breadboard, etc.) as required. Audit for proper handling and storage or materials.
3.5	Control of Raw Material	Ensure that physical and chemical test reports are furnished by the supplier. When deemed necessary, provide check analysis of supplier reports.

Table 5.2 - (cont'd)

NPC 200-3 Paragraph Number and Requirement		Proposed Effort
3.6	Inspections and Test	Perform inspections as required by inspection plan and applicable procedures. Provide procedures for special items. Develop inspection log concurrent with model development stage.
3.7	Process Control	Survey processes in accordance with applicable procedures. Ensure that all processes utilized are controlled. Perform audits to assure conformance.
3.8	Nonconforming Articles	Identify and segregate nonconforming articles. Prepare discrepancy report and make appropriate decision. Refer minor discrepancies which cannot be economically re-worked to materials review. Materials Review is to refer nonconformances affecting fit, form function.
3.9	Control of inspection, Measuring and Test Equipment	Ensure conformance of articles by providing for the use of equipment calibrated against standards traceable to national standards and displaying a sticker with the next calibration due date.

Table 5.2 - (cont'd)

NPC 200-3 Paragraph Number and Requirement		Proposed Effort
3.10	Indication of Inspection Status	Indicate inspection status of materials, parts and assemblies with stamps bearing individual inspectors identification number.
3.11	Preservation, Packaging, Packing and Shipping	Assure conformance to contractual requirements. Review drawings of shipping containers. Inspect articles prior to and subsequent to packing.
3.12	Sampling Inspection	Sampling Inspection, if employed, will be included in the Inspection Plan. Present plans do not envision sampling inspection for the proof of principle model.
3.13	Records of Inspections and Tests	Perform inspections as specified by the applicable procedure. Maintain records of all inspections and provide documented evidence of product quality. Make records available to the GSFC designated representative upon request.
3.14	Corrective Action	Take action to correct conditions which result or might result in substandard or defective articles being supplied to GSFC.

Table 5.3 RELIABILITY TASK LISTING

Task	Description
Document Review	A reliability engineer will review design specifications, drawings, processing procedures, test procedures and test reports for the purpose of ascertaining that these documents adequately and validly state the performance and environmental requirements, and that the test criteria is defined.
Reliability Analysis	The production model for the system shown in Section 2.0 will be revised as the detail design is evaluated and the reliability analysis progresses. The model will be utilized to identify potential problem areas, guide design trade-off, and determine areas where further reliability analysis is required. The possible modes of failure and the effects on mission success will be determined. The analysis will provide criterion for the establishment of checkout procedures.
Testing	The test program for Phase II is defined in Section 5.5. The test results will be used to verify the design performance of the Deployable Solar Array and to identify interactions and design weaknesses. Cycling tests to failure and overstress testing have not been incorporated into the test program; consequently, reliability demonstration is not a part of the Phase II Program.

Table 5.3 - (cont'd)

Task	Description
Testing (cont'd)	Testing will be performed to test procedures which will identify environmental and performance conditions, test sequence and time, data to be recorded, equipment to be used, and calibration requirements. Failures, should they occur, will be recorded and an analysis performed to isolate the cause for the purpose of initiating correction action. Test reports will identify all action taken.
Parts and Materials	Every effort will be made to select parts and materials on the basis of proven qualification. Parts and materials planned to be employed in the construction of the Deployable Solar Array will be adequately defined by Government specifications. In the event that adequate specifications do not exist, Fairchild Hiller will prepare supplementary specifications.

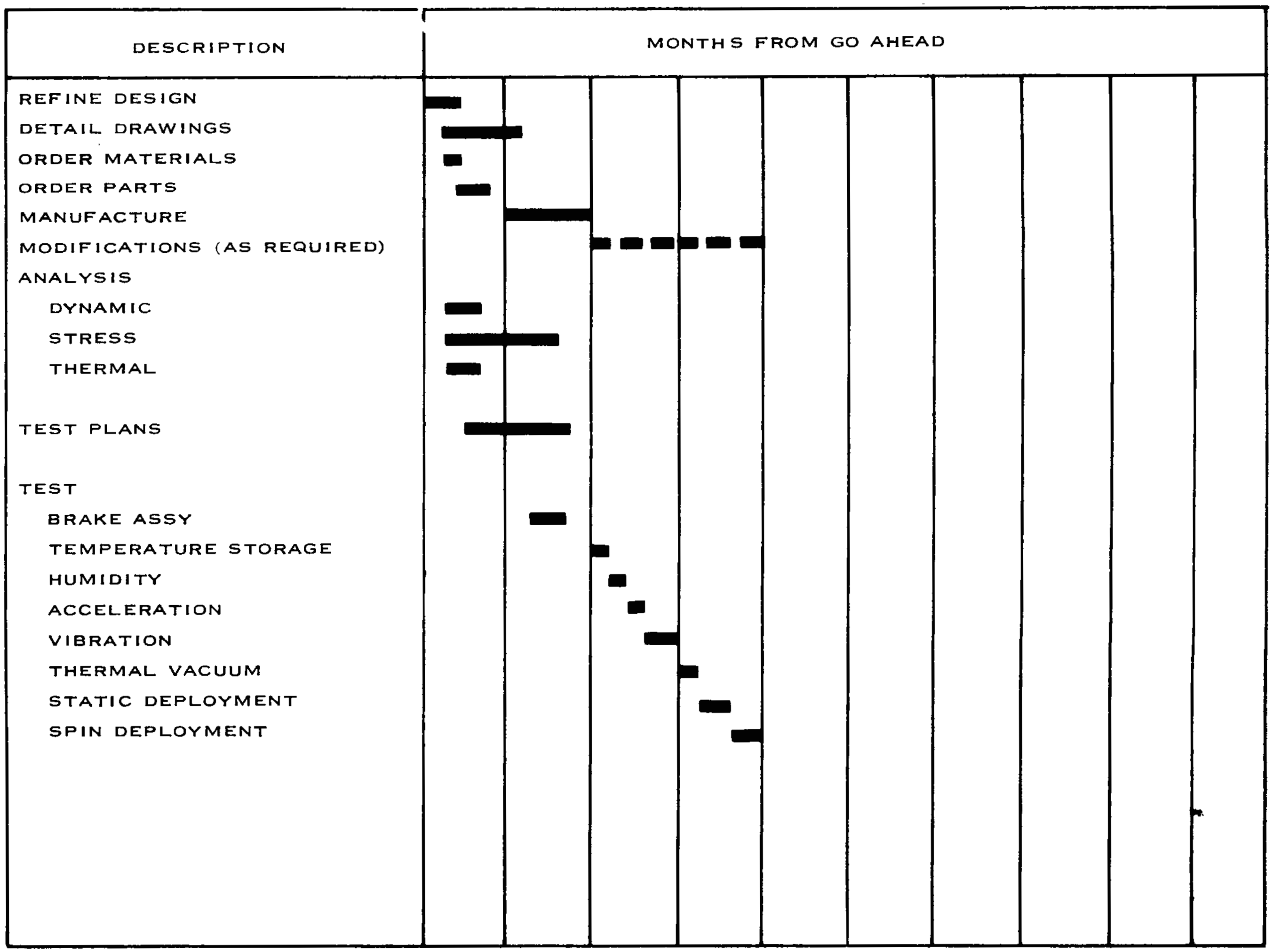

Figure 5.4
Phase II Schedule

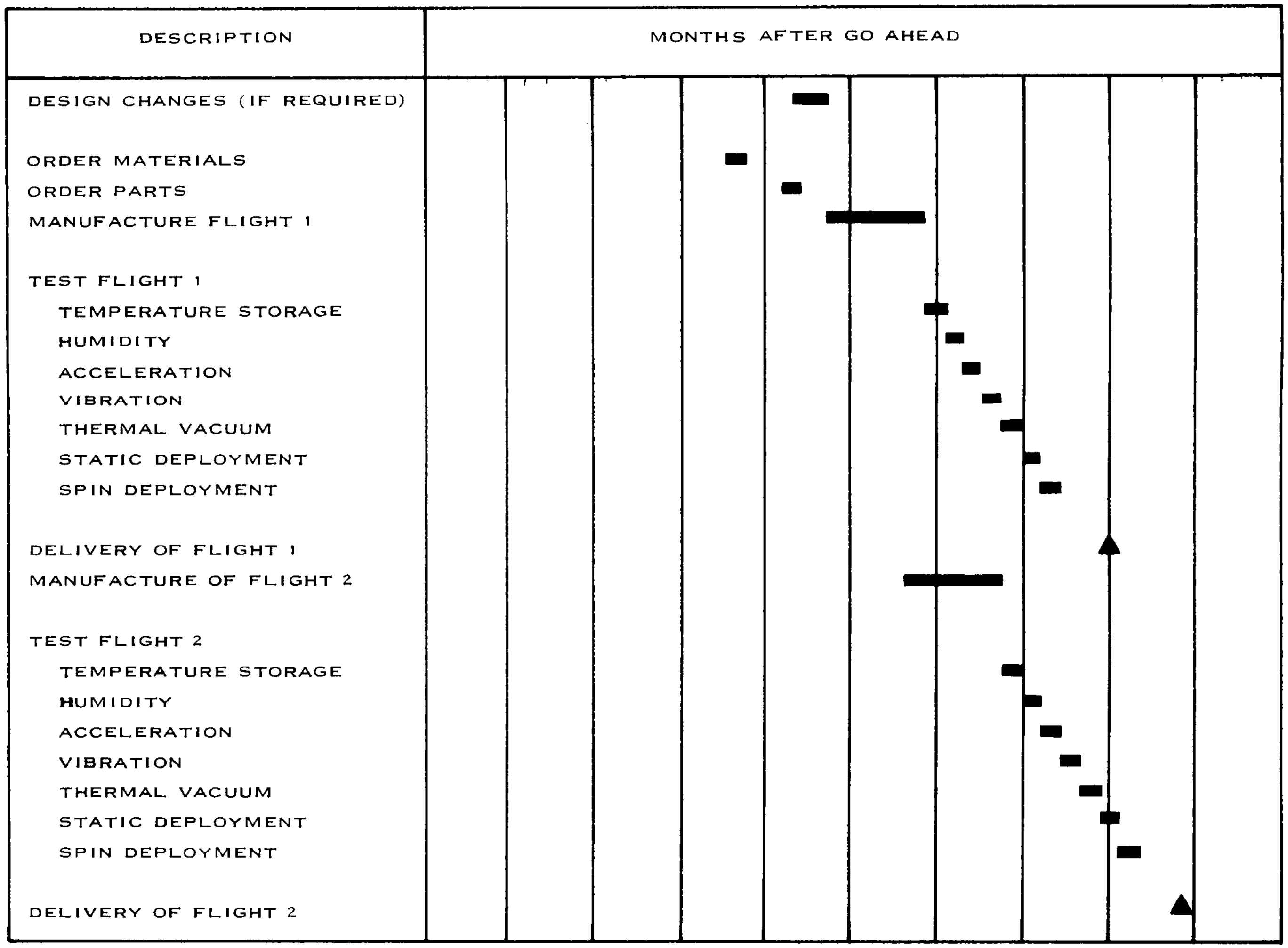

FIGURE 5.5
PHASE III SCHEDULE

6.0 NEW TECHNOLOGY

No new inventions have been disclosed as a result of this contract.

PRECEDING PAGE BLANK NOT FILMED.

7.0 BIBLIOGRAPHY

1. Formulas for Stress and Strain, Roark, R. J., McGraw Hill Book Company

2. MIL Handbook 5

3. MIL Handbook 17

4. Theory of Elastic Stability, Timoshenko and Gere, McGraw Hill Book Company

5. Applied Elasticity, Wang, C. T., McGraw Hill Book Company

6. Introduction to the Study of Aircraft Vibration and Flutter, Scanlan and Rosenbaum (Macmillan)

7. A General Computer Program for the Determination of Radiant - Interchange Configuration Factors, Tocips, K. A. ASD-TN-61-101, March 1963

8. Hunter Spring Company, Catalog 12c Hu

9. Report PDA 1-6 (15 January 1963) RCA Victor Company Ltd., Proposed Procedures for Reliability Assessment of Mechanical and Electromechanical Parts

PRECEDING PAGE BLANK NOT FILMED.

8.0 GLOSSARY

See Appendices. Separate glossaries are provided in each appendix as noted.

APPENDIX I

This appendix presents the development of the equations used in Section 3.1.3 pertaining to the deployment dynamics of the Deployable Solar Array.

MASS MOMENTS OF INERTIA

A. Deployable Solar Array About Spin Axis

The mass moment of inertia about the spin axis can be broken down into four (4) components

1. Cylindrical Centerbody: The centerbody is assumed to be a solid homogeneous cylinder of radius R_c for which the mass moment of inertia is

$$I_c = W_c R_c^2 / 2g \tag{A. 1}$$

2. Panel Housing Box: A panel housing box, which includes those portions of the deployment devices which do not move radially, is assumed to be a point mass located a distance R_c from the spin axis for which the mass moment of inertia is

$$I_b = W_b R_c^2 / g \tag{A. 2}$$

3. Scissors Unit: The scissors unit is assumed to be a uniformly distributed mass extending from R_c to X_e. The mass moment of inertia for one unit about the spin axis is

$$I_p = \frac{W_p(X_e - R_c)^2}{12\,g} + \frac{W_p(X_e + R_c)^2}{4\,g} \tag{A. 3}$$

4. Substrate: The substrate is assumed to be composed of an unrolled portion, located a distance R_c from the spin axis, and a deployed portion extending from R_c to X_e. The mass moment of inertia for one complete substrate about the spin axis is

$$I_r = \frac{\left[W_r - \mu(X_e - R_c)\right] R_c^2}{g} + \frac{\mu(X_e - R_c)^3}{12\,g} + \frac{\mu(X_e - R_c)(X_e + R_c)^2}{4\,g} \tag{A. 4}$$

The total mass moment of inertia of the Deployable Solar Array about the spin axis is

$$I = I_c + 4I_b + 4I_p + 4I_r \qquad (A.5)$$

Performing the addition and rearranging terms yields the following general equation

$$I = \left\{ \left[\frac{W_c}{2} + 4W_b + \frac{4}{3}W_p + 4W_r + \frac{8}{3}\mu R_c \right] R_c^2 + \frac{4}{3}W_p X_e^2 + \frac{4}{3}W_p X_e R_c - 4\mu X_e R_c^2 + \frac{4}{3}\mu X_e^3 \right\} \frac{1}{g} \qquad (A.6)$$

The time derivative of equation (A. 6) is required to evaluate the instantaneous angular acceleration of the Deployable Solar Array about the spin axis. The only time varying terms in equation (A. 6) are those containing X_e.

$$\dot{I} = 4\left[\mu(X_e^2 - R_c^2) + \frac{W_p}{3}(2X_e + R_c)\right]\dot{X}_e / g \qquad (A.7)$$

B. Undeployed Substrate (2 Rolls)

The undeployed substrate is considered to be two homogeneous masses of radius R_r wound around spools of radius R_{r_e} as shown in the following sketch

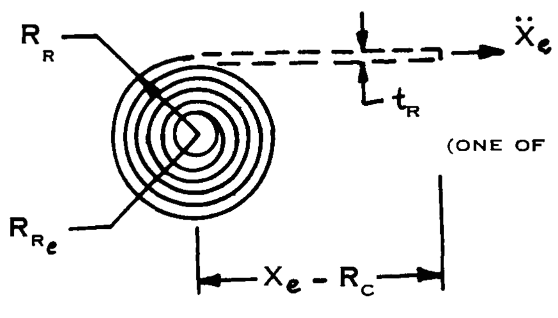

The mass moment of inertia of the substrate about the centerline of the spools can be approximated as follows, neglecting the spool radius and mass.

$$I_r = \left[W_r - \mu(X_e - R_c)\right] R_r^2/2g \qquad \text{(2 rolls)} \tag{A.8}$$

The inertia moment caused by angular acceleration of the two rolls is

$$T_r = - I_r \dot{\omega}_r = - I_r \ddot{X}_e / R_r \tag{A.9}$$

An equivalent inertia force restraining deployment acting tangentially to the roll and in the plane of the substrate may be taken as

$$F_{I_r}' = T_r/R_r = - I_r \ddot{X}_e / R_r^2$$

or

$$F_{I_r}' = - \left[W_r - \mu(X_e - R_c)\right] \ddot{X}_e / 2g \tag{A.10}$$

C. Total Substrate (Rolled Plus Deployed Portion)

The inertia force for the deployed portion of the substrate may be taken as

$$F_{I_r}'' = - \mu(X_e - R_c)\, \ddot{X}_e / g \tag{A.11}$$

Adding equations (A. 10) and (A. 11) to obtain the total equivalent inertia force in the plane of the substrate gives

$$F = - \left[W_r + \mu(X_e - R_c)\right] \ddot{X}_e / 2g \tag{A.12}$$

D. Speed Brake

It is convenient to transfer the inertia moment of the speed brake, due to $\ddot{X}_e$, to the axis of rotation of the undeployed substrate roll so that an equivalent inertia force similar to that of equation (A. 10) can be defined.

Neglecting the inertia of the gear train, the inertia of the speed brake about its axis of rotation can be taken as

$$I_f = W_f R_f^2 / g \tag{A.13}$$

The equivalent inertia referred to the axis of rotation of the undeployed substrate rolls is

$$I_f' = S^2 W_f R_f^2 / g \qquad (A.14)$$

where

$$S = \text{speed ratio, } W_f / W_r$$

noting that

$$\dot{\omega}_r = \ddot{X}_e / R_r$$

The equivalent inertia moment is

$$T_f = - I_f' \ \dot{\omega}_r = -S^2 W_f R_f^2 \ddot{X}_e / g R_r \qquad (A.15)$$

An equivalent inertia force restraining deployment acting tangentially to the roll and in the plane of the substrate may be taken as

$$F_{I_f} = T_f / R_r$$

or

$$F_{I_f} = -S^2 W_f R_f^2 \ddot{X}_e / g R_r^2 \qquad (A.16)$$

SCISSORS FORCE

The scissors unit depicted in the following sketch consists of N links and is driven by a constant torque spring system which applies a constant pair of opposing loads, F_{y_S}, tending to deploy the linkage outward.

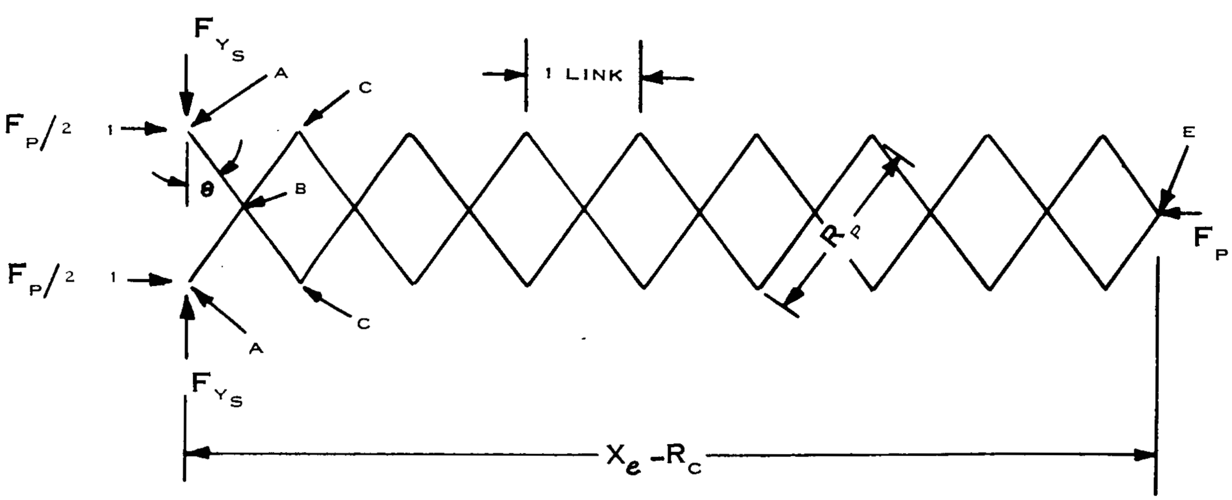

Two approaches are available to determine $F_p = f(F_{ys})$. The first is to start at point E and follow the load F_p through the linkage system ending with the forces F_{ys} which are required to support F_p. The second approach is an energy solution in which the instantaneous linear motions (dy) of the points denoted 'A' multiplied by the F_{ys} forces must equal the instantaneous linear motion (dx) of the point denoted 'E' multiplied by the F_p force. The $F_p/2$ reactions do not move in the direction of the forces and, hence, do not enter the calculation. Selecting the latter method for solution of $F_p = f(F_{ys})$ gives the following result.

Consider the half-link A-B:

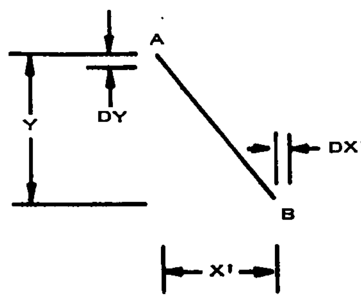

$$X' = \sqrt{\frac{R_p^2}{4} - y^2}$$

$$\frac{dX'}{dy} = -\frac{y}{\sqrt{\frac{R_p^2}{4} - y^2}}$$

$$= -\frac{y}{X'}$$

The minus sign merely indicates that the points A and B cannot both move away from the origin at the same time.

Denoting dy as a minus distance gives

$$dX' = dy \cot \phi$$

Since the points 'A' are restrained against motion in the X direction, it can be seen from proportionality (AC = 2AB) that the points 'C' will move a radial incremental distance 2 dX'.

Following this incremental motion through the links to point E will show that

$$dX_e = 2N dy \cot \phi$$

Writing the energy equation

$$F_p dX_e = 2F_{y_s}\, dy$$

or

$$F_p (2N\, dy \cot \phi) = 2\, F_{y_s}\, dy$$

It follows that

$$F_p = F_{y_s} \tan\phi / N \qquad \text{(A.17)}$$

where

$$\tan\phi = (X_e - R_c) / \sqrt{N^2 R_p^2 - (Xe - Rc)^2} \qquad \text{(A.18)}$$

SPEED BRAKE FRICTION

The speed brake mechanism consists of a "brake drum" housing two masses whose centrifugal forces cause two friction surfaces to bear against the brake drum creating a torque which opposes the angular velocity of the brake mechanism. A sketch of the mechanism is shown below to define nomenclature.

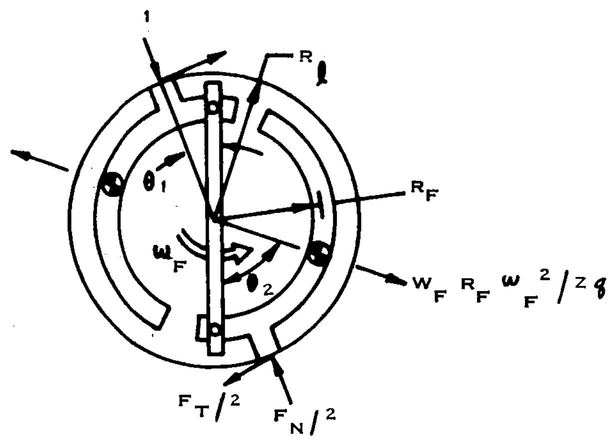

Noting that the forces and loads occur in pairs, the following equations are written for the entire brake mechanism.

Summing moments about the mass hinge points gives

$$\left(\frac{W_f R_f \omega_f^2}{g}\right) R_f \sin\theta_2 + F_t (R_1 - R_f \cos\theta_1) - F_n R_f \sin\theta_1 = 0 \quad \text{(A. 19)}$$

But

$$F_t = C_f F_n \quad \text{(A. 20)}$$

Substituting equation (A. 20) into (A. 19) and solving for F_n gives

$$F_n = \frac{W_f R_f^2 \omega_f^2 \sin\theta_2}{g\left[R_f \sin\theta_1 - C_f (R_1 - R_f \cos\theta_1)\right]} \quad \text{(A. 21)}$$

The friction torque about the axis of rotation is

$$T_f = R_1 F_t = R_1 C_f F_n \quad \text{(A. 22)}$$

Solving for the torque about the axis of rotation of the undeployed substrate rolls gives the following expressions.

Noting that

$$\omega_f = S \omega_r \quad \text{(A. 23)}$$

$$T_r = S T_f$$

and

$$\omega_r = \dot{X}_e / R_r \quad \text{(A. 25)}$$

it follows from equations (A. 22) that

$$T_r = ST_f = SR_1C_fF_n = \frac{C_fS^3W_fR_1R_f^2\dot{X}_e^2 \sin\theta_2}{g\left[R_f\sin\theta_1 - C_f(R_1 - R_f\cos\theta_1)\right] R_r^2} \quad (A.26)$$

An equivalent friction force restraining deployment acting tangentially to the undeployed substrate roll and in the plane of the deployed substrate may be taken as

$$F_f = T_r / R_r$$

Therefore,

$$F_f = \frac{C_fS^3W_fR_1R_f^2\dot{X}_e^2\sin\theta_2}{g\left[R_f\sin\theta_1 - C_f(R_1 - R_f\cos\theta_1)\, R_r^3\right]} \quad (A.27)$$

APPENDIX II

STRUCTURAL ANALYSIS CALCULATIONS

1. Analysis for axial loads in Scissors links

Forces applied to the scissors linkage through the screw jacks are constant but, the forces within the linkage are a function of the degree of deployment. The forces acting on the linkage system are shown in Figure B-1.

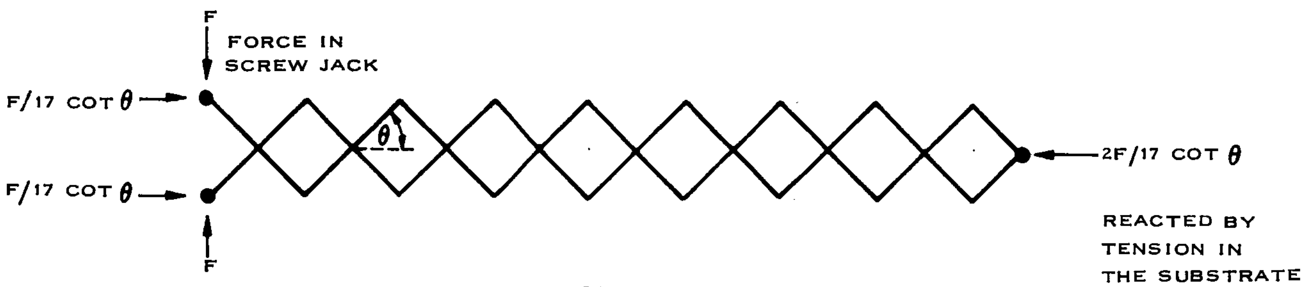

FIGURE B (1)

The axial compression and transverse shear in the scissors links caused by this loading is also a function of the degree of deployment and is different for each member of the linkage, the most inboard link being the most stressed. The shear and axial load for the most stressed link for $\Theta = 38.5^{o}$ (corresponding to maximum torsion) is computed below.

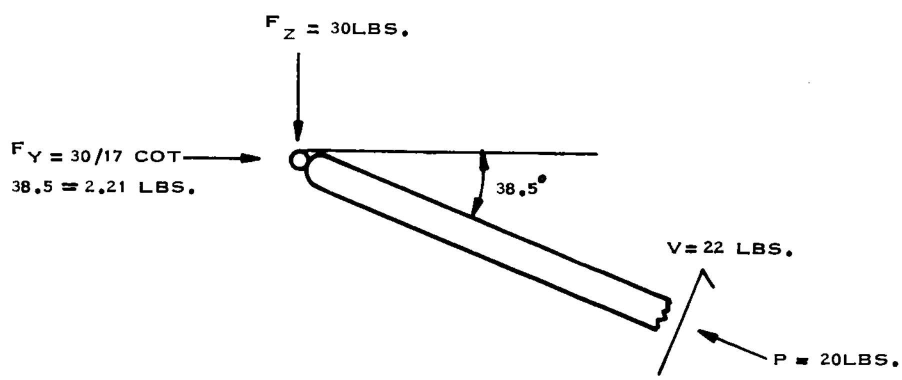

where:

$$P = 30 \text{ Sin } 38.5^{o} + 2.21 \text{ Cos } 38.5^{o}$$

$$V = 30 \text{ Cos } 38.5^{o} - 2.21 \text{ Sin } 38.5^{o}$$

$$P = 22.1 \text{ lbs.}$$
$$V = 20 \text{ lbs.}$$

2. Bending under 1 g Deployment

The scissors links were analyzed for the bending and torsional stresses under 1 g deployment. The loading of the system is shown in Figure B-2.

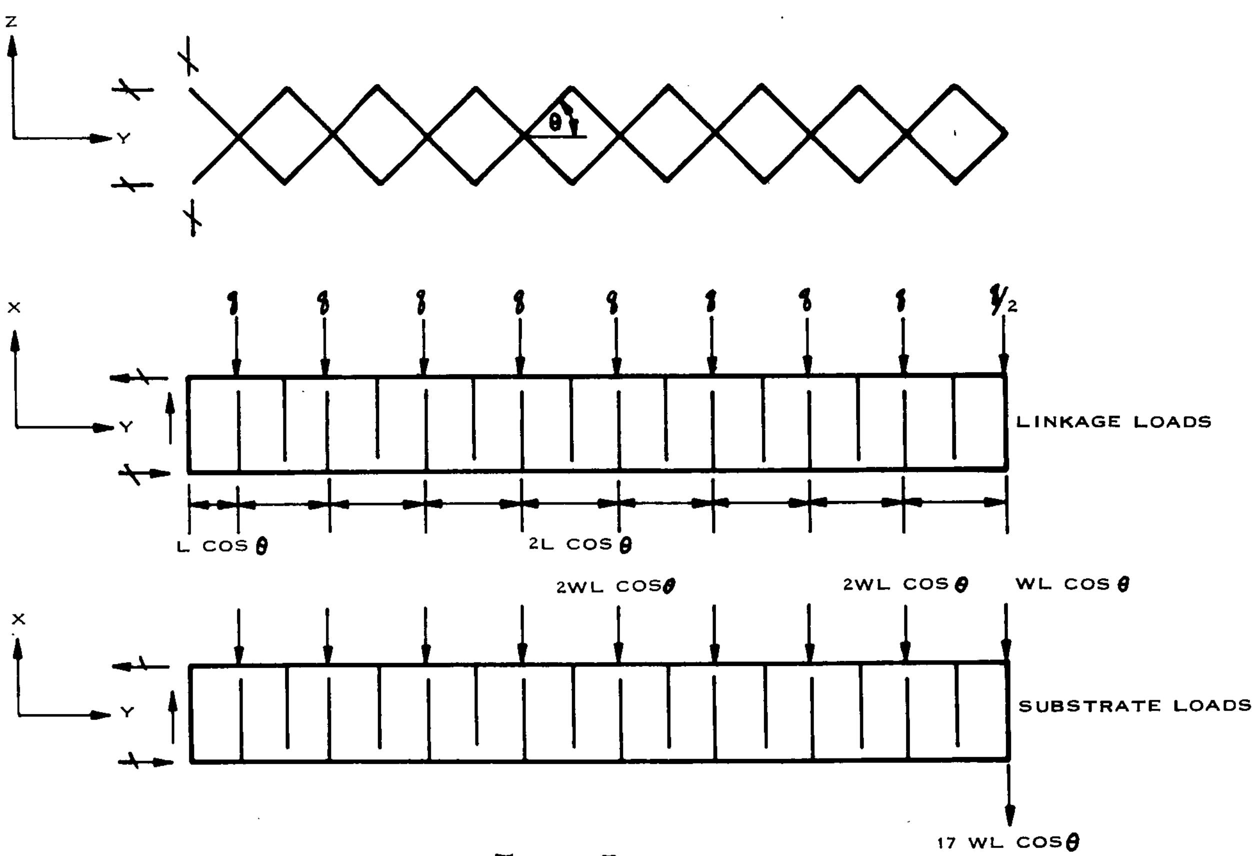

FIGURE B (2)

2L = length of link = 11.83 in.
W = weight of substrate and cells per inch = 0.026 lbs/in.
q = weights of scissor links 0.2325 lbs.

The moment in the last link is:

$$M = 344\ W^{2}\ \text{Cos}^{2}\ \Theta + 72.5\ qL\text{Cos}\ \Theta, \quad \text{ft-lbs.}$$

Part of this is carried by torsion M_T and part by bending M_b of the links

$$M_T = \overline{M}\ \text{Sin}\ \Theta$$

$$M_b = \overline{M}\ \text{Cos}\ \Theta$$

$$M_T = 344\ WL^2\ \text{Cos}^2\ \Theta\ \text{Sin}\ \Theta + 72.5\ qL\text{Cos}\ \Theta\ \text{Sin}$$

A plot of M_T versus Θ is shown in Figure B-3.

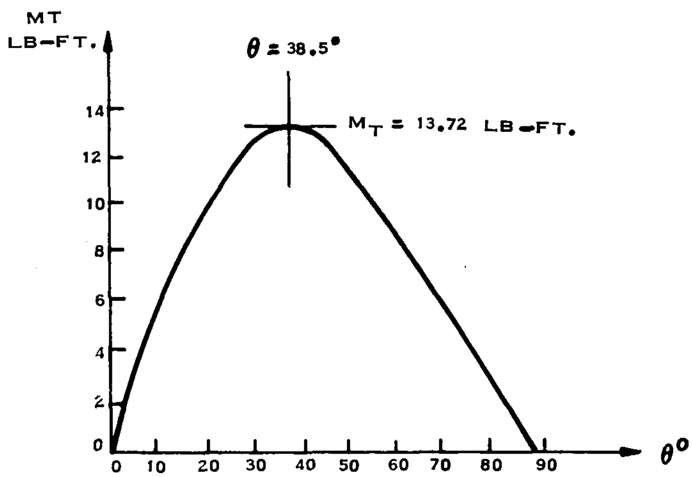

Figure B-3
Variation of torsional moment with angle of deployment

The maximum torsion in the links occurs for $\Theta = 38.5^{\circ}$. The distribution of moment to the channel and the box link of the scissors linkage can be determined by considering the condition that the vertical deflections are equal, and the conditions of equilibrium.

$$\delta_1 = \delta_2$$

$$\frac{M_1 L_1^2}{2E_1 I_1} = \frac{M_2 L_2^2}{2E_2 I_2}$$ (deflection condition)

$$\frac{M_1}{M_2} = \frac{I_1}{I_2} = \frac{0.138}{0.254}$$

where:

Subscript 1 refers to channel link

Subscript 2 refers to box link

but $M_1 + M_2 = \overline{M}$ (Equilibrium Condition)

$$M_1 = \frac{0.138}{0.392} \overline{M} = 0.35 \overline{M}$$

$$M_2 = \frac{0.254}{0.392} \overline{M} = 0.65 \overline{M}$$

Thus, the bending and torsional components in each member can be computed using a factor of 2 for all ultimate loads.

$M_{T1} = 0.35 \times 164 \times 2 = 115$ lb-in (Torsion in channel link)

$M_{T2} = 0.64 \times 164 \times 2 = 212$ lb-in (Torsion in Box link)

$M_{B1} = .35 \times 207 \times 2 = 125$ lb-in (Bending in channel link)

$M_{B2} = .65 \times 207 \times 2 = 270$ lb-in (Bending in Box link)

Stresses due to axial load, transverse shear, and bending shear are negligible.

3. Dynamic Deployment Loads

The Maximum bending moment (m), transverse shear force (v) and axial load (t) in each member of the scissors linkage can be related to the resultant moment M, shear V and axial force T acting at each section of the linkage for various degrees of deployment.

$$m = \frac{V}{2} L \cos\theta + \frac{T}{2} L \sin\theta + \frac{M}{2}$$

$$v = \frac{V}{2} \cos\theta + \frac{T}{2} \sin\theta + \frac{M}{2L}$$

$$t = \frac{T}{2} \cos\theta + \frac{M}{2L} \cot\theta - \frac{V}{2} \cos\theta$$

where:

$2L$ = length of a scissors link

θ = angle of deployment

The stresses resulting from these forces and moments are negligible.

4. Stress Calculations

a) Channel 7075 Al. Aly.

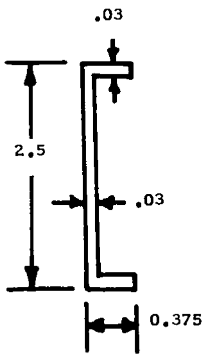

$$\sigma = \frac{MC}{I} = \frac{125 \times 1.25}{.138} = 1,400 \text{ psi}$$

$$\tau = \frac{Tc^1}{K} = \frac{114 \times .075}{24.4 \times 10^{-3}} = 35,000 \text{ psi}$$

$$\tau_{max} \sqrt{(\tau)^2 + (\tfrac{\sigma}{2})^2} = 35,000 \text{ psi}$$

$$\sigma_{max} = \frac{\sigma}{2} + \tau_{max} = 35,700 \text{ psi}$$

$$\text{M.S.} = \frac{48,000}{35,000} - 1 = \underline{\underline{0.37}}$$

where:

$I = .138 \text{ in.}^4$

$C_1 = 2.5 \text{ in.}$

$C = .075 \text{ in.}$

$K = 24.4 \times 10^{-3} \text{in.}^4$ Ref. 1

b) Box link 7075 al. aly.

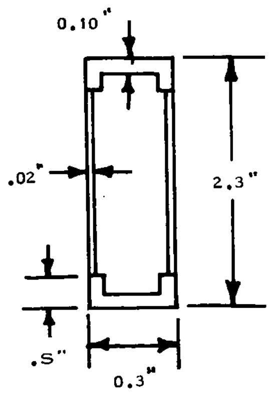

$$\sigma = \frac{270 \times 1.15}{.254} = 1,270 \text{ psi}$$

$$\tau = \frac{T}{2t_1(a-t)(b-t_1)} = \frac{212}{2 \times .02(2.2)(.29)} = 8,300 \text{ psi}$$ Ref. 1

$$\tau_{max} = 8,320 \text{ psi}$$

$$\sigma_{max} = 8,955 \text{ psi}$$

$$\text{M.S.} = \frac{48,000}{8,955} - 1 = \underline{\underline{4.36}}$$

where:

$I = .254 \text{ in.}^4$

$c = 1.15 \text{ in.}$

$a = 2.3 \text{ in.}$

$b = 0.3 \text{ in.}$

$t = 0.1 \text{ in.}$

$t_1 = .02 \text{ in.}$

c) Roller and Substrate (Response = 252 g ult.)

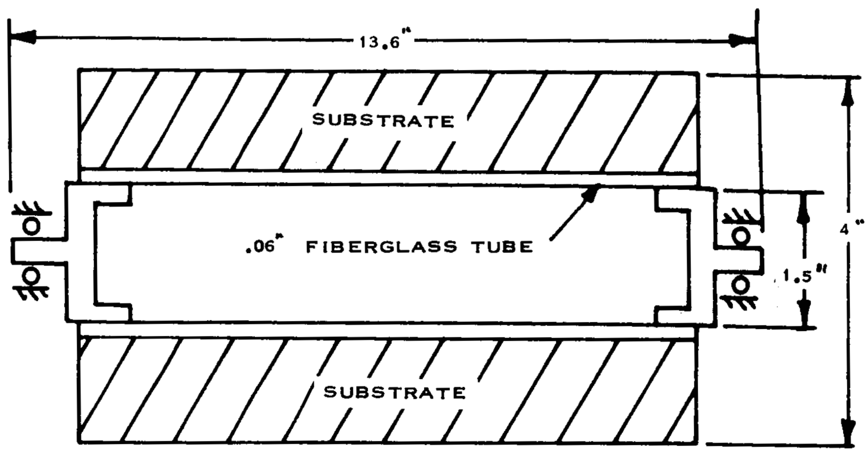

Weight of Substrate = 2.5 lbs.

$$W = \frac{2.5}{13.6} \times 252 = 46.3 \text{ lbs/in.}$$

$$M_{max} = \frac{WL^2}{8} \doteq \frac{46.3 \times (13.6)^2}{8} = 1070 \text{ lb-in.}$$

$$Z = \frac{I}{c} = \pi tr^2 = 0.106 \text{ in.}^3$$

$$\sigma = \frac{M}{Z} = \frac{1070}{0.106} = 11,000 \text{ psi}$$

Buckling of tube

$$\sigma_{cr} = Cb\frac{Et}{r} = 0.3 \times 2500 \times \frac{0.06}{.75} \times 10^3 = 80,000 \text{ psi}$$

($\therefore$ buckling not critical)

F_{TU} = 34,000 psi

$$M.S. = \frac{34,000}{11,000} - 1 = \underline{\underline{2.1}}$$

d) Housing (Vibration Loads)

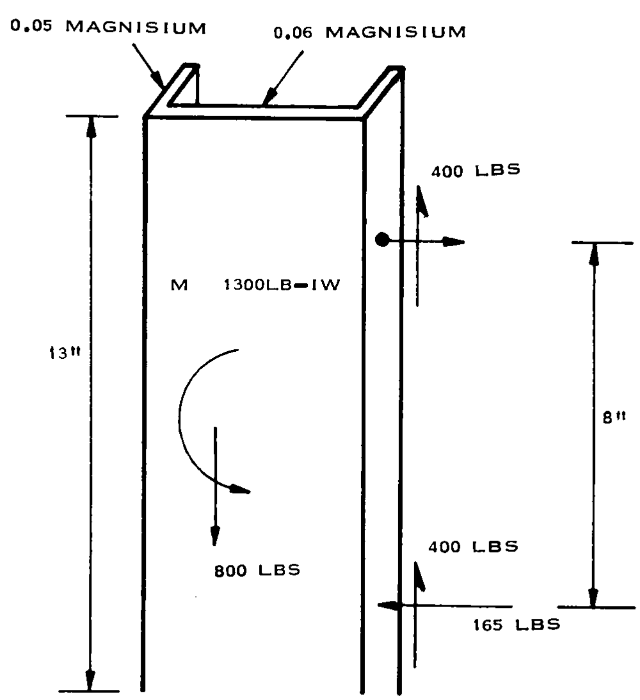

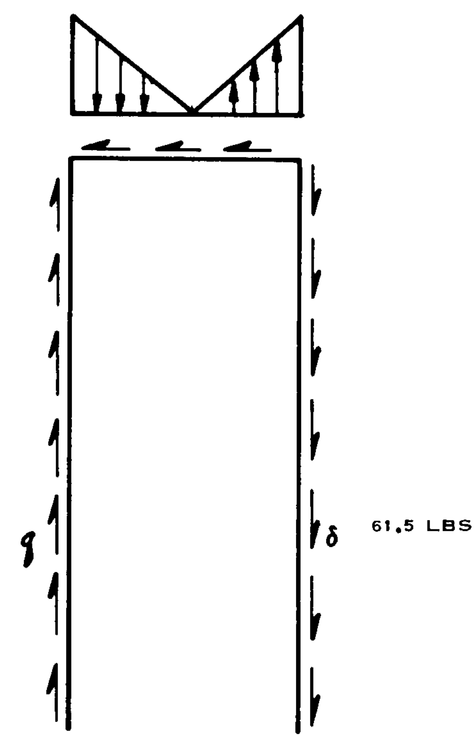

$$S_{cr} = K \frac{E}{1-\nu^2} \left(\frac{t}{b}\right)^2 \qquad K = 4.4$$

$$S_{cr} = 8,150 \text{ psi} \qquad q_{cr} = 440 \text{ lbs/in.} \qquad q = \frac{800}{13} = 61.5 \text{ lbs/in.}$$ (M.S. High

$$S^1{}_{cr} = K \frac{E}{1-\nu^2} \left(\frac{t}{b}\right)^2 \qquad K \approx 21$$

$$S^1{}_{cr} = 39,000 \text{ psi}$$

$$\sigma_{brwd} = \frac{MC}{I} = \frac{1300 \times 2.3}{1.08} = 2,830 \text{ psi} \quad \text{(M.S. High)}$$

Check housing for effect of locally applied concentrated loads.

Largest concentrated load = 330 lbs.

<u>Bearing Stress:</u> Plate is stiffened locally a one inch diameter

$$f_{br} = \frac{P}{Ab} = \frac{330}{.06 \times 1} = 5,500 \text{ psi.}$$

<u>Local buckling under concentrated loads</u>

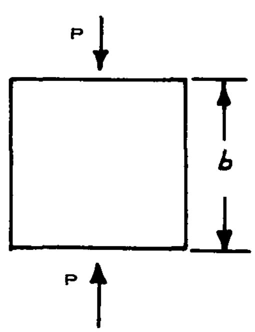

$$P_{cr} = \frac{\pi}{3} \frac{Et^3}{(1-\nu^2)b} = \frac{\pi}{3} \times \frac{6.5 \times 10^6 \times (0.06)^3}{.9\, b}$$

$$= \frac{1630}{b} \text{ lbs}$$

Assume that effect of concentrated load will not be felt more than 4" away from concentrated load (b = 4")

$$P_{cr} = \frac{1630}{4} = 408 \text{ lbs.}$$ Largest concentrated load = 330 lbs.

$$\text{M.S.} = \frac{408}{330} - 1 = \underline{\underline{0.23}}$$

e) <u>Hinge Pins of Scissors linkage</u>

The maximum moment transmitted by any hinge is for the fully deployed configuration $\Theta = 10^{o}$ at which point $M = 26.0\ S\ \cos^{2} 10^{o} + 7.64 \cos 10^{o} =$ 33.2 ft-lbs = 398 lb-in of this 0.65 M is carried by the Box link section. Using an ultimate factor of 2 g, the max moment across a hinge is 517 lb-in.

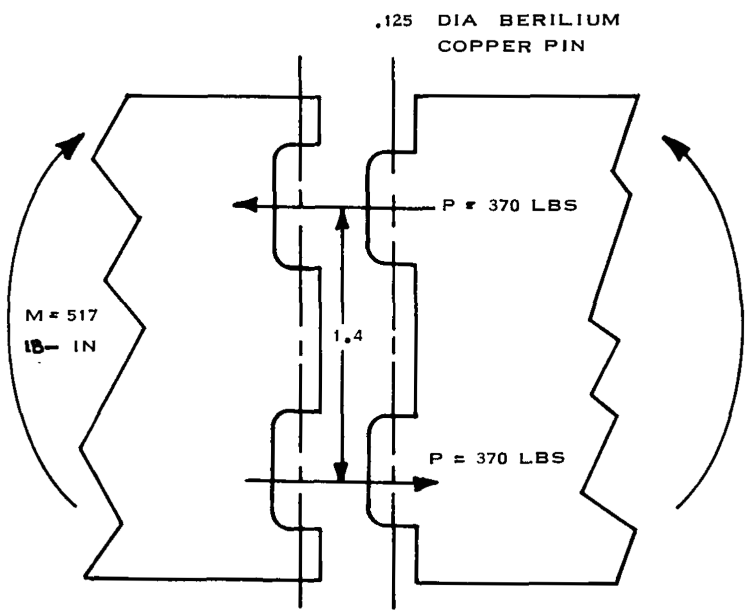

M = 517 lb-in

Pin is in double shear:

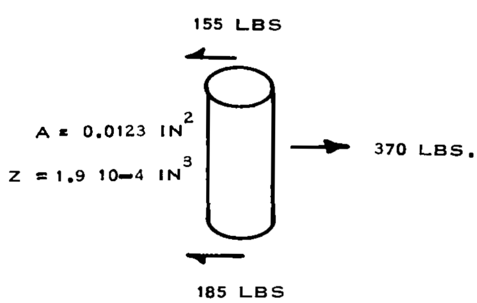

$$\text{Shear Stress} = \frac{P}{A} = \frac{185}{.0123} = \tau = 15,000 \text{ psi.}$$

Bending of Pin: Conservatively assume a gap of .05"

$$M = 185 \times .05 = 92.5 \text{ lb-in}; \quad \sigma = \frac{9.5}{1.9\text{x}10^{-4}} = 49,000 \text{ psi.}$$

Combined Stresses

$$\tau_{max} = \sqrt{\left(15\text{x}10^3\right)^2 + \left(\frac{49\text{x}10^3}{2}\right)^2} = 29,000 \text{ psi.}$$

$$\sigma_{max} = (24.5 + 29)\,\text{x}10^3 = 53,000 \text{ psi}$$

$$M_s = \frac{90,000}{29,000} - 1 = \underline{\underline{2.1}} \qquad \text{(Shear)}$$

$$M_s = \frac{100,000}{53} - 1 = \underline{\underline{0.9}} \qquad \text{(Tension)}$$

f) End Plate (181 Fiberglass 0.06 thickness)

The end plate supports the substrate tension load as a channel in bending about the end hinge of the scissors linkage.

$$\text{total Moment} = \frac{2\text{x}10}{2} \text{ lbs x } 3'' = 30 \text{ lb-in x Factor of } 2 = 60 \text{ lb-in}$$

Channel Section

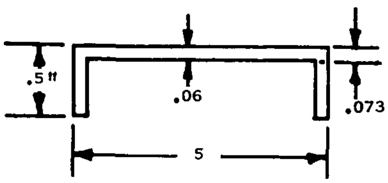

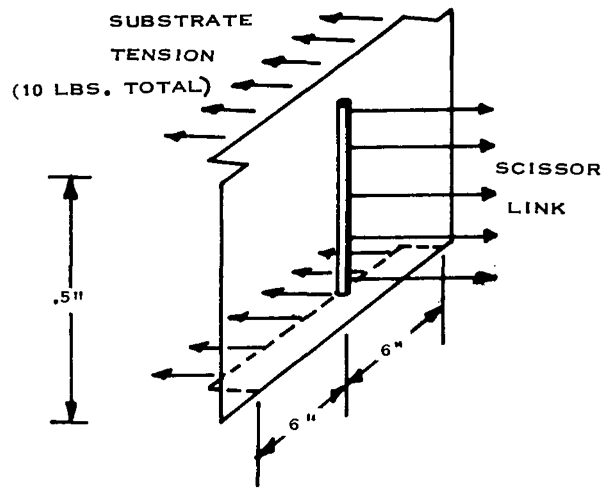

g) Screw Jack Bending Stress and Deflections

The location and magnitude of the linkage load on the screw jacks both depend on the degree of deployment. An overlapping assumption is made that the loads acting are the maximum loads possible but, act at the position along screw to cause maximum bending and maximum deflections.

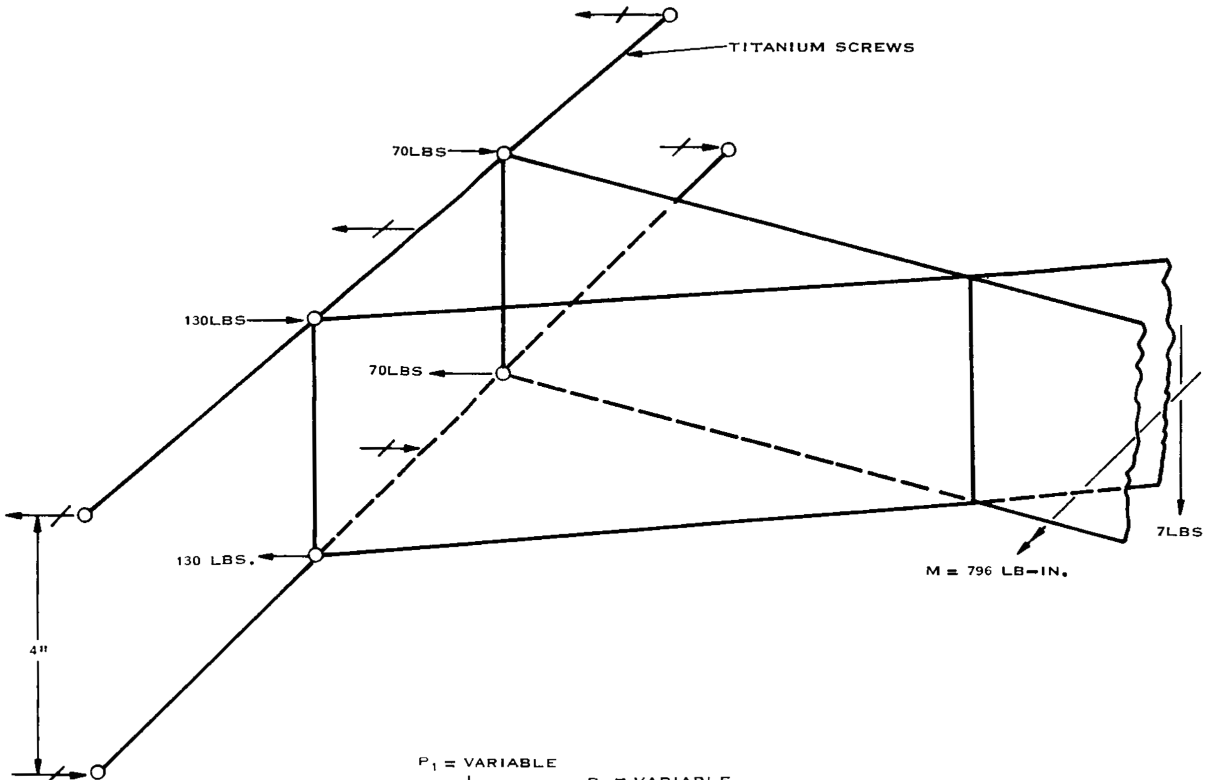

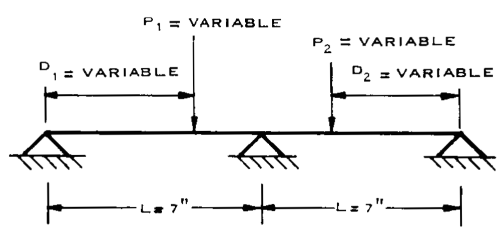

Absolute maximum moment = 157 lb-in

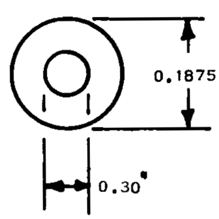

$$\sigma = \frac{M}{Z} = \frac{157}{23\times10^{-4}} = 68,000 \text{ psi.}$$

$$\text{M. S.} = \frac{70,000}{68,000} - 1 = \underline{\underline{0.03}}$$

where:

$$Z = 23 \times 10^{-4} \text{in.}^3$$

$$I = 6.9 \times 10^{-4} \text{in.}^3$$

Absolute maximum deflection

$$\delta = \frac{.0093PL^3}{EI}$$

$$\delta = \frac{.0093 \times 130 \times 7^3}{15 \times 10^6 \times 6.9 \times 10^{-4}} = .04 \text{ in.} \qquad \underline{\underline{\text{O.K.}}}$$

h) Substrate Loads

Maximum load in substrate during dynamic deployment = 25.5 lbs. = 2.1 lbs/in.

Allowable load in substrate = 140 lbs/in.

M.S. = high

APPENDIX III - RELIABILITY

This section of the Appendix presents the failure rate calculation.

1.0 BEARINGS

In the following analysis for the bearings the worst case was considered to be typical. It is apparent this approach is conservative and reliabilities will be higher than that computed. For the sleeve bearings on the scissors links this approach appears realistic when considering these bearings rotate at less than 1/2 RPM.

Duty Cycle - Assume one one-minute cycle per hour at 32 RPM

$$\text{RMS speed} = \sqrt{\frac{(32)^2(1) + (0)^2(59)}{60}} = 4.2 \text{ RPM}$$

$$\text{Equivalent Duty Cycle} = \frac{4.2}{32} \times 100 = 13\%$$

Speed Size Rating

Bearing Size = .375 x 25.4 = 9.53 mm

Shaft Speed = 32 RPM

DN Value = 9.53 x 32 = 305 DN

13% Duty at 305 DN = .13 x 305 = 40 DN

Hot Spot Temperature = 150°F

Enter Figure 5-1 of Reference 1 for failure rate.

Failure Rate = 1%/1000 hours (uncorrected)

Assuming resultant thrust load is 75% load limit, enter Figure 5-6 of Reference 1.

Failure Rate = 1%/1000 hours (corrected)

Degradation factor for launch environment = 100

Failure rate = 100 x 1%/100 = 100%/1000 hours

Wear out failure rate in %/1000 hours for calculated life period (t_c)

$$t_c = \frac{10^5}{FR} = \frac{100,000}{100} = 1000 \text{ hours}$$

The unit being analyzed will never be subjected to 1000 hours of operation; consequently, the only real possibility of failure for the mission as defined would be the probability of random failure. From Reference 1, Figure 4-1, the ratio of random to degradation in generic failure rate = 0.01.

Therefore, $\dfrac{F \text{ random}}{F \text{ degradation}} = .01$

FR = .01 (100) = 1.0%/1000 hours

$$R_{B_1} = e^{-\lambda t} = e^{-\left(\frac{0.1}{1000} \times \frac{25}{60}\right)} = e^{-4 \times 10^{-6}}$$

For total number of bearings (72)

$$R_B = \left(e^{-4 \times 10^{-6}}\right)^{72} = e^{-288 \times 10^{-6}}$$

2.0 BRAKE

The main wear effect on the brake will be in the bearing. Wear is influenced by shock loads on engagement, frequency, and speed of operation.

In this application, the DN value is less than 50 and the shock load experienced on engagement, frequency, speed of operation are low values. A base failure rate, without modification for the aforementioned factors of 1% are 1000 hours is assumed. The random failure rate is as follows:

Degradation factor due to launch = 100

$FR = 1 \times 100 = 100\%/1000$ hours

Ratio of F_{random} to $F_{degradation} = .02$

$F_R = .02 \times 100 = 2\%/1000$ hours

$$R_{BR} = e^{-\lambda t} = e^{-\left(\frac{.02}{1000} \times \frac{25}{60}\right)} = e^{-8 \times 10^{-6}}$$

3.0 GEAR REDUCTIONS

This prediction applies to instrument type reduction gear boxes. Degradation due to accuracy which is attributable to increase in back-lash resulting from wear which is a function of speed (ratio) duty cycle output loading, and frequency of reversal. Since correlation between this prediction and a prediction for larger reduction gear boxes is not available, this prediction will at least give an indication of the approximate failure levels to be expected.

Assume Precision Class I AGMA spur gears.

Substrate Gears

Reduction in three passes

Ratio 1:1

Speed Input = 32 RPM

Assume one one-minute cycle per hour at 32 RPM for calculating a duty cycle.

Duty cycle = 13% (reference Paragraph 1)

Effective Accuracy Failure Rate

EAFR = Base failure rate x duty cycle x number of passes

BRF = 10% failures per 1000 hours (reference 1)

$$EARF = \frac{10\%}{1000} \times .13 \times 3 = 3.9\%/1000 \text{ hours}$$

Effective reduction ratio failure rate

$$ERRFR = \frac{100}{\sqrt{\text{ratio}}} \times \text{duty cycle}$$

$$= \frac{100}{1} \times .13$$

$$= 13\ \%/1000 \text{ hours}$$

No factor for reverse drive or stops. Bearings have already been considered.

Calculated life period.

Total component failure rate = 13 + 3.9 = 16.9%/1000 hours

Degradation factor due to launch = 100

FR = 100 x 16.9 = 1690%/1000 hours

$$\text{Calculated life} = t_c = \frac{10^5}{FR} = \frac{100000}{1690} = 59.2 \text{ hours}$$

For this mission, the gears will never be operated 59.2 hours. The only real possibility of failure would be that of random failure.

$$\text{Ratio } \frac{FR}{FD} = .02$$

$$FR = .02 \times 1690 = 33.8\%/1000 \text{ hours} \qquad t = \frac{25}{60} \text{ hours}$$

$$R_{SG} = e^{-\lambda t} = e^{-\left(\frac{.338}{1000} \times \frac{25}{60}\right)} = e^{-141 \times 10^{-6}}$$

Drive Gears

Reduction in one pass

Ratio 1:2.4

Duty Cycle = 13% (Reference, Paragraph 1)

Effective Accuracy Failure Rate

EAFR = Base failure rate x duty cycle x number of passes

BFR = 10% failures per 1000 hours (Reference 1)

$$EAFR = \frac{10\%}{1000} \times .13 \times 1 = 1.3\%/1000 \text{ hours}$$

Effective Reduction Ratio Failure Rate

$$ERRFR = \frac{100}{\sqrt{\text{ratio}}} \times \text{duty cycle}$$

$$= \frac{100}{.645} \times .13$$

$$= 20.2 \%/1000 \text{ hours}$$

Calculated Life Period

Total component failure rate = 20.2 + 1.3 = 21.5%/1000 hours

Degradation factor due to launch = 100

FR = 100 x 21.5 = 2150%/1000 hours

$$\text{Calculated Life} = t_c = \frac{10^5}{FR} = \frac{100000}{2150} = 46.5 \text{ hours}$$

For this mission the gears will never be operated to the life of 46.5 hours. The only real possibility of failure being that of random failure.

$$\text{Ratio of } \frac{FR}{FD} = .02$$

FR = .02 x 21.50 = 43%/1000 hours

$$R_{DG_1} = e^{-\lambda t} = e^{-\left(\frac{.43}{1000} \times \frac{25}{60}\right)} = e^{-180 \times 10^{-6}}$$

For both drive gear meshes,

$$R_{DG} = .99964$$

$$= \left(e^{-180 \times 10^{-6}}\right)^2 = e^{-360 \times 10^{-6}}$$

Gear Reliability

$$R_G = (R_{SG})\ (R_{DG}) = e^{-141 \times 10^{-6}} \times e^{-360 \times 10^{-6}} = e^{-501 \times 10^{-6}}$$

4.0 SPRING MOTOR

Mean Cycles Between Failure

$$FR = \frac{1}{25} / 1000 \text{ cycles} = 40\%/1000 \text{ cycles (Reference 2)}$$

Launch Environment

Degradation factor = 100

FR = 40 x 100 = 4000%/1000 cycles

Ratio of $\frac{FR}{FD}$ = .02 Number of cycles = 1

FR = .02 x 4000 = 80%/1000 cycles

$$R_{M1} = e^{-\lambda c} = e^{-\left(\frac{.8}{1000} \times 1\right)} = e^{-800 \times 10^{-6}}$$

Test Environment

FR = 40%/1000 cycles

Ratio of $\frac{FR}{FD}$ = .02 Number of cycles = 24

FR = .02 x 40 = .8%/1000 cycles

$$R_{M2} = e^{-\lambda c} = e^{-\left(\frac{.008}{1000} \times 24\right)} = e^{-192 \times 10^{-6}}$$

Motor Reliability

$$R_M = R_{M1} \times R_{M2} = e^{-800 \times 10^{-6}} \times e^{-192 \times 10^{-6}}$$

$$= e^{-992 \times 10^{-6}}$$

5.0 SUBSTRATE

There are no failure rate data available on the flexural capabilities of the substrate. Therefore, the failure rate has been estimated at one failure per 5000 cycles. In addition, the fact that the substrate is rolled throughout the launch environment renders the launch environment degradation factor unrealistic, and is eliminated. In the interests of conservatism, any ratio of degradation to random failure rate is also eliminated.

$$FR = \frac{1}{5000} = .0002$$

$$R_S = e^{-.0002 \times 25} = e^{-5000 \times 10^{-6}}$$

6.0 CONDUCTORS

Failure rate data for the conductors is also unavailable, so the failure rate for this item is estimated at one failure in 500 cycles. Again, the launch factor and failure rate ratio are eliminated for the reasons stated above.

$$F_R = \frac{1}{500} = .002$$

$$R_C = e^{-.002 \times 25} = e^{50000 \times 10^{-6}}$$